

**MECHANISMS BY WHICH NONNUCLEOSIDE REVERSE TRANSCRIPTASE
INHIBITORS BLOCK HIV-1 REPLICATION ALONE AND IN COMBINATION WITH
OTHER REVERSE TRANSCRIPTASE INHIBITORS**

by

Jessica Ann Radzio

BS, Virginia Polytechnic Institute and State University, 2001

MS, Virginia Polytechnic Institute and State University, 2003

Submitted to the Graduate Faculty of
Graduate School of Public Health in partial fulfillment
of the requirements for the degree of
Doctor of Philosophy

University of Pittsburgh

2010

UNIVERSITY OF PITTSBURGH
GRADUATE SCHOOL OF PUBLIC HEALTH

This dissertation was presented

by

Jessica Ann Radzio

It was defended on

August 13, 2010

and approved by

Zandrea Ambrose, PhD, Assistant Professor
Department of Medicine, Division of Infectious Disease
School of Medicine, University of Pittsburgh

Velpandi Ayyavoo, PhD, Associate Professor
Department of Infectious Diseases and Microbiology
Graduate School of Public Health, University of Pittsburgh

John W. Mellors, MD, Professor
Department of Medicine, Division of Infectious Disease
School of Medicine, University of Pittsburgh

Tianyi Wang, PhD, Assistant Professor
Department of Infectious Diseases and Microbiology
Graduate School of Public Health, University of Pittsburgh

Dissertation Advisor: Nicolas Sluis-Cremer, PhD, Associate Professor
Department of Medicine, Division of Infectious Disease
School of Medicine, University of Pittsburgh

Copyright © by Jessica Ann Radzio

2010

**MECHANISMS BY WHICH NONNUCLEOSIDE REVERSE TRANSCRIPTASE
INHIBITORS BLOCK HIV-1 REPLICATION ALONE AND IN COMBINATION
WITH OTHER REVERSE TRANSCRIPTASE INHIBITORS**

Jessica Ann Radzio, PhD

University of Pittsburgh, 2010

Inhibition of reverse transcriptase (RT) is a vital tactic in the prevention of human immunodeficiency virus 1 (HIV-1). Nonnucleoside reverse transcriptase inhibitors (NNRTIs) are a class of compounds demonstrated to act as allosteric inhibitors of RT DNA polymerization. However, several lines of evidence suggest that polymerization may not be the main mechanism of inhibition of reverse transcription. It has been demonstrated that NNRTIs also have the ability to modulate RT ribonuclease (RNase) H cleavage. Additionally, recent evidence suggests that resistance to chain-terminating nucleoside reverse transcriptase inhibitors (NRTIs) is dependent on a balance between the polymerase and RNase H activities of the enzyme. In light of this, I hypothesize that NNRTIs block reverse transcription by exerting effects on both the DNA polymerase and RNase H active sites of the enzyme, significantly disrupting the equilibrium between these two enzymatic activities. Therefore, the ability for NNRTIs to be combined with other classes of RT inhibitors in antiretroviral therapies will depend on how these compounds respond to the NNRTI-induced shift in the polymerase/RNase H activity equilibrium. This study demonstrates that NNRTIs cause the accelerated appearance of secondary RNase H cleavage products that have decreased RNA/DNA hybrid structures. As a result, these template/primers

(T/Ps) are not sufficient substrates for NRTI removal and therefore, excision is less efficient in the presence of NNRTIs. Additionally, fluorescent resonance energy transfer experiments demonstrate that NNRTIs cause a shift in the binding of RT and T/P such that the RNase H domain is moved away from the 5' end of the primer. Finally, subunit-specific analysis shows that resistance to RTI combination therapy facilitated by the N348I mutation is a result of effects from the p51 subunit. I propose that the binding of NNRTIs cause RT to bind to T/P in a polymerase-incompetent mode, resulting in decreased polymerization and shorted RNase H cleavage products. Additionally, N348I can facilitate dual resistance by favoring the polymerase-competent binding mode. This work is of public health significance because it lays the foundation for the development of new reverse transcriptase inhibitors and highlights the importance of resistance in the connection domain of HIV-1 RT.

TABLE OF CONTENTS

1.0	INTRODUCTION.....	1
1.1	HUMAN IMMUNODEFICIENCY VIRUS.....	1
1.1.1	HIV-1 Origin.....	1
1.1.2	HIV-1 Structure.....	2
1.1.3	Virus Life Cycle.....	3
	1.1.3.1 Binding and Fusion.....	3
	1.1.3.2 Uncoating and Reverse Transcription.....	4
	1.1.3.3 Integration and Viral Gene Expression.....	18
	1.1.3.4 Virus Assembly and Egress.....	21
1.2	THERAPEUTIC INTERVENTIONS.....	22
1.2.1	Entry.....	22
1.2.2	Reverse Transcription.....	23
	1.2.2.1 NRTIs.....	25
	1.2.2.2 NNRTIs.....	30
1.2.3	Integration.....	34
1.2.4	Maturation.....	35
1.2.5	Combination Therapy.....	35
	1.2.5.1 Current Recommendations.....	36

1.3	HIV-1 RESISTANCE TO RT INHIBITORS.....	37
1.3.1	Nucleoside Reverse Transcriptase Inhibitors (NRTIs)	38
1.3.1.1	Discrimination Phenotype	39
1.3.1.2	Excision Phenotype.	40
1.3.2	Nonnucleoside Reverse Transcriptase Inhibitors (NNRTIs).....	42
1.3.3	Antagonism Between Resistance Mutations.....	43
1.3.4	Resistance Mutations in the Connection Domain.....	44
1.3.4.1	N348I	45
1.3.5	Resistance Mutations in the RNase H Domain	47
2.0	SPECIFIC AIMS.....	49
2.1	BACKGROUND AND PRELIMINARY DATA.....	49
2.2	HYPOTHESIS AND SPECIFIC AIMS.....	53
3.0	CHAPTER ONE: EFAVIRENZ ACCELERATES HIV-1 REVERSE TRANSCRIPTASE RIBONUCLEASE H CLEAVAGE, LEADING TO DIMINISHED ZIDOVUDINE EXCISION.....	54
3.1	PREFACE	54
3.2	ABSTRACT.....	55
3.3	GOAL OF THE STUDY.....	56
3.4	MATERIALS AND METHODS.....	56
3.4.1	Materials.....	56
3.4.2	Template/Primer Substrates.....	57
3.4.3	Assays for Inhibition of AZT-TP Incorporation and AZT-MP Excision by HIV-1 RT	58

3.4.4	RNase H Assays	59
3.4.5	Gel Mobility Shift Assays.....	60
3.5	RESULTS AND DISCUSSION	60
3.5.1	Effect of Efavirenz on Excision and Incorporation.....	61
3.5.2	Effect of Efavirenz on RNase H Activity	64
3.5.3	Excision from T/Ps with Decreasing Template Lengths	67
3.5.4	Effect of Efavirenz on RT-T/P Association	67
4.0	CHAPTER TWO: EFAVIRENZ ALTERS THE INTERACTION BETWEEN HIV-1 REVERSE TRANSCRIPTASE AND TEMPLATE/PRIMER	71
4.1	PREFACE	71
4.2	ABSTRACT.....	72
4.3	GOAL OF THE STUDY	73
4.4	MATERIALS AND METHODS.....	74
4.4.1	Materials.....	74
4.4.2	Template/Primer Substrates.....	74
4.4.3	Generation and Characterization of Labeled Recombinant Mutant Enzymes	75
4.4.4	FRET Assays	75
4.4.5	Analysis of Data	76
4.5	RESULTS AND DISCUSSION	77
4.5.1	Characterization of Labeled RT	77
4.5.2	Effect of NNRTI Binding as Evaluated by FRET Analysis.....	80

5.0	CHAPTER THREE: N348I REVERSE TRANSCRIPTASE PROVIDES A GENETIC PATHWAY FOR HIV-1 TO SELECT TAMS AND MUTATIONS ANTAGONISTIC TO TAMS.....	85
5.1	PREFACE	85
5.2	ABSTRACT.....	86
5.3	GOAL OF THE STUDY.....	86
5.4	MATERIALS AND METHODS.....	87
5.4.1	Materials.....	87
5.4.2	Single-Round AZT-MP Excision Assays.....	88
5.4.3	Assay for RT RNase H Activity.....	88
5.4.4	RT Polymerization Products Formed Under Continuous DNA Polymerization Conditions.....	89
5.5	RESULTS AND DISCUSSION.....	89
5.5.1	N348I Rescues the Excision Phenotype on RNA Templates.....	90
5.5.2	N348I Decreases RNase H Cleavage Alone and When Combine with Antagonistic Mutations.....	92
5.5.3	N348I in HIV-1 RT Also Compensates for the Antagonism of K70R by L74V and M184V.....	97
6.0	CHAPTER FOUR: SUBUNIT-SPECIFIC MUTATIONAL ANALYSIS OF RESIDUE N348 IN HIV-1 REVERSE TRANSCRIPTASE.....	100
6.1	PREFACE	100
6.2	ABSTRACT.....	101
6.3	GOAL OF THE STUDY.....	102

6.4	MATERIALS AND METHODS	103
6.4.1	Materials	103
6.4.2	Cloning, Expression and Purification of Recombinant HIV-1 RT	103
6.4.2.1	Asn348 Mutations in Both Subunits	103
6.4.2.2	Subunit-Specific Mutagenesis	104
6.4.3	Recombinant Enzyme Characterization	104
6.4.4	Evaluation of RT Polymerization Products Formed Under Continuous DNA Polymerization Conditions	105
6.5	RESULTS AND DISCUSSION	106
6.5.1	Comparison of Polymerization Activity.	107
6.5.2	Evaluation of RNase H activity	108
6.5.3	Analysis of RT Polymerization Under Continuous DNA Polymerization Conditions in the Presence of AZT-TP	111
6.5.4	Nevirapine Resistance of Recombinant Mutant HIV-1 RTs	112
7.0	CONCLUSIONS AND FUTURE DIRECTIONS	115
7.1	SUMMARY OF PROJECT	115
7.1.1	Mechanisms of Synergy Between NRTIs and NNRTIs	117
7.1.2	Mechanisms by Which HIV-1 RT is able to Circumvent Combination Therapy	120
7.2	PUBLIC HEALTH SIGNIFICANCE	124
7.3	FUTURE DIRECTIONS	126
7.3.1	Mechanism(s) by which NNRTIs inhibit RT and reverse transcription	126

7.3.2 More questions about N348I and the connection between decreased RNase H activity and NNRTI-resistance.	127
7.3.3 Resistance Mutations in Non-subtype B.....	128
BIBLIOGRAPHY	130

LIST OF TABLES

Table 1. Select clinically relevant drug resistance mutations	38
Table 2. Inhibitory and binding constants determined for NNRTIs using various assay systems	52
Table 3. Efficiency of energy transfer (E) and distances (r) calculated.....	84

LIST OF FIGURES

Figure 1. The human immunodeficiency virus structure.....	3
Figure 2. HIV-1 life cycle.....	5
Figure 3. HIV-1 reverse transcriptase.....	8
Figure 4. Pre- and post-translocation states of HIV-1 RT during processive DNA synthesis.....	10
Figure 5. Modes of RNase H cleavage during reverse transcription.....	15
Figure 6. Reverse Transcription.....	17
Figure 7. FDA-approved reverse transcriptase inhibitors.....	24
Figure 8. Mechanism of inhibition by zidovudine.....	27
Figure 9. HIV-1 RT containing nevirapine bound in the NNRTI-BP.....	31
Figure 10. Location of N348I in HIV-1 RT complexed with RNA/DNA T/P.....	47
Figure 11. HIV-1 RT RNase H cleavage in the presence of efavirenz.....	50
Figure 12. Inhibition of RT-mediated AZT-TP incorporation and AZT-MP excision on RNA/DNA and DNA/DNA T/P by efavirenz.....	63
Figure 13. Efavirenz accelerates HIV-1 RT RNase H activity.....	66
Figure 14. Ability of HIV-1 RT to incorporate or excise AZT on RNA/DNA T/P with decreasing duplex lengths.....	69
Figure 15. Mobility gel shift assays to assess RT-T/P interactions.....	70
Figure 16. Characterization of modified recombinant RT function.....	79

Figure 17. Fluorescence spectra for donor dye AlexaFluro555 and acceptor dye AlexaFluor647.	81
Figure 18. FRET analysis of RT-AF555 bound to a AF-647 labeled T/P in the absence and presence of 1 μ M efavirenz.....	83
Figure 19. Model depicting effect of efavirenz on T/P association.....	84
Figure 20. ATP-mediated AZT-MP excision activity of HIV-1 RT on RNA/DNA and DNA/DNA T/Ps.....	91
Figure 21. RNase H cleavage activity of HIV-1 RT that occurs during the AZT-MP excision reaction.....	94
Figure 22. Autoradiogram of steady-state DNA synthesis by WT and mutant HIV-1 RT in the presence of AZT-TP and 3 mM ATP	96
Figure 23. AZT-MP excision activities of WT and mutant HIV-1 RT on an RNA/DNA T/P.....	98
Figure 24. RNase H cleavage during ATP-mediated AZT-MP excision by WT and mutant HIV-1 RT.	99
Figure 25. Molecular models of the β 14- β 15 loop in the p51 subunit of HIV-1 RT in complex with an RNA/DNA duplex that extends into the RNase H active site.....	107
Figure 26. Polymerase activity of Asn348 mutants.....	108
Figure 27. RNase H cleavage activity of WT and N348 mutant HIV-1 RT.....	110
Figure 28. DNA synthesis by WT and mutant HIV-1 RT in the presence of AZT-TP and 3 mM ATP.....	112
Figure 29. Nevirapine resistance of WT and N348 HIV-1 RTs.	113
Figure 30. N348I confers NNRTI resistance by favoring a polymerase-competent binding mode.	124

1.0 INTRODUCTION

1.1 HUMAN IMMUNODEFICIENCY VIRUS

1.1.1 HIV-1 Origin

Four independent interspecies crossover events of simian immunodeficiency virus (SIV) have shown to be the origin of the human immunodeficiency virus type 1 (HIV-1) pandemic in humans [1]. Phylogenetic relationships have indicated that HIV type 1 and type 2 arose from the closely related SIV-infected chimpanzees (*Pan troglodytes troglodytes*) and sooty mangabeys (*Cercocebus atys*), respectively. The evolution of HIV-1 led to four distinct phylogenetic groups termed M (main), O (outlier), N (non-M, non-O) and P (putative) [1-2]. The origins of group M can be traced back to chimpanzees in Cameroon while group O seems to be prevalent in gorillas (*Gorilla gorilla*) in the same region [3]. The origins of groups N and P are still unknown.

HIV-1, the causative agent of acquired immunodeficiency syndrome (AIDS), has a high replication rate, producing 10^9 to 10^{10} virions per day, and a high mutation rate, approximately 1.4×10^{-5} per nucleotide base per cycle of replication, resulting in extreme heterogeneity and a very complex pattern of evolution within the host [4]. These genotypically related viruses within one host comprise a quasispecies [5]. As a result, three of the four groups have diverged into numerous subtypes since the early 1900s [6]. Group M, being the most widespread, has expanded into nine subtypes including A-D, F-H, J and K. Phylogenetic analyses have shown that overall these subtypes have 70-90% sequence similarity (diversity is 20-30% in *env*, 15-22%

in *gag* and 15% in *pol*) [7]. Subtypes A-D are responsible for 90% of today's current pandemic, with subtype B being most prominent in the industrialized world (12% of worldwide infections) and subtype C being the most prevalent overall (50% of world-wide infections) [7]. Additionally, at least 21 subtype circulating recombinant forms (CRFs) have been identified [8].

1.1.2 HIV-1 Structure

HIV-1 is a lentivirus in the retroviridae family. As with other viruses in this family, HIV-1 has an outer layer derived from its host cell plasma membrane which can contain up to 200 copies of the envelope glycoprotein (gp160). In its native form on the surface of a virion, the envelope is a heterotrimer consisting of three gp120 molecules and three gp41 molecules. The gp120 and gp41 molecules interact through non-covalent interactions [9]. The gp120 molecule binds to the receptors on the target cells while gp41 is involved in fusion. In a mature virion, just below the surface of the outer shell, is a layer of matrix (MA, p17) followed by a cone-shaped core formed from capsid (CA, p24), which protects the innermost contents of the virion, and the p6 protein (Fig. 1). The content of the core includes two copies of the RNA genome protected by a coating of nucleocapsid protein (NC). The core also contains the non-structural proteins reverse transcriptase (RT) and integrase (IN), in addition to viral protein R (Vpr), and host cell factors [10]. The protease (PR) is found within the virion but outside the core structure. The viral infectivity factor (Vif) and negative factor (Nef) accessory proteins are found closely associated with the core of the virion.

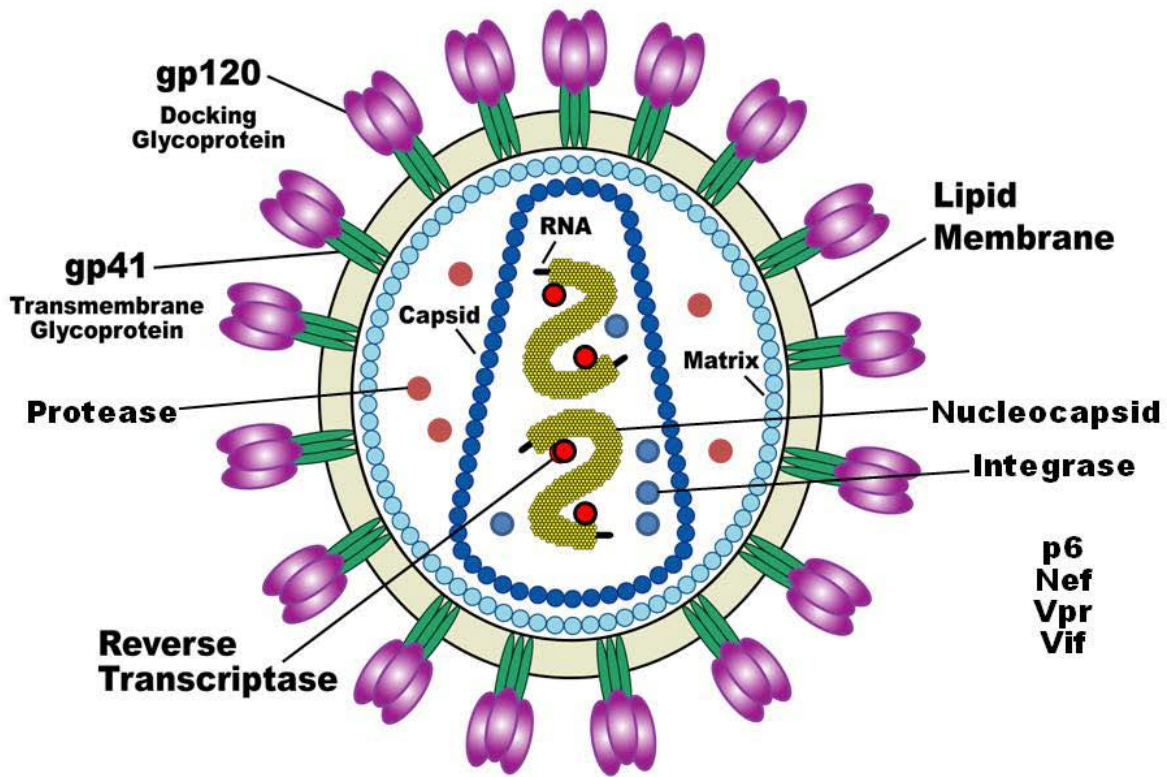


Figure 1. The human immunodeficiency virus structure.

Shown are all virion components. The listed proteins are found in the virion but are not pictured. Adapted from an open source (<http://amath.colorado.edu/index.php?page=hiv-early-infection-pathogenesis-modeling>).

1.1.3 Virus Life Cycle

1.1.3.1 Binding and Fusion

Despite the fact that HIV-1 is able to infect a variety of cell types, AIDS is largely the result of depletion of CD4⁺ T cells. As mentioned above, the process of viral replication begins with the binding of gp120 to the CD4 receptor (Fig. 2, step 1), causing a structural change in both molecules and exposing the chemokine co-receptor binding site. This allows the engagement of

a chemokine receptor expressed at the cell surface, depending on the tropism of the virus. HIV-1 most commonly uses the CCR5 (R5) or CXCR4 (X4) co-receptor for viral entry and this tropism is dictated by the sequence of the V3 and V1/V2-variable regions of gp120. The hydrophobic ectodomain of the N-terminal fusion peptide, gp41, can then penetrate the cell membrane, leading to fusion of the two and allowing release of the viral core into the cytoplasm of the cell (Fig. 2, step 2).

1.1.3.2 Uncoating and Reverse Transcription

After virus entry, a process known as uncoating occurs (Fig. 2, step 3). The capsid core undergoes morphological changes in the cytoplasm, and the subunits are disassociated from the viral genome [11-12]. Proper uncoating appears to be essential for efficient HIV-1 infection and nuclear import and requires host cell factors [13-14]. For example, cyclophilin A has been shown to increase viral infectivity by its interaction with capsid during uncoating [15]. Conversely, host factors present in certain mammalian cell types cause restrictions to infection at the step of uncoating [16].

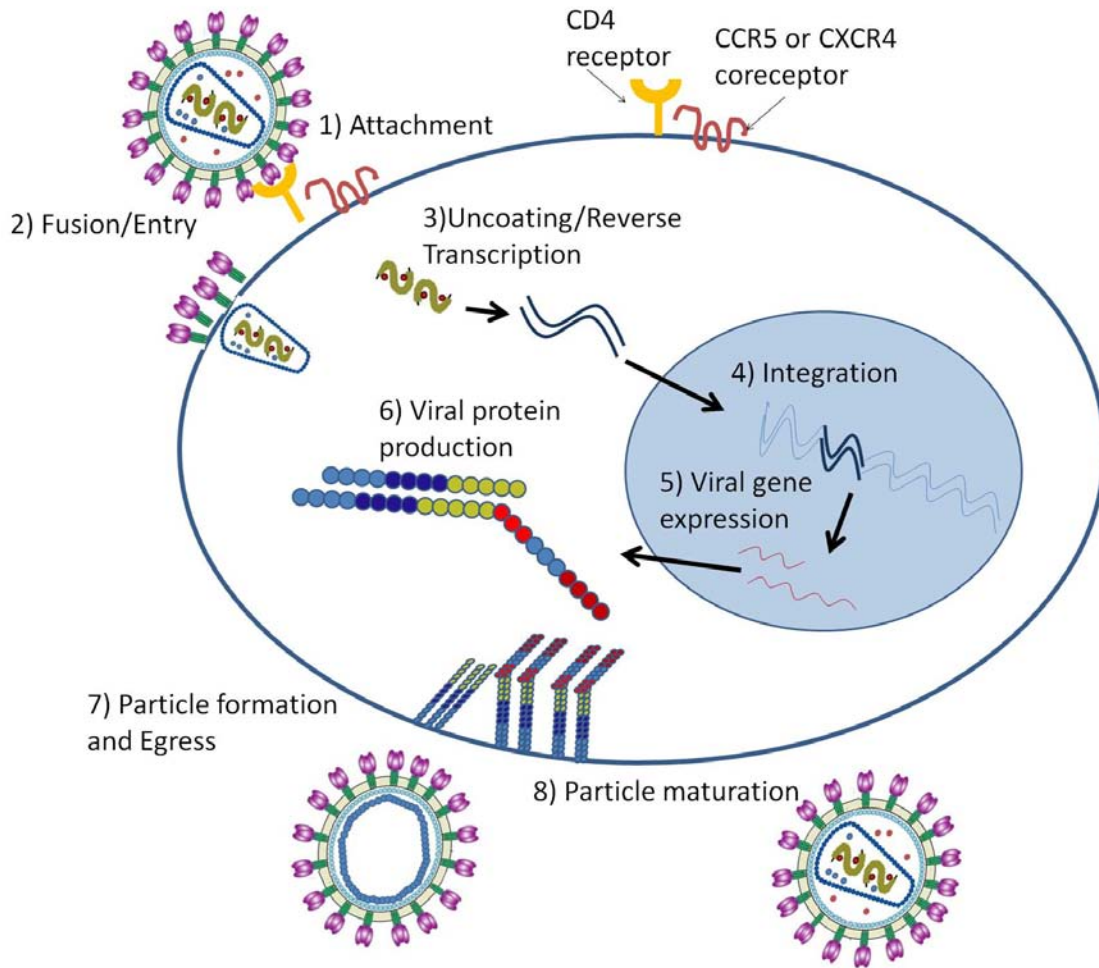


Figure 2. HIV-1 life cycle.

The HIV-1 life cycle begins with virus attachment to the host cell receptors (step 1). The virus envelope then fuses with the host cell membrane to allow entry of the viral contents into the cytoplasm (step 2). Uncoating and reverse transcription occur in the cytoplasm (step 3) and then the cDNA is imported into the nucleus. The viral cDNA is integrated into the host genome (step 4) and the viral RNA is produced by the cellular machinery (step 5). Translation in the cytoplasm is also performed by the cellular components (step 6) and the viral polyproteins assemble at the cell surface. Immature particles bud from the cell (step 7) and as the viral polyproteins are cleaved by the viral protease, the virion matures and becomes infectious (step 8).

Reverse transcription is the process whereby the single-stranded plus-sense RNA genome is converted to double-stranded cDNA for integration into the host genome. Despite a lack of

detailed understanding of the timing of initiation of reverse transcription, evidence suggests it is coupled with uncoating [17]. At some point between viral entry into the host cell and completion of viral cDNA, reverse transcription complexes (RTCs) are formed. The association of RT, viral RNA (vRNA) and the tRNA^{Lys3}, the minimal components of the RTC, is thought to occur in the virion prior to fusion with the host cell [18]. Live cell imaging of HIV-1 through the labeling of Vpr and IN suggests that, once in the target cell, the RTC associates with the cytoskeleton [19]. Recent studies done with fluorescence microscopy have shown that the RTC is attached to the microtubules and is actin-dependent, but the viral proteins that interact with the host cell transport machinery are unknown [20]. This association seems to require CA subunits, but is shed early, suggesting that the formation of the RTC during the first few hours of infection is likely due to the acquisition of host cell factors, of which, 51 individual proteins have been identified [21]. It is believed that the process of reverse transcription is completed as the RTC travels along the cytoskeleton from the distal regions of the cell, to the nucleus. Once the double-stranded viral DNA is complete (the details of reverse transcription will be described further in a later section), the RTC becomes integration competent and is then termed the preintegration complex (PIC) [22].

The lines separating the steps in the virus life cycle between host cell entry and cDNA integration are blurred by the inability of researchers to purify the undisturbed RTC from an infected cell [23]. As a result, the interdependence of uncoating and reverse transcription remains a mystery. It has recently been shown that reverse transcription can occur in an intact core structure prior to uncoating [24].

Reverse Transcriptase

In 1975, Howard Temin, David Baltimore, and Renato Dulbecco shared the Nobel Prize for Physiology or Medicine for the discovery of the viral enzyme RT. This enzyme is found in a variety of virus classes and retrotransposons. It has also been invaluable to molecular biology by allowing the development of new, more sensitive techniques. HIV-1 RT (Fig. 3) was first characterized by Rey *et. al.*[25] and was found to have various activities including DNA-dependent DNA polymerization (DDDP), RNA-dependent DNA polymerization (RDDP) and ribonuclease H (RNase H) activity. These studies also found that RT was responsible for catalyzing the conversion of RNA to DNA by way of a Mg^{+} as a divalent cation. It was later discovered that active HIV-1 RT exists as a heterodimer of two subunits, p66 and p51, formed by the proteolytic cleavage of a 15 kDa segment of the carboxyl terminus of the p66 subunit [26].

The p66 subunit of RT contains three domains: the polymerase, RNase H and connection domains [27]. The connection domain (residues 322-440) serves as a bridge between the polymerase (residues 1-321) and RNase H domains (residues 441-560) and plays a key role in dimerization of the two subunits [28]. The polymerase domain has three subdomains that contribute to the catalytic activity: fingers, palm and thumb. Between the fingers and thumb, along the palm, lies the temple/primer (T/P) binding cleft, which extends through the connection and RNase H domains. The cleft allows the nucleic acid strand to bind to the enzyme and exposes the 3' hydroxyl end of the primer to the catalytic triad (Asp110, 185 and 186), part of the highly conserved YMDD motif found in RNA-dependent DNA polymerases. Binary [29] and tertiary [30] structures revealed conformational changes that occur in the enzyme during active polymerization. The thumb domain is known to be flexible and, upon T/P binding, will close around the nucleic acid complex through conformational changes. Binding of a

deoxyribonucleic acid triphosphate (dNTP) causes many changes in the structure of RT, including rotation of the thumb domain and a clamping motion of the fingers.

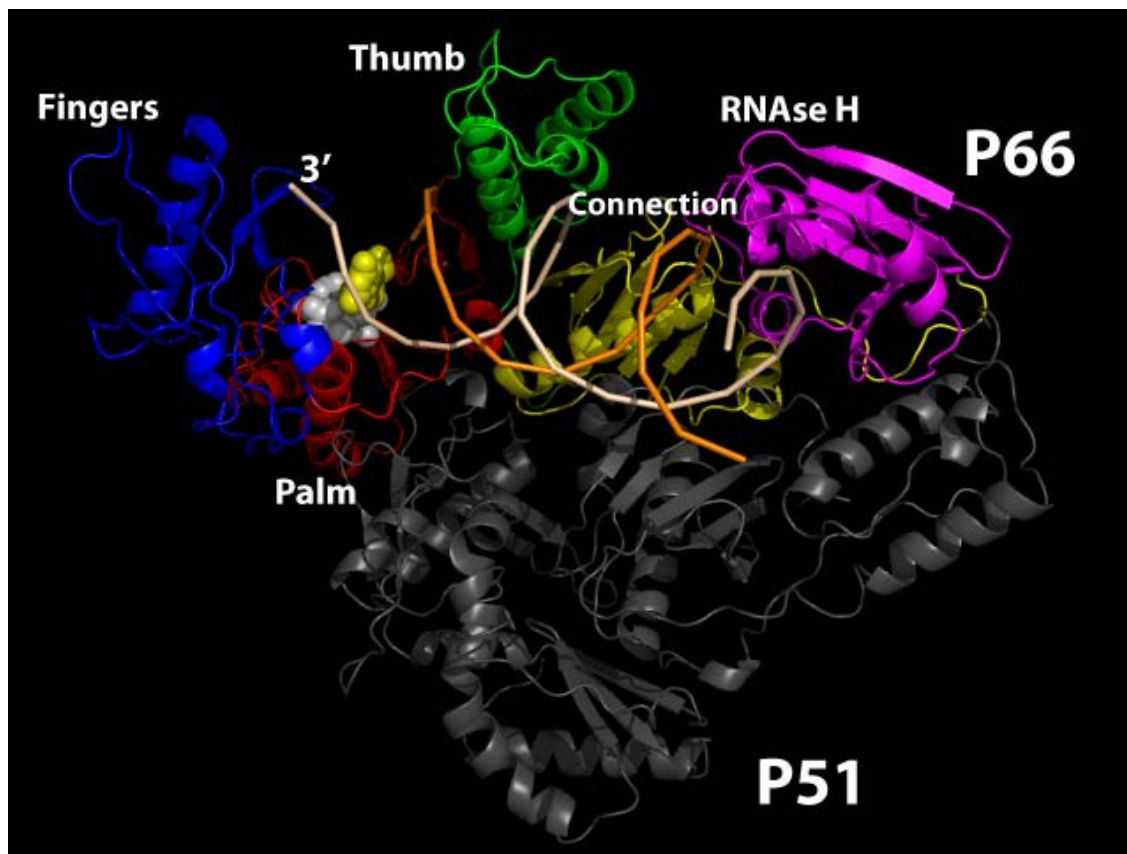


Figure 3. HIV-1 reverse transcriptase.

The ternary complex of HIV-1 RT shown is based on the crystal structure 1RTD [30]. The p51 subunit is shown in gray. The polymerase subdomains, fingers (blue), palm (red) and thumb (green), are shown. The connection (yellow) and RNase H (purple) domains of the p66 subunit are also shown. The double stranded DNA template (yellow) and primer (orange) is situated in the binding cleft, and the incoming dNTP (yellow spacefill) is shown in the active site. Residues that make up the polymerase active site are shown in white spacefill (D110, D185 and D186) Image reproduced from a publically available source; <http://hivdb.stanford.edu/pages/3DStructures/rt.html>

RT requires a T/P to which it will bind with the primer or product site (P-site) of the palm subdomain over the 3'-OH group (Fig. 4A), forming the binary complex. This causes the thumb

subdomain to transition from a closed to an open position. Next, the incoming nucleotide binds in the nucleotide binding site (N-site), forming the ternary complex (Fig. 4B). The final association of the dNTP to RT-T/P seems to be a two-step process [31]. During the first interaction hydrogen bonds are formed between K65 and the γ -phosphate of the incoming dNTP, between R72 and the α -phosphate and β -phosphate, and between Q151 and the sugar 3'-OH [30]. The secondary stage requires a conformational change in the enzyme and brings the next correct dNTP into proper alignment for catalysis [32]. The α -phosphate of the dNTP and the 3'OH of the primer then become properly aligned for nucleophilic attack by the transitioning of the fingers from an open to a closed conformation. This conformational change is the rate-limiting step of polymerization and requires complementarity between the incoming dNTP and the template. The formation of a new phosphodiester bond, facilitated by the presence of Mg^{+} , leads to the exclusion of pyrophosphate which exits the active site with the opening of the fingers (Fig. 4C). Processive DNA synthesis then requires RT to translocate to position the newly formed free 3'OH group in the P-site (Fig. 4D).

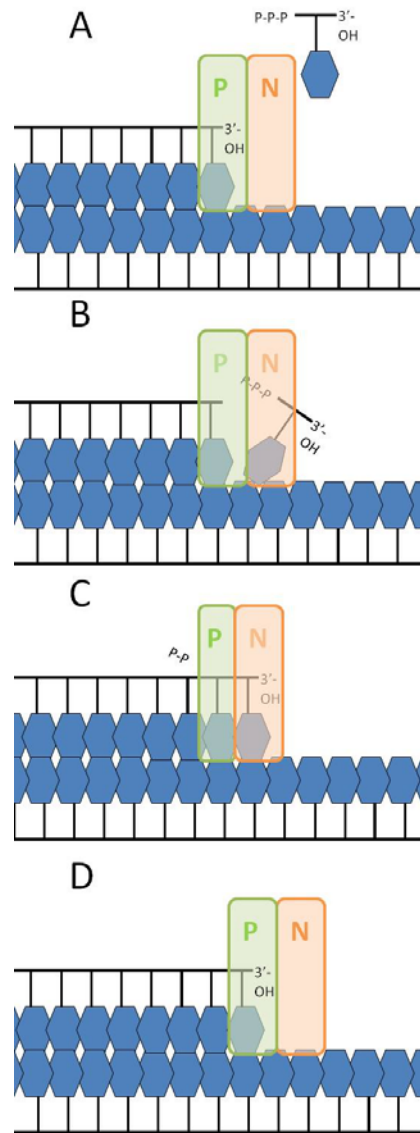


Figure 4. Pre- and post-translocation states of HIV-1 RT during processive DNA synthesis.

A, After association with the T/P, RT positions such that the primer or product site (P-site) contains the last nucleic acid added in the nascent DNA chain. B, The next complementary nucleotide then binds in the nucleotide binding site (N-site). C, Catalysis occurs, forming a new phosphodiester bond and extending the DNA primer by one base. At this point, RT is in the pre-translocation state. Binding of the next complementary nucleotide requires loss of the PP_i molecule from the product complex. D, The enzyme must translocate a single position further downstream to clear the nucleotide (N) binding site. This brings the 3'-end of the primer to the P-site referred to as the post-translocation state.

RT-associated RNase H activity

There are two types of RNase H enzymes and, although they share an overall fold, they differ in active site configuration and substrate preference. RNase H1 (activity found in HIV-1 RT) is found in a variety of organisms including prokaryotes and eukaryotes. It is a non-specific endonuclease – in regard to specific nucleotide sequence composition - which catalyzes the cleavage of RNA by a hydrolytic mechanism. All eukaryotic RNase H1 have highly conserved regions at their N- and C-termini separated by a variable sequence. Although the cellular and retroviral RNase H enzymes share similar structures and modes of action, their substrate binding structure within the active site provides grounds for designing specific inhibitors [33].

The HIV-1 RT RNase H active site is composed of four residues (D443, Q478, D498 and D549) and the RNase H primer grip, a network of six amino acids (T473, I505, K476, Q475, Y501, R448, N474 and Q500), which contact the DNA primer strand and/or the RNA template. The active site resides ~18 base pairs upstream of the polymerase active site and is more than 60Å away in space. Because it cleaves in such a way that leaves a 3'-OH and a 5'-PO₄, the RNA strand left annealed to the DNA is able to function as a primer for subsequent DNA synthesis. As with the polymerase activity, Mg⁺ is required for RNase H hydrolysis. Although there is no strict sequence requirement, there does seem to be specificity, possibly with regard to T/P secondary structure, RT-T/P interactions and the dimensions of the minor groove [34]. Additionally, mutational analyses suggest that the residues that contact the primer strand of the hybrid through the RNase H primer grip are more valuable than those that contact the template itself [35].

Several studies have demonstrated interdependence between the polymerase and RNase H domains. Both the polymerase and RNase H domains of the RT molecule contact the T/P

simultaneously and both contribute to proper positioning and binding to the nucleic acids [36]. The polymerase domain is required for efficient substrate binding and cleavage by the RNase H domain [37]. Despite this, it is believed that the two activities are not strictly coupled. The rate of polymerization is 7-10 times faster than that of the RNase H domain [31] and RNA molecules can be cleaved in the absence of polymerization [38]. Conversely an enzyme with a nonfunctional RNase H domain, still has polymerase activity, albeit attenuated [39]. Although it is not known whether RT has the ability to simultaneously incorporate dNTPs while cleavage is occurring, biochemical studies performed with the inhibitor foscarnet, a pyrophosphate analog, suggest that both active sites can be engaged concurrently [40].

Steps of Reverse Transcription

Formation of minus strong stop DNA

Once in the target cell, RDDP is initiated from the 3'-end of the annealed tRNA^{Lys3} primer. Like many other polymerases, RT requires a primer for initiation of polymerization. The tRNA anneals to a specific 18-nucleotide sequence within the vRNA termed the primer binding site (PBS) and forms a highly structured scaffold for the association of RT [41]. This annealing is facilitated in the producer cell by the interaction of NC [42]. Polymerization from this primer region towards the 5'-end of the genome generates a DNA intermediate termed minus-strand strong-stop DNA (-sssDNA, Fig, 6, step 1).

First Strand Transfer

During polymerization, RNase H-mediated degradation of the RNA template from the -sssDNA allows it to anneal to the complementary R region on the 3'-end of the RNA genome. This can be an inter- or intramolecular occurrence and is known as the first strand transfer event [43]. It is

facilitated by NC protein [44], genome dimerization [45], and RNA secondary structure [46], allowing minus strand synthesis to continue from the 3' end of the genome back to the PBS region (Fig. 6, step 2). The result of this strand transfer event is the formation of the direct repeats flanking the genome (long terminal repeats or LTRs).

There are three different prevailing models to describe the first strand transfer event. In the “forced copy choice” model, a break in the RNA genome induces the transfer to the other co-packaged RNA molecule based on homology [47]. The “copy choice” model relies on pausing or stalling of RT during synthesis as a driving force for template switching [48]. Finally, “dynamic copy choice” model dictates that both the polymerase and RNase H activity dictate the efficiency of strand transfer [49]. Data supporting this model include the observation that decreased dNTP concentrations or mutations in the dNTP binding pocket in RT that decreased affinity resulted in a high recombination efficiency. Additionally, mutations in the RNase H domain of RT that decreased cleavage caused a slower rate of template switching. There are also three mechanisms by which strand transfer can occur. All three rely heavily on the functioning of the RNase H domain. In each case, RNase H cleavage allows removal of the template RNA strand to allow for homologous recombination. An RNase H-deficient RT fails to perform the strand transfer reaction, reinforcing the necessity of the function [49].

Two distinct modes of RNase H cleavage have been described during reverse transcription: 3'-end-directed (polymerase-dependent) and 5'-end-directed (a form of polymerase-dependent) cleavage. When the enzyme is bound under polymerization conditions, such as during active minus-strand elongation, the polymerase active site is positioned over the 3' end of the growing DNA strand while RNA hydrolysis is occurring at the opposite end of the enzyme in an incomplete and irregular manner based on enzyme pausing and T/P structure (Fig.

5A). It has been observed that as the pausing of RT increases, the RNase H cleavage events increase as well. Because there are 50-100 RT molecules and only two RNA templates to process, the excess RT is thought to degrade the remaining bound RNA segments annealed to the nascent minus-strand DNA [50]. This occurs through a mode of polymerase-independent cleavage where the polymerase active site binds on the DNA opposite the 5'-end of the RNA. This positioning results in internal cleavage events ~18 bases away from the 5'-end of the RNA (Fig. 5B) which are also dependent on T/P sequence and structure [51]. The RNase H activity of RT is also responsible for the precise removal [52-53] of the tRNA^{Lys3} and PPT primers during reverse transcription. The final positioning of RT on the T/P is a result of the nature of the T/P as well as the cellular milieu (i.e., absence or presence of dNTPS and/or inhibitors) [54]. Some have suggested that the main mode of RNase H cleavage during this process is polymerase-dependent and the polymerase-independent mode plays only a minor role [55]. However, studies using an RNase H-deficient RT coupled with *Escherichia coli* RNase H (supplying the polymerase-independent cuts) was able to perform strand transfer efficiently [56].

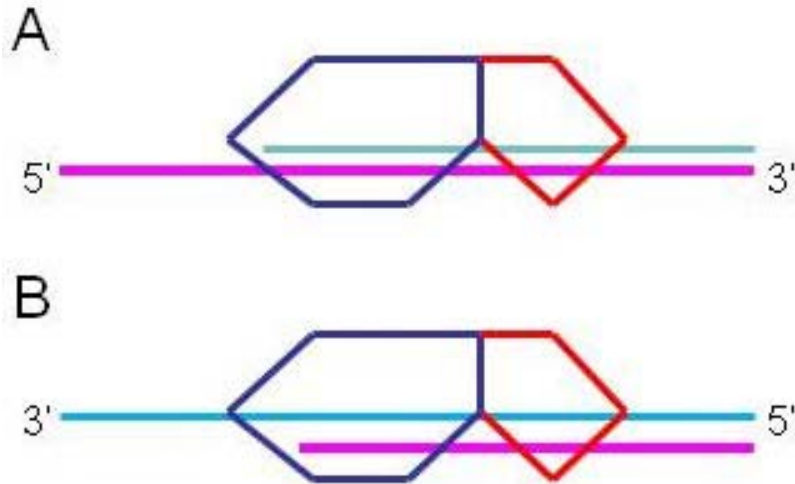


Figure 5. Modes of RNase H cleavage during reverse transcription.

A, During RDDP, RT binds with the polymerase domain (dark blue) positioned over the 3' end of the growing DNA strand (light blue). This is termed polymerase-dependent or 3' end directed cleavage. B, To removed fragments of RNA (pink) annealed to the nascent DNA strand after completion of minus strand synthesis, free RT molecules can bind with the polymerase domain over the 5' end of the RNA. This is termed 5' end directed cleavage.

Completion of minus strand DNA

At pausing events during continued minus strand synthesis, the RNA genome is degraded by the RNase H activity of the RT. Two regions, known as the polypurine tract (PPT) and the central polypurine tract (cPPT), are protected from this degradation by mispairing of bases. This allows at least a short stretch of RNA to remain annealed to the newly synthesized cDNA to act as a primer for plus strand synthesis. DDDP begins from this point and continues through the retained tRNA^{Lys3} primer.

Second Strand Transfer

After using the tRNA primer as a template for the PBS region of the plus strand, synthesis terminates. At this point, the RNase H of the RT molecule removes the tRNA primer, leaving a

short single-strand cDNA complementary to the PBS sequence at the 3'-end of the extended minus strand. RT cleaves the tRNA primer leaving the last two nucleotides behind, allowing for efficient integration later. Using complementarity and NC, these ends anneal and plus strand synthesis resumes, engaging the 3'-end of the newly synthesized minus strand template. This constitutes the second strand transfer event and allows plus strand synthesis to continue in a bidirectional fashion (Fig. 6, step 3). This event is largely intramolecular [43]. Completion of integration-competent DNA requires displacement synthesis in order to achieve the full LTRs on each end of the viral DNA (Fig. 6, step 4).

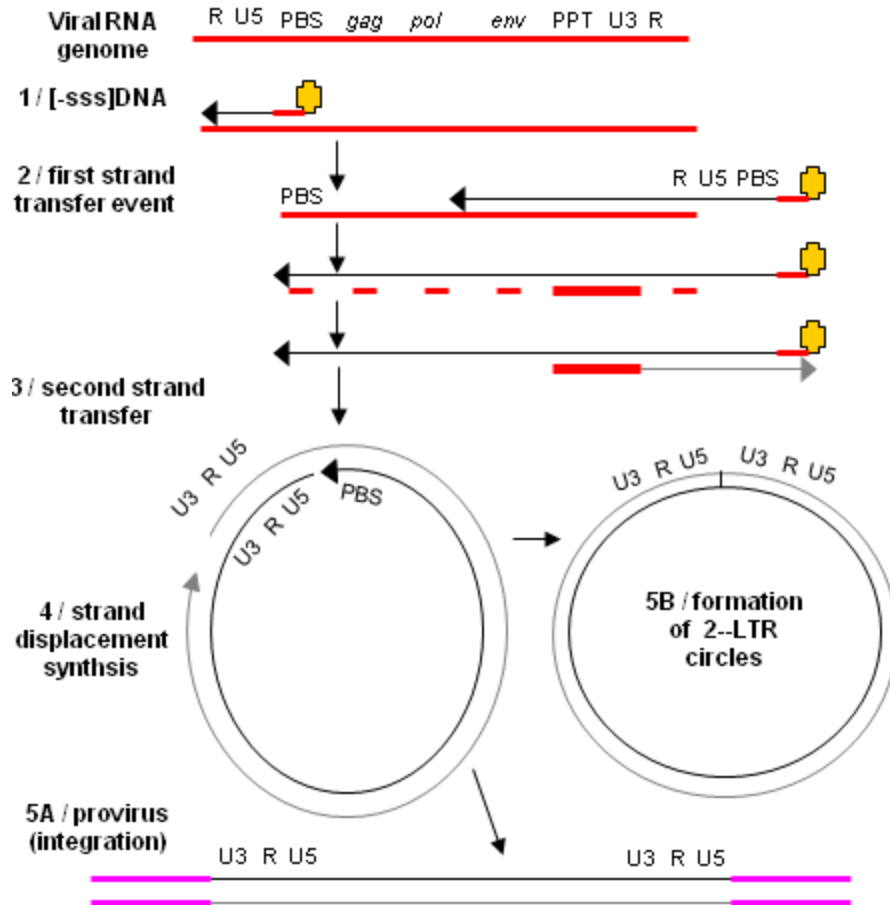


Figure 6. Reverse Transcription.

Reverse transcription begins from the annealed tRNA^{Lys3} primer and RNA-dependent DNA polymerization proceeds to the 5' end of the RNA, generating the minus strand strong-stop DNA intermediate (-sssDNA, step 1). Once the template RNA is degraded, this allows the 5' end of the nascent DNA to anneal to the 3' end of the template RNA as a result of complementary R regions (first strand transfer event, step 2). Synthesis proceeds to the 5' end of the RNA while the RNase H activity of the RT incompletely degrades the template strand. Because of mismatched base pairing, the PPT region is saved from degradation and serves as the primer for plus strand synthesis. RT then begins DNA-dependent DNA polymerization towards the 5' end of the newly formed DNA strand. Once the tRNA^{Lys3} is reached, RT removes it, leaving a complementary PBS region which can now bind to the PBS region on the opposite end of the DNA strand (second strand transfer event, step 3). The genome is completed by strand displacement synthesis (step 4). The provirus is then complete and ready for integration (step 5A). A small percentage of this proviral DNA can undergo ligation in the nucleus to form 2-LTR circles (step 5B).

1.1.3.3 Integration and Viral Gene Expression

Integration

Unlike other retroviruses, HIV-1 does not have to wait for the nuclear envelope to breakdown during cell division; the PIC can be imported through the nuclear membrane [20]. In addition to its association with microtubules, other components are required for the PIC to traverse the nuclear envelope via nuclear import pathways. The accessory protein Vpr plays a controversial role in this process. Even though it alters the structure of the nuclear lamina in a manner that leads to the formation of nuclear herniations that intermittently rupture (presumably allowing PIC entry) [57], some studies have shown the nuclear import can occur in arrested cells in its absence [58]. MA has also been shown to possibly play a role in nuclear import, as it contains two weak nuclear localization signals [59], although the importance of this has been debated [60]. It is thought that cellular importins α , β and possibly γ are required to bind the nuclear localization signals present in the PIC and target them to the nucleus by docking the complexes to nuclear pore complex proteins and translocating through the pore [61-62]. Additionally, fasciculation and elongation protein zeta-1 (FEZ1), Nup98, Nup358, Nup153 and transportin 3/transportin SR-2 (tnp3) have been shown to be involved in nuclear import [63-65].

After nuclear entry, the irreversible process of integration is mediated by IN. HIV-1 has a preference for integration into actively expressed genes [66] however integration in resting T-cells has been shown to be in suboptimal locations [67]. Host factors have been shown to play a role. For example, integrase binding protein lens epithelium-derived growth factor (LEDGF/p75) has been shown to tether the PIC to the host cell's genome [68]. Additionally,

SWI/SNF chromatin-remodeling [69] or DNA-repair [70] complexes and Polycomb-group proteins [71] have also been shown to interact with integrase.

Two reactions are required to integrate the viral DNA into the host genome. First, IN binds to the LTR at each end of the viral DNA and catalyzes the removal of two nucleotides from the 3'-end, leaving a C-A with a free 3'-OH group. This process is known as endonucleotide cleavage or 3'-processing. This can happen in the cytoplasm of the cell, directly after the production of cDNA [72]. Next, IN binds to both ends of the viral DNA simultaneously with an offset of five base pairs between the two opposite points of insertion. IN uses that free OH group to carry out nucleophilic attacks that result in cuts in the host genome, a process known as strand transfer [72]. Finally, the host cell DNA repair enzymes join the viral cDNA and cellular genome after extra nucleotides are trimmed from the 5'-end [73] and integration is complete (Fig. 2, step 4).

Viral gene expression.

The HIV-1 genome contains 9.8 kilobases (kb) of genetic information for the expression of nineteen proteins spread out across nine gene sequences. From 5' to 3', the HIV-1 genome contains the *gag* (group-specific antigen), *pol* (polymerase) and *env* (envelope) open reading frames (ORFs). Expression of these is regulated by a number of structural components within the RNA genome. Many *cis*-acting elements, both host- and virus-derived, bind to the proviral LTRs which contain the U3, R and U5 regions. This repeated sequence flanks the functional genes of the HIV genome and acts like a viral promoter containing a number of *cis*-acting elements, most found in the 5' U3 region. It contains binding sites for cellular factors such as nuclear factor kappa B (NFκB), CAT-box enhancer binding proteins, positive transcription

elongation factor b (P-TEFb)–cyclin T complex and nuclear factor of activated T cells (NFAT) [74], as well as viral factors including Tat and Vpr.

There are two phases of HIV gene expression. During the early phase of gene expression, the local genome microenvironment is responsible for the level of viral gene expression. Production of Tat, a very potent virus-derived *trans*-activator, allows the recruitment of P-TEFb to the trans-activation response element (TAR), a stem-loop structure present at the 5' end of the RNA. In the second phase of viral gene expression, the presence of Tat allows for hyperphosphorylation and, therefore, activation of RNA polymerase II, which in turn facilitates high levels of processive transcription [75].

Both full length and subgenomic RNA molecules are produced to serve as genomic RNA (to be packaged into nascent virions) and mRNA (to be translated into viral proteins), respectively (Fig. 2, step 5). Fully spliced early transcripts are exported from the nucleus by the cellular machinery and translated in the cytoplasm. Rev, an early protein, is imported into the nucleus where it binds to the *rev* response element (RRE) on unspliced and single-spliced RNA (i. e. *env*, *vpu*, *vif* and *vpr*) to facilitate their export [76].

The production of viral genes is also regulated at the level of translation through a programmed -1 ribosomal frameshift (PRF). Both Gag (Pr55) and Gag-Pol (Pr160) are translated from full-length vRNA (Fig. 2, step 6) using the same start codon but different ORFs [77]. The *pol* ORF is out-of-frame in reference to the *gag* ORF and, therefore, requires a frameshift for translation. The mechanism is thought to occur as a result of a translocation ribosome pausing over a “slippery” site as a consequence of 3' RNA structure. When this occurs and a frameshift happens, the resulting protein is the full Pr160 polyprotein. If there is no frameshift event, the ribosome encounters a stop codon at the end of the *gag* gene and produces

the Pr55 polyprotein. In addition to the *cis*-acting elements in the viral RNA, the frequency of the frameshift is also controlled by host translational factors [78]. In this way, the production of the 160 kDa polyprotein Gag-Pol is highly regulated and is approximately 5 to 10% of the total Gag produced by the PRF [79].

1.1.3.4 Virus Assembly and Egress

HIV-1 virus particles can form at the plasma membrane and bud from the surface as immature, noninfectious virions (Fig. 2, step 7) or form intracellularly within multivesicular bodies (MVBs). The driving force behind particle assembly is the Gag polyprotein. Gag is produced and co-translationally myristoylated in the cytosol [80]. The N-terminal myristoylation works in synergy with the 31 basic amino acids present in the N-terminus of the protein (within the MA region) to allow stable association of the Gag molecules with the lipid bilayers of the plasma membrane [80]. The newly produced proteins are inserted into the membrane of MVBs and trafficked to the plasma membrane through the ESCRT machinery, a pathway important for endocytosis in mammalian cells. The Gag at the surface is found at lipid rafts in the membrane which contain high concentrations of cholesterol, glycosphingolipids and sphingomyelin [81]

As the virus buds from the cell, it matures through cleavage of its viral proteins by the virally encoded PR (Fig. 2, step 8). Cleavage is initiated by the dimerization of the Gag-Pol polyprotein, which thereby allows autoprocessing of PR to occur in a two-step process. In the initial, rate-limiting step, cleavage of the N-terminus occurs to release the intermediate, which has enzymatic activity equivalent to that of the fully mature protein [82]. The second event is the subsequent cleavage of the C-terminus to release the mature enzyme [83]. Also arising from the processing of the Pol portion of the Gag-Pol polyprotein are RT and IN, which, like PR, are required to form dimers for full activity. Subsequently, Gag is cleaved into three structural

proteins, MA, CA, and NC. Additionally, p2 and p1 spacer proteins are produced from these cleavage events in a specific series of cleavage events during maturation, inhibition of which renders the virus particles noninfectious [84-85].

1.2 THERAPEUTIC INTERVENTIONS

In the absence of an effective vaccine to prevent HIV-1 infection, patients must rely on chemotherapeutics to delay the onset of AIDS. Experiments with 3'-azidothymidine (zidovudine, AZT) first demonstrated that HIV-1 infection could be controlled by chemotherapy [86-87]. Thanks to the advancement of antiretroviral therapy (ART) during recent years, the prognosis for patients infected with HIV-1 has greatly improved. Because HIV-1 is incurable, the inhibitors must be taken for the life of the patient, which requires that the compounds be relatively nontoxic and easily administered. Although HIV-1 relies heavily on the host cell machinery for replication, specific steps in the virus life cycle have been targeted for therapeutic interventions. Currently, there are approximately thirty drugs, formulated either individually or in combination, available to physicians for the treatment of HIV-1 infected patients [86]. These inhibitors span six subclasses and inhibit various stages of the HIV-1 life cycle, including fusion, reverse transcription, integration and proteolytic cleavage (maturation).

1.2.1 Entry

As previously discussed, the initial step in the viral life cycle is attachment and entry into the host cell, which is a multi-step process that provides opportunities for drug development. In the

mid-1990s, CCR5 and CXCR4 co-receptors were identified as essential for HIV-1 entry into the CD4⁺ cell [88-90]. HIV-1-infected individuals with decreased CCR5 co-receptor expression on their CD4 cells, due to polymorphisms, had a longer period until disease progression and lower viral loads. Additionally, individuals homozygous for a null mutation on both CCR5 alleles appeared to have a strong protection against HIV-1 infection [91]. In light of these observations, co-receptor antagonists were developed for use as therapeutics. There is currently one CCR5 inhibitor which was approved by the US Food and Drug Administration (FDA) in 2007, maraviroc.

Enfuvirtide, in contrast, is a peptide-based fusion inhibitor which mimics the C-terminal domain of the gp41, thereby preventing the formation of the helical hairpin required for fusion of the virus envelope with the cellular membrane [92]. Although there is considerable variability in the efficacy of this compound against primary HIV-1 strains, a number of next-generation fusion inhibitors are being developed [93].

1.2.2 Reverse Transcription

The most heavily targeted step in the virus life cycle is reverse transcription, which comprises over 50% of the compounds approved by the US FDA to treat HIV-1 infection. The two main classes of reverse transcriptase inhibitors are NRTIs (Fig. 6A) and NNRTIs (Fig. 6B). In addition, the pyrophosphate (PP_i) analog, foscarnet (PFA) also inhibits RT but is rarely used in the clinic as a result of toxic side effects and limited bioavailability. Other RT inhibitors are under development, such as those that target RNase H activity, but many of these have limited cell uptake ability or result in high toxicity [94].

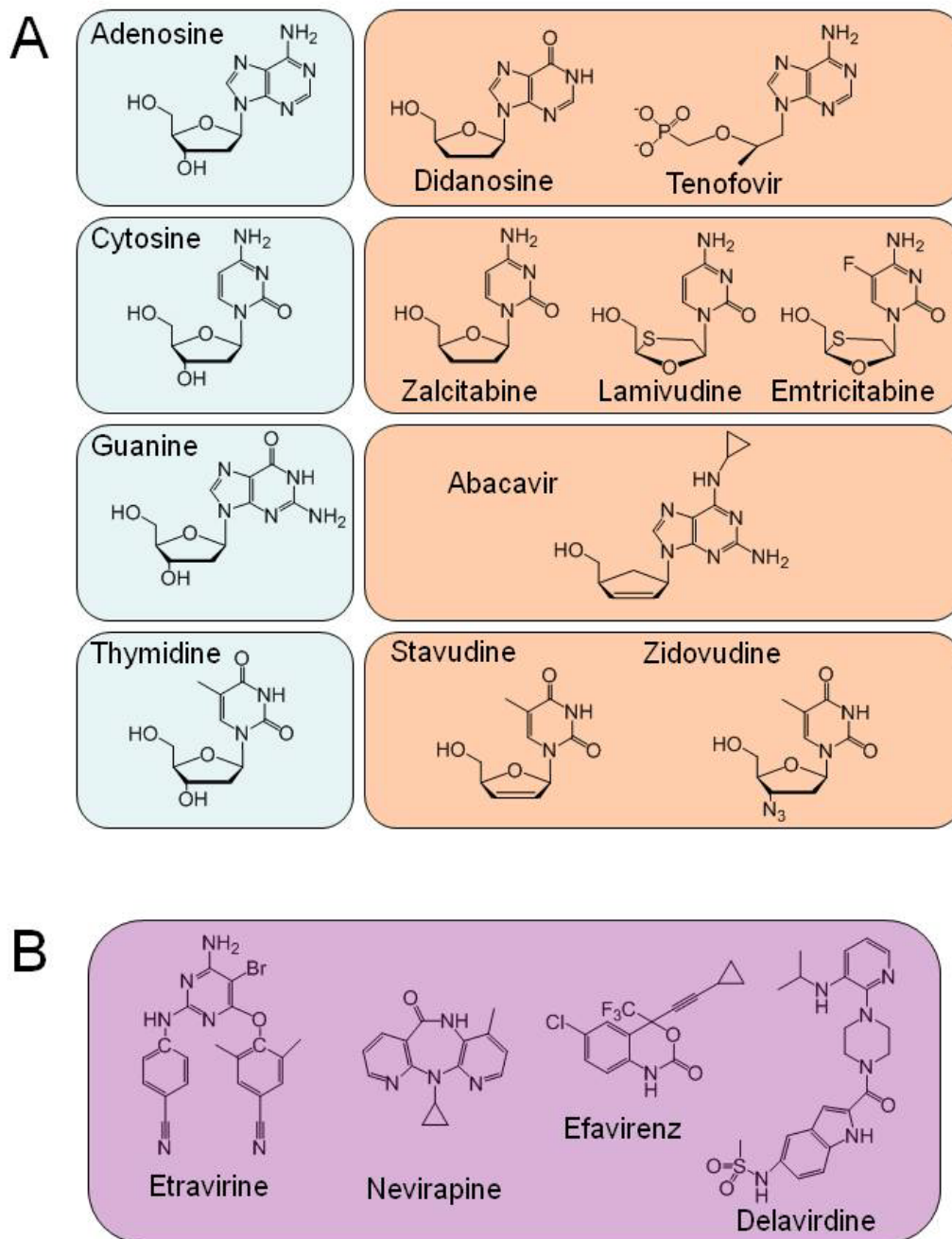


Figure 7. FDA-approved reverse transcriptase inhibitors

A, Chemical structure of nucleoside reverse transcriptase inhibitors paired with the natural nucleoside they compete with *in vivo* (NRTIs). and B, nonnucleoside reverse transcriptase inhibitors (NNRTIs).

1.2.2.1 NRTIs

NRTIs were the first compounds approved by the FDA for the treatment of HIV-1. Currently, there are eight available for treating HIV-infected individuals, although zalcitabine (ddC) is no longer used clinically. As described earlier, these compounds are analogs of naturally occurring nucleotides which lack the 3'-OH group required for catalysis during polymerization. They are inactive in their parent form and require the action of host cellular kinases and phosphotransferase to form deoxynucleoside triphosphates that can then compete with natural nucleotides for binding in the N-site of RT during polymerization [95]. Incorporation of an NRTI into the nascent viral DNA chain by RT results in termination of DNA synthesis (Fig 7). Many of the compounds approved for HIV-1 therapy were first described as anticancer therapies, years before the clinical onset of HIV.

Although these compounds are analogs of the natural substrate for DNA polymerization, there is great diversity in their structures (Fig. 7A). Two of the eight compounds, didanosine (ddI) and ddC, completely lack the 3'-OH group, while compounds such as AZT have a substituted azido group at this position. Two compounds, emtricitabine (FTC) and lamivudine (3TC), have a ribose in the L-enantiomer form. Most of the active, metabolized compounds have natural purine or pyrimidine base structures, with the exception of FTC. Despite their structural diversity, these compounds are able to mimic the structural contacts made by natural dNTPs in the N-site of the RT during polymerization and therefore can be efficiently incorporated into the nascent DNA strand during reverse transcription. Unfortunately, not all of the NRTIs make good substrates for the cellular kinases and require high levels in the bloodstream to be effective HIV inhibitors [96].

These compounds have their advantages and disadvantage. Unfortunately, because the compounds are designed to mimic the natural dNTP substrate for polymerization, they have a significant level of toxicity due to their incorporation during cellular DNA polymerization. For example, AZT is limited by its toxic effects to bone marrow cells, manifested as anemia and neutropenia [97]. Mitochondria are particularly sensitive to toxicity because of the compartmentalization of nucleoside/nucleotide phosphorylating enzymes and the inability of the mitochondrial DNA polymerase γ to distinguish between dNTPs and NRTIs [98-100]. However, one major advantage of NRTIs is their intracellular persistence, which allows for more constant viral inhibition.

Zidovudine (AZT)

AZT was the first inhibitor available to combat HIV-1. Although it was first described in the literature as an anticancer drug in 1964 [101], it was found to inhibit HIV-1 in 1985 [87] and approved by the FDA in 1987. This compound (3'-azido-3'-deoxythymidine) contains an azido group instead of the 3'-OH. As a result, polymerization is terminated upon incorporation (Fig. 7). This compound selects resistance mutations termed thymidine analog mutations (TAMs) which includes M41L, D67N, K70R, L210W, T215F/Y and K219Q/E. It also selects for Q151M which allows RT to discriminate between this compound and the natural dNTP in association with A62V, V75I, F77L and F116Y. Interestingly, HIV-2 does not acquire resistance to AZT via TAMs, rather it typically gains the Q151 mutation [102].

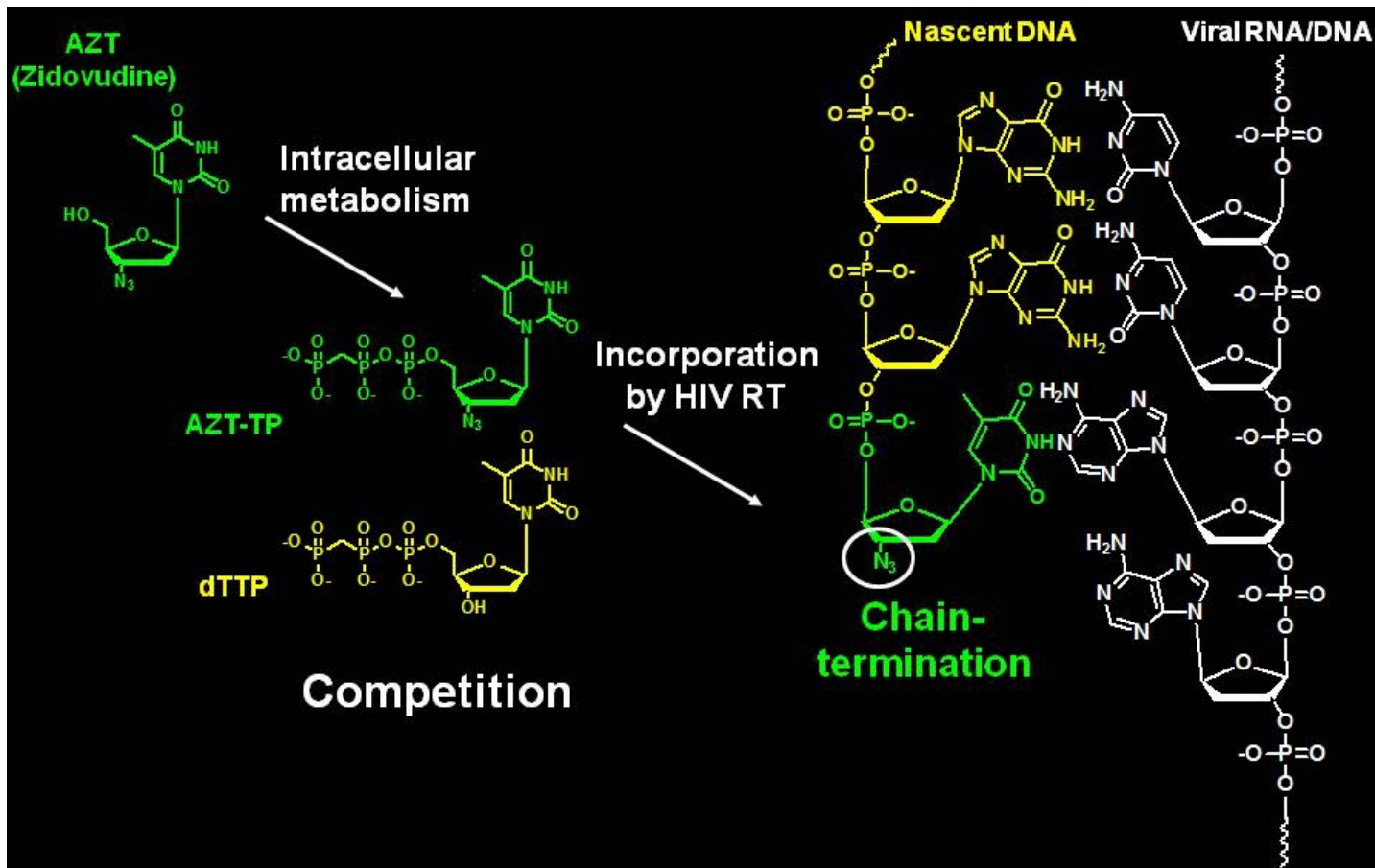


Figure 8. Mechanism of inhibition by zidovudine.

After phosphorylation by cellular kinases, zidovudine (and other NRTIs) compete with natural dNTPs for incorporation by RT into the growing nascent DNA strand. Once incorporated, polymerization stops due to the lack of 3'-OH group on the NRTI. In the case of zidovudine, the 3'-OH group has been replaced with an azido group.

Didanosine (ddI)

Approved in 1991, ddI (2', 3'-dideoxyinosine) is metabolized in the host to the active compound dideoxyadenosine 5'-triphosphate (ddATP). Earlier studies investigating 2',3'-dideoxyadenosine (ddA) as a potential drug found that it was metabolized into 2,8-dihydroxyadenosine, a nephrotoxic compound [103]. Additionally, oral administration was not an option for the compound because it was degraded by the acidity in the stomach [103]. Treatment with ddI leads to resistance through the L74V and/or K65R mutations. Although use of this compound has declined, it is still used as an alternative choice for first-line therapy in the US and is predominantly used as first-line therapy in the developing world as a result of its low manufacturing costs [104].

Stavudine (d4T)

The d4T (2',3'-didehydro-2',3'-dideoxythymidine) compound was already described in the literature as a potential anticancer agent when it was found to inhibit HIV-1 RT [105]. Although it turned out to be less potent than some NRTIs such as AZT, it had a far better safety profile in humans and animals [106]. Treatment with d4T selects for TAMs and V75I.

Tenofovir (TFV)

Tenofovir (*R*-9-(2-phosphonomethoxypropyl)adenine) was first described in 1993 [107]. Since its approval by the FDA in 2001, its prodrug, tenofovir disoproxil fumarate, has become one of the most frequently prescribed RTIs [104]. TNF was also the first inhibitor used in post-exposure prophylaxis [108]. In cells, the phosphorylated compound selects for K65R and K70E.

Abacavir (ABC)

Abacavir, a carbocyclic '2 -deoxyguanosine nucleoside, was approved by the FDA in 1998. Since this time, it has been used to simplify treatment because of its dosing flexibility. Abacavir can be prescribed either once daily or twice daily to match the dosing patterns of other regimen components, and its availability in fixed-dose combination (FDC) tablets containing lamivudine or lamivudine plus zidovudine has allowed regimens with low pill counts. It is metabolized to carbovir triphosphate and competes with dGTP for incorporation in the nascent DNA strand [109]. Analyses using peripheral blood mononuclear cells (PBMCs) demonstrated that abacavir is significantly more potent than ddI and as effective as AZT [110]. This compound selects for combinations of K65R, L74V and M184V.

Lamivudine (3TC)

Lamivudine was the first L-nucleoside analogue developed for the treatment of HIV-1 and was approved for use in 1995 [111]. It is a highly effective agent that can be dosed once or twice daily due to its long intracellular half-life. It also has one of the best tolerability and long-term safety profiles among all antiretroviral agents and continues to be preferred as part of initial or subsequent combination therapy in HIV-infected patients. Like FTC, it has the ability to delay resistance to AZT or resensitize AZT-experienced patients. Additionally, like FTC, the M184V/I mutations lead to resistance.

Emtricitabine (FTC)

Emtricitabine, the (-)-enantiomer of 2,3' -dideoxy-5-fluoro-3'-thiacytidine, in combination with other inhibitors, is indicated for treatment of HIV-1-infected adults in the US. Structurally, emtricitabine is a fluorinated derivative of lamivudine. This structural alteration increases the

binding affinity for RT and enhances the antiviral activity of emtricitabine relative to that of lamivudine [112]. In addition, by decreasing binding affinity for DNA polymerase γ , the potential for mitochondrial toxicity was reduced as compared to the original compound [112]. Because the two compounds are structurally related, FTC-resistant isolates are cross-resistant to lamivudine. Most often the M184V/I mutations are observed, however the K65R mutation also reduces susceptibility [113].

1.2.2.2 NNRTIs

Although there are NNRTIs at various stages in clinical development, currently there are only four approved for use in the United States: efavirenz, nevirapine, delavirdine and etravirine (Fig. 7B). Chemically, NNRTIs are small compounds, structurally distinct from NRTIs that do not require cellular metabolism. Functionally, NNRTIs are highly specific allosteric inhibitors of HIV-1 RT, which bind to a hydrophobic pocket in the palm domain of the p66 subunit of RT, approximately 10Å away from the polymerase catalytic site of the enzyme [27].

When crystal structures of RT in complex with these inhibitors became available, the location and composition of the NNRTI-binding pocket (NNRTI-BP, Fig. 9) was revealed [27, 114]. It is formed by 16 amino acids from p66 and 2 residues from p51 and, despite a vast array of NNRTI chemical structures, crystal structures reveal similar binding for many NNRTIs in the pocket. From these studies, it is known that the binding of NNRTIs cause local distortions in RT within the NNRTI-BP as well as long-range alterations in the overall enzyme structure. The pocket is located 10-15Å from the polymerase active site and in both the apo (or unliganded) and substrate-bound RT structure, the NNRTI-BP is occluded by the Y181 and Y188 side chains indicating that this binding region is closed in the absence of drug [27]. When an NNRTI binds to RT, residues Y181 and Y188 in the palm domain rotate and are displaced, creating the

NNRTI-BP [115]. The residues which form the walls of the pocket include L100, V109 and L234. The front of the pocket includes K101, K103, P225, P236 and Y318. More than 30 structurally distinct classes of compounds have proven to bind to this pocket and inhibit polymerization [116].

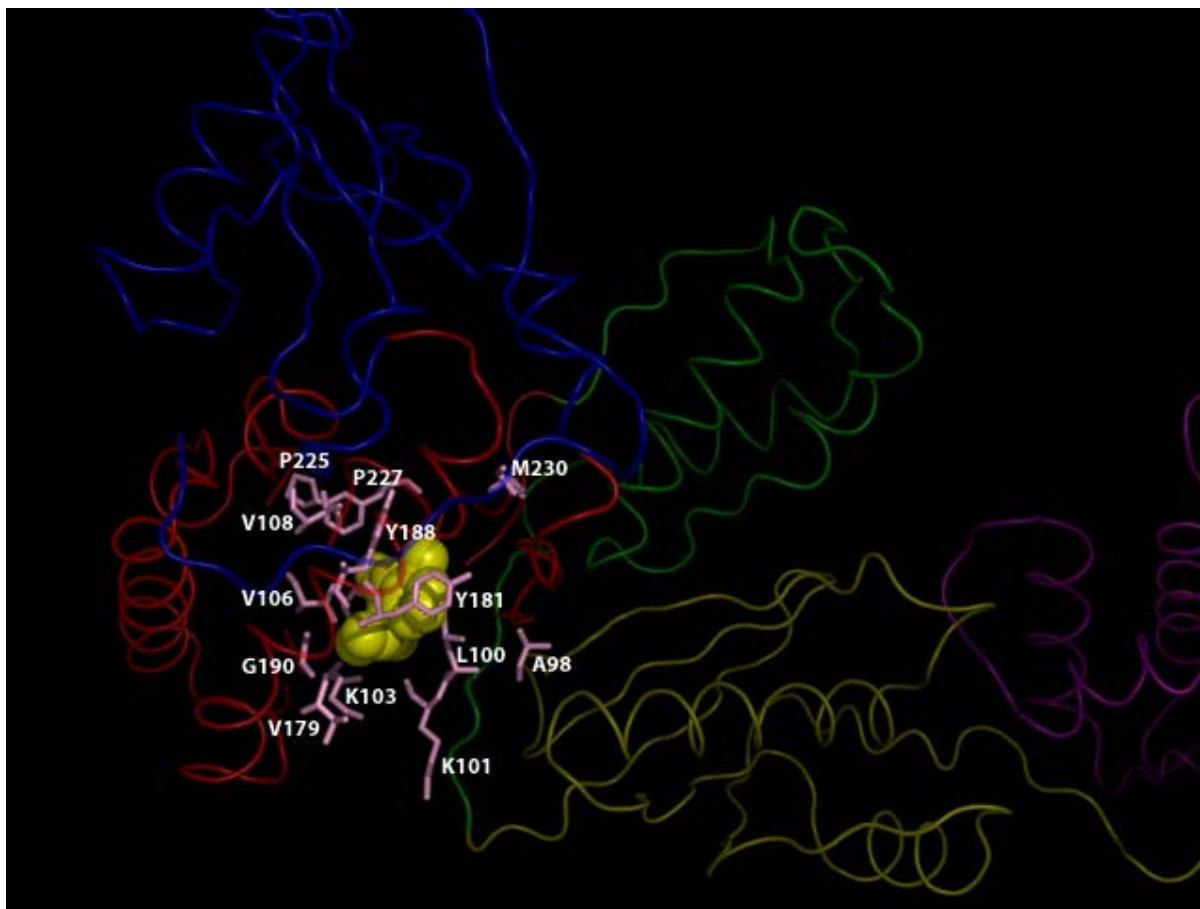


Figure 9. HIV-1 RT containing nevirapine bound in the NNRTI-BP.

The amino acid positions associated with NNRTI resistance that make up the central NNRTI binding pocket are shown: L100, K101, K103, V106, V108, V179, Y181, Y188, G190, F227. Additional positions that make up the pocket include E138 in the p51 subunit is not pictured. Residues M230, L234, P236, K238, and L318 form part of an extended pocket. The fingers (blue), palm (red) and thumb (thumb) subdomains are shown. Also the connection (yellow) and RNase H (purple) domains are pictured. (Image reproduced from a publically available source; <http://hivdb.stanford.edu/pages/3DStructures/rt.html>)

When DNA is bound to RT, most structural changes occur in the fingers and thumb domain, while the primer grip region is stationary. When an inhibitor is bound (NNRTI), significant distortion is noticeable in the catalytic triad as well as the primer grip region, suggesting a mechanism of inhibition. Based on this structural evidence, it has been suggested that polymerization is decreased because the highly conserved YMDD motif is altered and the primer grip region, responsible for positioning the T/P for catalysis, is perturbed [117]. During polymerization in the absence of an inhibitor, the $\beta 9$ - $\beta 10$ loop which contains the YMDD motif flexes and moves downward by 2Å to bind the dNTP and the metal ions [118]. When NNRTIs are present, the loop is fixed in the up position, resisting the conformational change [119]. This observation has been bolstered by biochemical evidence suggesting that the chemical process of phosphodiester bond formation is not slowed by the NNRTI but rather by the rate limiting step of conformational change [120].

Interestingly, it has been demonstrated that some NNRTIs can abrogate initiation from the PPT primer under conditions that do not inhibit minus strand elongation and that the binding of the drug may cause RT to favor one binding mode over another [121]. Recently, single-molecule fluorescence resonance energy transfer (FRET) assays have determined that the binding of nevirapine causes a destabilization of the RT-T/P complex and leads to enzyme reorientation on its substrate, specifically at the PPT region [54, 122]. This could explain why NNRTIs preferentially inhibit plus strand synthesis, decrease initiation from the PPT primer, and possibly enhance the enzyme's ability to remove the PPT primer.

Delavirdine (U-90152, Rescriptor®)

As with many NNRTIs, this compound exhibits low toxicity, due to its relative lack of inhibition of human DNA polymerases [123]. It was first described in the literature in 1993 [123] but is

rarely used today as a result of its inconvenient dosing schedule and low potency as compared to other NNRTIs such as efavirenz. It is significantly bulky and protrudes from the binding pocket [124]. It forms a hydrogen bond with the lysine at position 103 in the binding pocket and is further stabilized through hydrophobic interactions with the proline at position 236. Therefore, the most common resistance mutations seen are K103N and P236L. Additionally, Y181C is seen in therapy, which confers resistance to nearly all NNRTIs.

Nevirapine (BI-RG-587, Viramune®)

Nevirapine was first developed in 1990 [125]. Nevirapine in combination with 2 NRTIs is the recommended first-line therapy in resource-limited countries. It is also often used to prevent mother-to-child transmission in developing countries, however this has been shown to lead to resistance in the mother and affect future treatment outcomes [126]. The most commonly seen resistance mutation to nevirapine is Y181C, but substitutions at positions 103, 106, 108, 188 and 190 are often observed [127].

Efavirenz (DMP-266, Sustiva™, Stocrin™)

Efavirenz was first described in the literature in 1995 [128]. Although it is more potent than nevirapine or delaviradine, it is considered teratogenic and is contraindicated in women who are pregnant or wish to become so [129]. The most commonly selected resistance mutation is K103N, but many others were observed during clinical trials [130]. Efavirenz has been shown to greatly enhance enzyme heterodimerization, resulting in changes in molecular flexibility, which may result in effects on the later stages of viral replication such as premature Gag-Pol processing [131-133]. Efavirenz has also been shown to increase homodimerization, which may lead to

enhanced processing as a result of increased oligomerizing of the Gag-Pol polyprotein. Currently, efavirenz is the most used NNRTI in treatment-naïve patients [134].

Etravirine (TMC-125, Intelence™)

The most recent addition to the list of FDA-approved NNRTIs is etravirine. It was approved for use in 2008 and is known to be active against RTs that have resistance to other currently available NNRTIs [135]. This is a result of torsional flexibility in the molecule, which allows for various binding conformations within the NNRTI-BP [135]. Resistance can be achieved when multiple mutations are present, but the exact resistance profile of etravirine is not known because it has not been studied in treatment-naïve individuals.

1.2.3 Integration

Raltegravir is a strand transfer inhibitor which blocks the joining of the processed viral DNA ends with the host chromosome and was the first of its kind on the market in 2007. Importantly, the compound is active against drug resistant strains of HIV-1 and is considered to be additive or synergistic with current treatments [136]. Resistance to this compound has been observed and cross-resistance has been noted with investigational integrase inhibitors [137]. An early crystal structure of the catalytic core of IN revealed the similarities between it and nucleotidyl strand transferases, a recent crystal structure of the prototype foamy virus in complex with viral DNA may serve as an appropriate proxy for the study of HIV-1 IN inhibitors [138].

1.2.4 Maturation

Protease inhibitors were the second class (following NRTIs) to be introduced in the market in 1995, beginning the era of highly active antiretroviral therapy (HAART), or the therapeutic approach to viral inhibition using combinations of inhibitors. These inhibitors were also the product of structure-based drug design which employs the current knowledge of the target structure [139]. Currently there are 10 protease inhibitors on the market, all of which are competitive inhibitors binding at the active site of protease. Because they all interact with the same hydrophobic pockets on the enzyme, accumulation of only a few resistance mutations can lead to resistance to this class of inhibitors [140].

1.2.5 Combination Therapy

HIV-1 inhibitors are given in combination for two main reasons: (1) using drug combinations has proven to delay the onset of resistance (which will be discussed in a later section) and (2) some inhibitor combinations were determined to act in a synergistic fashion. The success of a multidrug regimen in the clinic is dependent not only on pharmacokinetic and pharmacodynamic parameters but also on any effect that the compounds may have on each other at the enzymatic and cellular levels. For this reason, a number of studies have focused on the synergy or antagonism of drug combinations.

Synergy was first noted between AZT and ddI [141]. Since this time, a number of studies have demonstrated synergy between NRTIs [142-143] as well as NRTIs in combination with NNRTIs at the cellular level [144-146]. A mechanism for synergy at the enzyme level between NRTIs and NNRTIs has been described. Excision is one of the two main mechanisms of

resistance to NRTIs and will be discussed in detail in a later section (Section 1.3.1.2). Briefly, after the incorporation of a terminating nucleoside, excision allows RT to use cellular ATP to perform the reverse reaction and remove the NRTI. The bound NNRTI negatively affects both affinity of ATP for RT and the rate of the chemical step in the excision reaction [147] decreasing NRTI removal. Additionally, synergy can be the result of NNRTI-mediated stable complex formation prolonging and enhancing the chain-termination effects of NRTIs possibly as a result of the enzyme “flipping” that can occur at the PPT region when NNRTIs are bound [54].

Importantly, studies have also determined that some compounds, when given in combination, act in an antagonistic fashion. This is especially true for specific combinations of NRTIs. For example, it has been well described in cell-based and enzyme-based studies that AZT combined with d4T is less efficacious than either compound alone. This is believed to be a result of the antagonistic effect that the combination has on the cellular thymidine kinase [148]. This was also found to be true in clinical studies where patients responded better to monotherapy than the combination of the two [149]. Some treatment combinations also lead to high levels of toxicity. For example in initial studies, ddI and d4T demonstrated good antiviral activity and was well tolerated. However, upon further analysis, this combination was associated with a significant increased risk of lactic acidosis, peripheral neuropathy, pancreatitis, lipodystrophy, and hepatitis, all believed to result from mitochondrial toxicity [150-151].

1.2.5.1 Current Recommendations

Since their inception, NRTIs are considered to be the backbone of HIV-1 therapeutic strategies. The current Adult and Adolescent Antiretroviral Treatment Guidelines (published by the US Department of Health and Human Services and the International AIDS Society–USA Panel) for first-line therapy consists of 2 NRTIs (preferably tenofovir and FTC) in combination with either

1) a protease inhibitor (either atazanavir, darunavir, fosamprenavir, or lopinavir) boosted with low-dose ritonavir, 2) an NNRTI (usually efavirenz) or, more recently, 3) an integrase inhibitor [152-153]. To increase adherence and decrease the pill burden for patients, combination therapies have been condensed into single pills including: AZT/3TC (Combivir), AZT/ABC/3TC (Trizivir), ABC/3TC (Epzicom), TDF/FTC (Truvada) and TDF/FTC/efavirenz (Atripla). In the case of treatment experienced patients, more and more physicians are relying on genotyping to determine the best clinical combination. As will be discussed in the next section, resistance mutations that are present in a virus population <1% can affect treatment outcomes [154].

1.3 HIV-1 RESISTANCE TO RT INHIBITORS

Despite the increased drug availability and decreased mortality rate as a result of fewer infection complications, a major hurdle yet to be scaled is antiretroviral resistance. The development of resistant variants is an issue for all HIV-1 inhibitors. HIV-1 RT is error prone and the errors that arise during the viral life cycle, together with the rapid replication of the virus in patients, allow the virus to escape the host immune system and develop resistance to antiretroviral drugs. In the milieu of low drug concentrations, which allows low levels of viral replication, drug resistant variants are rapidly selected.

Complete inhibition of viral replication stops the development of resistance. A combination of drugs (usually three) and absolute drug adherence on the part of the patient is required to completely block viral replication. Unfortunately, drug resistance is not only a problem for treated HIV+ individuals, but it affects untreated infected and uninfected people as well. The rate of transmission of antiretroviral drug resistant virus has risen during the past

decade. Estimates suggest that 3.4-26% of treatment-naïve patients already have resistance to at least one class of inhibitor [155]. Table 1 lists examples of resistance mutations in the polymerase and connection domain of HIV-1 RT that confer resistance to NRTIs and NNRTIs by different mechanisms.

Table 1. Select clinically relevant drug resistance mutations.

Mutation(s)	Domain of RT	Confers Resistance	Mechanism
K65R	polymerase	ddC, ddI, 3TC, TDF	Discrimination; Decreased K_{pol}
K70R	polymerase	AZT	Excision
L74V	polymerase	ddI, ddC	Decreased K_{pol}
K103N	polymerase	EFV, NEV	Increased K_D
Q151M	polymerase	multiple	Discrimination
Y181C	polymerase	NEV	Increased K_D
M184V/I	polymerase	3TC	Discrimination; Increased K_D
Y318F	connection	DEL, NEV	?
G333D/E*	connection	AZT/3TC	T/P binding
N348I*	connection	AZT/NEV	Excision; Indirect Effect
A360I/V*	connection	AZT	Excision; Indirect Effect

*indicates that mutation is typically found with other resistance mutations to confer high level drug resistance.

1.3.1 Nucleoside Reverse Transcriptase Inhibitors (NRTIs)

There are two main mechanisms for NRTI resistance at the enzyme level: discrimination and excision. By definition, discrimination dictates that RT can acquire mutations which allow it to preferentially bind the natural dNTP over the analogue. With most compounds, usually only one residue change is required for this phenomenon. Discrimination can occur by two mechanisms: decreased binding affinity of the compound for the active site of RT (increased K_D) or decreased

incorporation of the compound into the nascent strand of DNA (decreased k_{pol}). Mutations that allow RT to discriminate include K65R, K70E, L74V, Q151M and M184V. In the case of excision, RT acquires mutations that allow it to remove the chain-terminating nucleoside from the end of the primer. These mutations are collectively referred to as thymidine analog mutations or TAMs (because they primarily develop under AZT or d4T drug pressure) and include M41L, D67N, K70R, L210W, T215F/Y and K219Q/E.

1.3.1.1 Discrimination Phenotype

Discrimination involves the acquisition of one or more mutations that improve the ability of RT to discriminate between the natural dNTP and the NRTI-TP. This typically results in decreased catalytic efficiency of NRTI-TP incorporation. The catalytic efficiency is driven by two factors: the affinity of the nucleotide for RT (K_D) and the rate of nucleotide incorporation (k_{pol}). Typically, discrimination is achieved by the effect of the mutation on one of these two parameters.

Residues in and around the RT polymerase active site dictate resistance as a result of their role in polymerization. The K65 residue resides in the $\beta 3$ - $\beta 4$ loop of the fingers subdomain of RT. Crystal structures reveal that this residue interacts with the γ -phosphate of the incoming dNTP [30]. As a result, the K65R mutation distorts optimal positioning of the NRTI-TP in the active site, which reduces the catalytic efficiency of incorporation. This mutation confers resistance to all FDA-approved NRTIs with the exception of AZT [156]. Similarly, molecular modeling suggests that residue L74 makes van der Waals contacts with the nucleotide base of the incoming dNTP. The resistance mutation L74V can cause loss of stabilizing interaction that leads to a base rotation indirectly affecting the position of the phosphates of the incoming ddNTP [157]. This causes resistance to NRTIs such as ddI, ABC and ddC [158].

Discrimination can also occur by steric hindrance (increased K_D). For example, the M184V mutation causes high-level resistance to 3TC and FTC. This residue forms part of the highly conserved YMDD motif. Ternary crystal structures of M184V RT reveal that this residue contacts both the dNTP and the 3'-end of the primer terminus and suggests steric hindrance between the oxathiolane ring of 3TC-TP and the branched side chain of the residue [29]. This affects both the initial binding and the catalysis of the compound resulting in resistance [159]. Additionally, as a result of this effect, the presence of the M184V mutation causes a decrease in viral fitness [160].

1.3.1.2 Excision Phenotype.

The major mechanism of resistance to AZT is excision [161]. This typically requires more than one residue change for RT to acquire high levels of resistance. After the observation that many AZT resistance mutations clustered around the dNTP binding pocket, it was demonstrated that these mutations increased the rate of phospholytic removal of the chain-terminating NRTI from the end of the primer, a process termed excision [162-163]. A variety of mutation combinations can lead to this phenotype, however they often appear in a distinct order where K70R is the earliest and most frequent TAM to arise. Additionally, RTs harboring these mutations tend to be more processive and associate more tightly to the AZT-terminated primer [164-165]. These mutations can also confer high-level resistance to ABC, d4T, ddI, ddC and TFV [166].

The excision reaction is dependent on the terminating NRTI residing in the N-site of the RT active site. The presence of the next correct nucleotide can push RT in an orientation such that the NRTI is located in the P-site, in which excision is prevented. This is referred to as “dead-end complex” (DEC) formation because RT is unable to polymerase as a result of the

incorporated NRTI and is unable to excise the compound due to its position [167]. Biochemical analyses have suggested multiple mechanisms for increased excision as a result of TAMs, including increased binding affinity for ATP [168], increased rate of NRTI removal [169], decreased sensitivity to DEC formation [162], and a shift in the equilibrium between N- and P-sites where the N-site is favored [170].

A number of factors influence the ability of a terminating nucleoside to be excised, including the base structure of the NRTI [171]. Other NRTIs can be excised, albeit not as efficiently as AZT-MP. Some reports suggest that the excision of TFV can be as efficient as AZT [172]. Additionally, the azido group is not the primary determining factor for excision. 3'-azido-ddC, and -ddU are also efficiently removed from the end of a terminated primer by RT harboring TAMs. The removal rates for 3'-azido-ddA and -ddG were greatly reduced as compared to the previous [171].

The sequence and nature of the template (RNA or DNA) can also influence the efficiency of NRTI removal. Excision and resumption of DNA synthesis occurs with similar rate constants on both DNA and RNA, however, the amount of terminating nucleoside removed on the RNA template is half what was seen on the DNA template, suggesting that excision on RNA and DNA is not equivalent. Additionally, the RT containing TAMs was unable to excise a terminating nucleoside during initiation of minus-strand synthesis [173-174]. This suggests that efficacy of TAMs varies during different stages of the production of viral DNA.

Additionally, the RNase H domain of RT has recently been suggested to play a role in excision. As described earlier, decreased RNase H activity leads to decreased template switching and an increased time period available for nucleoside excision. This is supported by the observation that mutations that decrease RNase H activity also increase resistance to AZT

[175]. More specifically, mutations at positions within the RNase H primer grip region were shown to increase AZT resistance in the presence of TAMs [176].

1.3.2 Nonnucleoside Reverse Transcriptase Inhibitors (NNRTIs)

Although NNRTI-based therapy is an attractive therapeutic option based on superior virologic outcomes, lower pill burden and less toxicity than the protease inhibitor regimen [177], the low genetic barrier to resistance is of concern. As with the NRTIs, NNRTI resistance emerges as a result of many reasons, including non-adherence. Unlike the other classes of inhibitors mentioned, these compounds all bind in the same location, the NNRTI-BP, resulting in a single mutation that can lead to reduced susceptibility to the entire class of NNRTIs [178]. Primary NNRTI resistance mutations are the most prevalent and their rate in the infected population continues to rise [177]. Currently, 6.9% of patients who are screened have at least one NNRTI resistance mutation [177].

The described mechanism of resistance to NNRTIs results in a loss of interaction between the inhibitor and the binding pocket. Decreased association can occur for a variety of reasons, such as a loss of interaction between the compound and the binding pocket or steric hindrance [118]. Loss of interaction can happen by alteration of key hydrophobic residues, causing a loss of aromatic ring interactions with changes such as Y181C [27]. Steric hindrance between the pocket and the compound can also occur with mutations in the central region. Alterations at G190 can cause a “bulge” in the pocket, preventing inhibitor association [179]. Certain changes in the outer rim of the pocket can also prevent drug from entering the pocket. In the case of K103N, an additional network of hydrogen bonds is formed that keeps the NNRTI-BP closed [180]. Because NNRTIs such as nevirapine and delaviradine have little flexibility in

the NNRTI-BP, they make similar side chain interactions and, therefore, cross-resistance occurs. Loss of aromatic interaction between the side chains of Y181 and Y188 in RT and some NNRTIs is thought to be the main mechanism of resistance [181].

The development of novel NNRTIs is underway. New generation NNRTIs such as etravirine (recently approved) and rilpivirine (in late stage clinical trials) do not rely on interactions with Y181 and Y188 like the earlier compounds [182]. Instead, because these compounds have flexibility between their aromatic rings, they have flexible binding orientations in the pocket and have tighter interactions with W229, a residue less prone to mutation [182]. As a result, resistance to these second generation NNRTIs requires multiple mutations in the binding pocket. Unfortunately, it has been shown that patients failing first-line therapies infected with non-B subtypes may not respond to etravirine [183].

1.3.3 Antagonism Between Resistance Mutations

As mentioned earlier, one of the main reasons RT inhibitors are given in combination is to delay the onset of resistant phenotypes. This phenomenon occurs because many RT inhibitors give rise to mutational patterns which are antagonistic. This has been well described in the case of the excision phenotype where mutations such as K65R, L74V and M184V resensitize RT to AZT in the presence of TAMs. For example, AZT/3TC dual therapy gives rise to the M184V mutation but delays AZT resistance [184]. Similarly, AZT/ddI dual therapy gives rise to the AZT resistance mutation T215Y, but delays the onset of ddI resistance [185]. Additionally, it has been demonstrated that the nevirapine resistance mutation, Y181C, can resensitize the virus to AZT in the presence of TAMs [186]. This mutation is also associated with reduced ATP-dependent excision and reduced affinity of the RT-T/P binary complex for ATP [187-188]. The

cause of this may be due to an effect on ATP binding to RT and/or a decrease in the overall rate of the excision reaction [189-190]. Yet another example of antagonism is the K65R mutation. This is a discrimination mutation that confers resistance to various NRTIs including abacavir, tenofovir, d4T and ddI. Although discrimination between AZT and dTTP is increased, K65R suppresses the excision phenotype and for this reason it is not found on the same genome as TAMs [191-192]. Structurally, this could be a result of decreased flexibility of the fingers loop subdomain [193].

1.3.4 Resistance Mutations in the Connection Domain

All NRTI mutations included in the most widely used resistance tables (such as the from the International AIDS Society – USA expert panel [194]) map to the DNA polymerase domain of HIV-1 RT. As a result, genotyping has focused on the N-terminal 300 nucleotides of RT, encompassing only the polymerase domain. This standard is a result of mutational clustering around the active site and NNRTI-BP. Most research also focuses on this area as it typically correlates with the catalytic activity of the enzyme. However, strong evidence suggests that mutations outside the polymerase domain can affect inhibitor susceptibility. Kagan and colleagues analyzed mutations spanning codons 1-400 (which includes the connect domain) in over 40,000 clinical samples [195]. From this analysis, six mutations were identified that appeared more frequently in samples from ART-experienced patients as compared to naïve patients. These mutations included N348I, G359S, E370D/G and A371V. Another study performed by Galli and colleagues also examined RT between codons 240 and 400 and

compared treatment-naïve and -experienced patients [196]. In this analysis, N348I increased in prevalence from less than 1% in treatment-naïve to over 11% in treatment-experienced individuals.

A polymorphism, G333D/E, has been reported in 6% of treatment-naïve patients and increases to 12% in individuals having received NRTI therapy [197]. It has been demonstrated that this mutation facilitates resistance to both AZT and 3TC in the background of mutations that cause a loss of sensitivity to both drug [198]. Interestingly, G333 resides ~35Å from the polymerase active site of RT, at the base of the thumb subdomain, which is known to be involved in T/P interactions. Biochemical studies revealed that rather than directly affecting the ability of the RT to excise, mutations at residue 333 affect the association of RT and the AZT-terminated T/P [199].

In an effort to determine whether mutations in the C-terminal domains of RT confer inhibitor resistance, Nikolenko and colleagues performed genotypic and phenotypic analyses from 8 treatment-naïve and -experienced patients [200]. This study demonstrated that the C-terminal regions from the treatment-experienced patients did, in fact, confer AZT resistance alone and when paired with TAMs. In contrast, the same domains from treatment-naïve patients did not, reinforcing the role of N-terminal residues in drug resistance.

1.3.4.1 N348I

Recently, the N348I mutation was identified which confers resistance to both AZT and NNRTIs [201]. It is known to appear early in therapy and is highly associated with TAMs, M184V/I and NNRTI resistance mutations K103N, Y181C/I and G190A/S [201-202]. Clinically, this mutation has been associated with patients being treated with AZT and nevirapine and has been seen in small patient cohorts at a frequency of up to 40% [202] and in larger cohorts at approximately

13% frequency [201, 203]. Biochemical analysis of this mutation revealed that increased excision was only observed on RNA and not DNA templates [201]. Therefore, it was determined that a decrease in RNase H activity led to increased AZT excision. More specifically, it was found that N348I reduces the affinity of RT for the RNA/DNA substrate in the RNase H competent complex and increases processive DNA synthesis [204]. By this mechanism, the N348I mutation in combination with TAMs can increase the resistance two-fold as compared with TAMs alone [201]. However this mutation disappears in the absence of chemotherapy, which may be due to its effect on viral replication kinetics [203].

The location of this mutation in the context of the RT structure does not reveal a mechanism by which NNRTI resistance can be achieved (Fig. 10). The N348 residue lies 27Å away from the polymerase active site and 20Å or 60 Å away from the NNRTI binding pocket in the p66 or p51 subunits, respectively. This residue does lie at the base of the thumb domain, which may contribute to flexibility and T/P interactions. The mechanism by which it confers resistance to NNRTIs or the biochemical effect it has in an antagonistic background remains to be investigated.

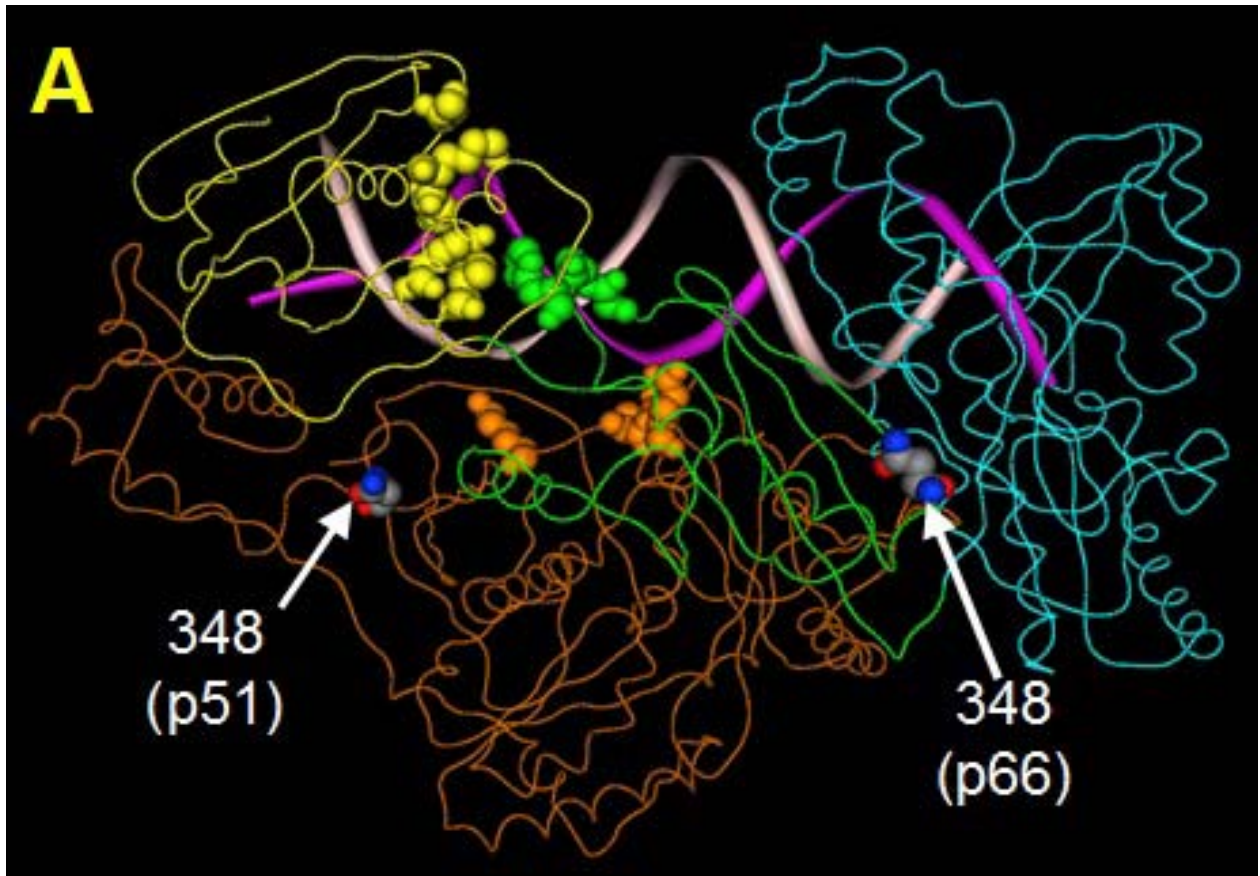


Figure 10. Location of N348I in HIV-1 RT complexed with RNA/DNA T/P.

Crystal structure of RT in complex with the polypurine tract RNA/DNA. The p66 polymerase (blue), connection (green) and RNase H domains (yellow) are shown. The p51 subunit is colored orange. The DNA and RNA strands are in white and purple, respectively. Residues in the connection and RNase H domain that form part of the nucleic acid binding tract are shown in spacefill.

1.3.5 Resistance Mutations in the RNase H Domain

Mutations in the RNase H domain were proven to decrease the frequency of RT template switching, reducing recombination, as well as confer resistance to AZT, d4T and ddi [49, 175]. Nikolenko and colleagues recently showed that a mutation that decrease RNase H activity

increase AZT and d4T resistance alone and in combination with TAMs [175]. From this observation it was hypothesized that after incorporation of a chain terminating nucleoside (i. e., AZT), there is competition between excision and RNase H activity. If cleavage of the template reduces the T/P hybrid significantly before the terminating nucleoside is removed, excision becomes impossible. Therefore, if RNase H cleavage is decreased, additional time is available for the excision reaction. However, the mutations identified in this study (D549N and H539N) have not been observed in clinical samples.

To identify additional mutations that could contribute to AZT resistance, *in vitro* selection experiments were carried out using increasing concentrations of AZT [205]. These studies identified A371V (in the connection domain) and Q509L (in the RNase H domain) that confer high-level resistance to AZT in combination with TAMs. Interestingly, these mutations also confer high-level resistance to 3TC and ABC but not d4T and ddI. Again, these mutations have not been identified in clinical samples. Whether or not codons located beyond the polymerase domain should be included in standard genotype testing is under debate [206].

2.0 SPECIFIC AIMS

2.1 BACKGROUND AND PRELIMINARY DATA

Although it is well known that NNRTIs inhibit polymerization, there is evidence to suggest that this is not the main mechanism by which reverse transcription is inhibited. The work presented here is born from observations that IC_{50} values determined using recombinant RT suggest that NNRTIs are less effective inhibitors of *in vitro* polymerization alone as compared to the overall process of reverse transcription *in vivo*. Overall, the ability of NNRTIs to inhibit RT or HIV-1 depends on the assay system used (Table 2). Recent studies described below suggest that NNRTIs may inhibit various stages of reverse transcription. Cell-free studies designed to determine the relationship between RT-mediated polymerization and inhibitors of the reaction revealed that inhibition by nevirapine is template length-dependent [207-208]. This suggested that slowed catalysis results in fewer full length products for longer templates (in the range of 186-370 nucleotides). Despite this, cell-based assays reveal nearly uninhibited levels of -sss DNA product in cells infected with virus in the presence of nevirapine (a product of approximately 200 nucleotides) [209]. Data presented at the *XV International HIV Drug Resistance Workshop* in 2006 demonstrated that NNRTI-resistant HIV-1 RT is 30-fold more resistant to inhibition in strand transfer assays than polymerase or RNase H assays [210], indicating that NNRTIs may be more effective during strand transfer.

To further understand the disconnect between enzyme-based assays and cell-based assays, evaluation of the effect of NNRTIs on different functions of RT was necessary. I began

by determining the effect of NNRTIs on the RNase H function (Fig. 11). Both NNRTIs and mutations that confer resistance to these inhibitors have been shown to impact the cleavage rate and pattern. For example, some studies have shown that RNase H cleavage is partially inhibited by NNRTIs [125]. However, other groups have shown no effect [211-212] or even enhancement of activity [213]. A study investigating various NNRTIs determined that the nature of the cleavage (position of RT on the T/P) and the structure of the T/P (primer overhangs) affected the outcome of RNase H function assays in the presence of NNRTIs [214]. It was concluded that previous conflicting data was generated from different T/P systems. This study suggested that NNRTIs can have enhancing, inhibitory or no effect on the function of RNase H, depending on how RT associates with the substrate. Therefore, NNRTIs can have varied effects on the process of reverse transcription depending on the nature of the T/P at each stage.

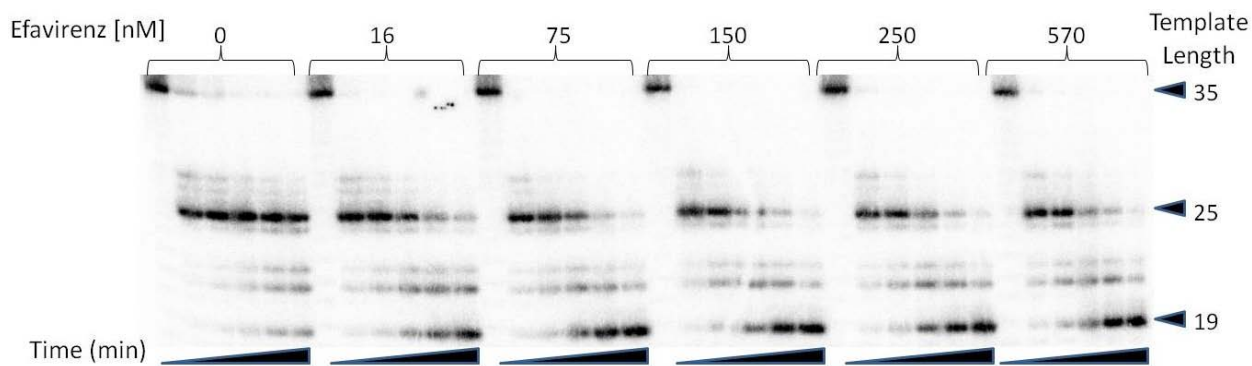


Figure 11. HIV-1 RT RNase H cleavage in the presence of efavirenz.

Audioradiogram of the cleavage activity of WT HIV-1 RT in the absence and presence of increasing concentrations of efavirenz. Fifty nanomolar HIV-1 RT was incubated with varying concentrations of efavirenz, 50 nM $T_{RNA}/pr26$ and reaction buffer (Section 3.4.2-3.4.4). Samples were quenched at 0, 3, 6, 9, 12 and 15 minutes.

More recently, it was shown that there is a correlation between RNase H activity and polymerase activity. It has been previously observed that there is a relationship between the two active sites [37, 215-216], but it was only recently demonstrated that decreased RNase H activity

could decrease RT template switching during reverse transcription [175]. This study revealed that a shift in the equilibrium between the two activities could affect the efficiency of the overall reverse transcription process. The authors also observed a correlation between decreased RNase H activity and increased NRTI resistance, suggesting that drug resistance could be affected by the interplay between the two active sites.

Given the known effects of NNRTIs on the function of RT, it is possible that perturbation of both the polymerase and RNase H activities, in addition to the effects on the molecular dynamics of the enzyme and T/P, may affect other aspects of reverse transcription. From the observation that NNRTIs are more effective in the context of the virus as compared to polymerization assays and because NNRTIs have varied effects on RNase H activity, it seems that NNRTIs could have effects on steps of reverse transcription which require RNase H cleavage, such as strand transfer and primer removal. Additionally, because a correlation between RNase H activity NRTI resistance has been demonstrated [200], it is logical to anticipate that inhibitors (or mutations) that affect RNase H activity (i. e. NNRTIs) may affect the efficacy of these compounds.

Table 2. Inhibitory and binding constants determined for NNRTIs using various assay systems

Assay	Virus - cell type	T/P substrate	EC ₅₀ or IC ₅₀ or K _D (nM)		
			Nevirapine	Delaviradine	Efavirenz
Antiviral ^a (EC ₅₀)	LAI - P4/R5	--	85.5 ± 27	63.3 ± 19	1.46 ± 0.29
Antiviral ^b (EC ₅₀)	NL4-3 - HeLa-CD4	--	490 ± 18	290 ± 10	10 ± 0.5
Antiviral ^c (EC ₅₀)	HXB2 - MT4	--	99 ± 32	18 ± 6	1.6 ± 0.8
Antiviral ^c (EC ₅₀)	HXB2 - PBMC	--	--	--	2.1 ± 0.5
Polymerase ^d (IC ₅₀)	--	poly (rC)/oligo (dG)	200 ± 45	5.4 ± 0.4	7.7 ± 0.9
Polymerase ^e (IC ₅₀)	--	poly (rA)/oligo (dT)	7222 ± 138	2180 ± 62	94.2 ± 6.3
Polymerase ^f (IC ₅₀)	--	heteropolymeric (RNA/DNA)	2217 ± 954	--	3.9 ± 0.2
RNase H (IC ₅₀)	--	polymerase-independent	216 ± 40	--	4.5 ± 0.8
RNase H	--	polymerase-dependent	Accelerated ^b	Accelerated ^b	Accelerated ^b
Biacore ^g	--	--	1550 ± 441	6.19 ± 0.15	0.63 ± 0.34

Data published ^a[217], ^b[218], ^c[219], ^d[220], ^e[221], ^f[222], ^g[223], ^h[224], [222] and [225].

2.2 HYPOTHESIS AND SPECIFIC AIMS

I hypothesize that NNRTIs block reverse transcription by exerting effects on both the DNA polymerase and RNase H active sites of RT, which significantly disrupt the equilibrium between these two enzymatic activities. I also hypothesize that the feasibility of NNRTIs to be combined with other classes of RT inhibitors in antiretroviral therapies will depend on how these compounds respond to the NNRTI-induced shift in the polymerase/RNase H activity equilibrium. In this study, I propose to investigate these hypotheses by determining the mechanisms by which NNRTIs inhibit RT and by examining the interactions between NNRTIs and the nucleoside analog AZT. These studies will be achieved through two Specific Aims.

In **Aim 1**, I will determine the molecular mechanism for synergy between the NNRTIs and the nucleoside analog AZT and I will investigate the structural changes that occur in RT when bound to an NNRTI.

In **Aim 2**, I will investigate the mechanism(s) by which HIV-1 can evade therapies containing combinations containing nevirapine and AZT by determining the molecular mechanism(s) by which N348I confers dual resistance.

**3.0 CHAPTER ONE: EFAVIRENZ ACCELERATES HIV-1 REVERSE
TRANSCRIPTASE RIBONUCLEASE H CLEAVAGE, LEADING TO DIMINISHED
ZIDOVUDINE EXCISION**

3.1 PREFACE

This work was presented at the *14th Annual Conference on Retroviruses and Opportunistic Infections*. February 25-28, 2007; Los Angeles, California (abstract 490; Radzio J, Sluis-Cremer N. Mechanism of Synergy Between Efavirenz and Zidovudine: Role of HIV-1 Reverse Transcriptase RNase H Activity.)

Additionally, this chapter was adapted from a published study (Radzio J, Sluis-Cremer N. Efavirenz accelerates HIV-1 reverse transcriptase ribonuclease H cleavage, leading to diminished zidovudine excision. *Molecular Pharmacology* 2008 Feb;73(2):601-6), reprinted with permission from the *American Society for Pharmacology and Experimental Therapeutics*.

This work is in partial fulfillment of Specific Aim 1.

3.2 ABSTRACT

Previous biochemical studies have demonstrated that synergy between NNRTIs and NRTIs is due to inhibition by the NNRTI of the rate at which HIV-1 RT facilitates ATP-mediated excision of NRTIs from chain-terminated T/P. However, these studies did not take into account the possible effects of NNRTI on the RNase H activity of RT, despite recent evidence that suggests an important role for this activity in the NRTI excision phenotype. Accordingly, in this study, we compared the ability of efavirenz to inhibit the incorporation and excision of AZT by HIV-1 RT using DNA/DNA and RNA/DNA T/Ps that were identical in sequence. Whereas IC_{50} values for the inhibition of AZT-TP incorporation by efavirenz were essentially similar for both DNA/DNA and RNA/DNA T/P, a 19-fold difference in IC_{50} was observed between the AZT-MP excision reactions, the RNA/DNA T/P substrate being significantly more sensitive to inhibition. Analysis of the RNase H cleavage events generated during ATP-mediated excision reactions demonstrated that efavirenz dramatically increased the rate of appearance of a secondary cleavage product that decreased the T/P duplex length to only 10 nucleotides. Studies designed to delineate the relationship between T/P duplex length and efficiency of AZT excision demonstrated that RT could not efficiently unblock chain-terminated T/P if the RNA/DNA duplex length was less than 12 nucleotides. Taken together, these results highlight an important role for RNase H activity in the NRTI excision phenotype and in the mechanism of synergy between NNRTI and NRTI.

3.3 GOAL OF THE STUDY

Previous studies investigating the effect of NNRTIs on excision were carried out using DNA/DNA T/P only and, as such, they ignored the potential contribution of the enzyme's RNase H activity in the NRTI excision phenotype. We have recently determined that the polymerase-dependent RNase H activity of HIV-1 RT can be modulated by the presence of efavirenz (Fig. 11). It has not been determined if the same effect is seen on a nucleoside-terminated T/P system. Additionally, it has been shown that a balance between nucleotide excision and template RNA degradation plays an important role in NRTI resistance [175], therefore, the effect of NNRTIs on RNase H activity could contribute to synergy noted between NRTIs and NNRTIs. To determine if the modulation of RNase H activity affects excision, I will compare the ability of RT to excise a terminating nucleoside on an RNA and DNA template under equivalent conditions. Additionally, I will evaluate the effect of efavirenz on RNase H activity on an AZT-terminated T/P system and compare and contrast the ability of NNRTIs to inhibit the ability of RT to unblock chain-terminated primers using both RNA/DNA and DNA/DNA T/P substrates.

3.4 MATERIALS AND METHODS

3.4.1 Materials

HIV-1 RT was overexpressed as an N-terminal hexahistidine fusion protein from the prokaryotic expression vector p6HRT-PROT [226] and purified to homogeneity as described previously [226-227]. Briefly, expression of the recombinant enzyme was induced with 1 mM isopropyl β -

D-1-thiogalactopyranoside (IPTG) in JM109 strain of *E. coli* overnight at 30°C. The cells were lysed and the tagged protein was purified using TALON HIS-tag Metal Affinity Resin from Clontech (Mountain View, CA). Enzyme concentration was determined spectrophotometrically at 280 nm using an extinction coefficient (ϵ_{280}) of 260,450 M⁻¹ cm⁻¹. The activity of the enzyme was evaluated using a polymerase activity assay where 25 nM enzyme was incubated in reaction buffer [10 mM MgCl₂, 50 mM Tris-HCl, pH 7.5 and 50 mM KCl], with 600 nM biotinylated oligo (dT) primer (18 nucleotides in length) annealed to poly (rA) (with an average length of 600 bases) and 1 μM dTTP containing trace amounts of ³H-labeled dTTP. The reaction was incubated at 37°C for 10 minutes then quenched with 0.25 M EDTA containing SPA scintillation beads (Perkin Elmer). SPA scintillation beads are microspheres containing scintillant which are streptavidin conjugated. When mixed with the reaction, they bind to the biotinylated primer and emit light when in the proximity of the incorporated ³H. The activity was quantified using a MicroBeta liquid scintillation counter from Perkin Elmer (Waltham, MA). Efavirenz was obtained from the National Institutes of Health AIDS Research and Reference Reagent Program. Both RNA and DNA oligonucleotides were synthesized by Integrated DNA Technologies (Coralville, IA). The AZT-TP was purchased from Sierra Bioresearch (Tuscon, AZ). All other reagents were of the highest quality available and were used without further purification.

3.4.2 Template/Primer Substrates

All assays were carried out using a 26-nucleotide DNA primer (pr26, 5'-CCTGTTCGGGCGCCACTGCTAGAGAT-3') annealed to either a 35-nucleotide RNA template (RNA-T, 5'-AGAAUGGAAAAUCUCUAGCAGUGGCGCCCGAA CAG-3') or to a DNA

template that was identical in sequence to the RNA template (DNA-T, '5-AGAATGGAAAATCTCTAGCAGTGGCGCCCGAACAG-3'). The pr26 primer was 5'-end labeled with [γ - 32 P]ATP (from Amersham Biosciences) according to the manufacturer's instructions. For some experiments, the primer was chain-terminated with AZT-monophosphate (AZT-MP) to generate pr26-AZT, as described previously [171-172]. Briefly, the pr26 primer was annealed to the DNA-T then incubated with wild-type (WT) RT and 100 μ M AZT-triphosphate (AZT-TP) at 37°C for 30 minutes. The 32 P-labeled chain-terminated primer was purified by elution of the appropriate band following resolution by 7 M urea, 16% acrylamide denaturing gel electrophoresis. The purified chain-terminated primer was then annealed to the appropriate DNA primer for use in phosphorolysis experiments. Depending on the nature of the assay (described below), the 5'-end of the DNA primer or RNA template was radioactively labeled with [γ - 32 P]ATP (GE Healthcare, Piscataway, NJ).

3.4.3 Assays for Inhibition of AZT-TP Incorporation and AZT-MP Excision by HIV-1

RT

Inhibition of AZT-TP incorporation by efavirenz was determined using a fixed-time assay. In brief, 200 nM HIV-1 RT was preincubated with 20 nM T/P (RNA-T/pr26 or DNA-T/pr26) and varying concentrations of efavirenz (0-300 nM) in 50 mM Tris-HCl, pH 7.5 and 50 mM KCl at 37°C for 5 min. Reactions were initiated by the addition of 0.1, 1, or 10 μ M AZT-TP and 10 mM MgCl₂. Reactions were quenched after a defined time (15 s, 1 min, or 15 min) by the addition of an equal volume of sample loading buffer (98% deionized formamide, 10 mM EDTA, and 1 mg/ml each of bromphenol blue and xylene cyanol). Inhibition of AZT-MP excision by efavirenz was determined using both fixed-time and time-course assays. In brief, 200 nM HIV-1 RT was

preincubated with 20 nM T/P (DNA-T/pr26-AZT or RNA-T/pr26-AZT) in 50 mM Tris-HCl, pH 7.5, and 50 mM KCl and varying concentrations of efavirenz (0-500 nM) at 37°C for 5 min. Reactions were initiated by the addition of 3 mM ATP and 10 mM MgCl₂. Excision reactions carried out on the DNA-T/pr26-AZT and RNA-T/pr26-AZT were quenched with an equal volume of sample loading buffer after 30, 60, or 90 min, respectively. Reaction products were separated using denaturing polyacrylamide gel electrophoresis and analyzed by densitometry using a GS525 Molecular Imager FX (Bio-Rad Laboratories, Hercules, CA). Data analyses were carried-out using SigmaPlot 8.02 and/or SigmaStat 3.00 (Systat Software, Inc., San Jose, CA). Statistical significance was determined using the two-sample Student's *t* test. The results demonstrated that the IC₅₀ values for efavirenz calculated at different AZT-TP concentrations (i.e., 0.1, 1.0 or 10 μM), or time points (15 s, 1 min or 15 min), were similar. Likewise, IC₅₀ values calculated for AZT-MP excision from the fixed time assay (from different time points) or time course assays were also similar. Accordingly, for inhibition of AZT-TP incorporation data are reported from 1 min assays that contained 1.0 μM AZT-TP, and for inhibition of AZT-MP excision data are reported from a fixed time assay that was carried out for 30 min (Figure 12).

3.4.4 RNase H Assays

The effect of efavirenz on RNase H activity was evaluated using the RNA-T/pr26-AZT T/P that was used in the ATP-mediated excision assays described above. HIV-1 RT (200 nM) was preincubated with 20 nM T/P in 50 mM Tris-HCl, pH 7.5, and 50 mM KCl and varying concentrations of efavirenz (0 and 150 nM) at 37°C for 5 min. Reactions were initiated by the addition of 3 mM ATP and 10 mM MgCl₂. Aliquots were removed and quenched at varying times and analyzed as described above.

3.4.5 Gel Mobility Shift Assays

Gel mobility shift assays were used to evaluate the thermodynamics of RT-T/P interactions. In these assays, the amount of T/P-bound RT present in an equilibrium solution was assayed by native polyacrylamide gel electrophoresis. RT (0-10 μ M total) was equilibrated with 100 nM T/P in 50 mM Tris-Cl, pH 7.5, and 50 mM KCl for 15 min at 37°C. Gels were run at room temperature for 30 min (100 V constant voltage) and quantified as described above. Discontinuity of sample and gel buffers can cause severe streaking of the bands. To correct for this, the area of the unshifted band was estimated from the lane containing DNA alone, and the area between shifted and unshifted bands was counted as the shifted band. The percentage of DNA-bound RT was calculated assuming that the amount of DNA in the shifted band represented a 1:1 complex of RT-T/P.

3.5 RESULTS AND DISCUSSION

This study compared the ability of the NNRTI efavirenz to inhibit HIV-1 RT-catalyzed incorporation and excision of the NRTI AZT in reactions carried out on DNA/DNA and RNA/DNA T/P that are identical in length and sequence. In this regard, previous detailed biochemical studies designed to delineate the molecular mechanism of synergy between NRTIs and NNRTIs measured inhibition of NRTI-MP excision on DNA/DNA T/P only [147]. Other studies [228-229] evaluated NNRTI-mediated inhibition of NRTI-MP excision on RNA/DNA T/P but did not provide a direct comparison with results obtained from complementary DNA/DNA T/P. Furthermore, none of these studies considered the possible effects of RNase H

activity on the NRTI excision phenotype, despite ample evidence in the literature that this activity was modulated by NNRTI binding to RT [213-214, 230-232].

3.5.1 Effect of Efavirenz on Excision and Incorporation

To determine whether efavirenz differentially inhibited the incorporation and/or excision of AZT by HIV-1 RT on RNA/DNA and DNA/DNA T/P, IC_{50} values for these reactions were determined (Figure 12E). In all experiments described, the same DNA primer (pr26 or pr26-AZT) was annealed to DNA or RNA templates (RNA-T or DNA-T) that were identical in length and sequence (Figure 12A). The IC_{50} values for efavirenz inhibition of AZT-TP incorporation by HIV-1 RT were calculated to be 19.6 ± 8.5 and 10.2 ± 4.0 nM for the DNA/DNA and RNA/DNA T/P, respectively (Figure 12C). The small difference (~ 1.9 -fold) between these values was found to be statistically nonsignificant. By contrast, the IC_{50} values for efavirenz inhibition of AZT-MP excision by HIV-1 RT were calculated to be 108.1 ± 32.3 and 5.8 ± 1.1 nM for the DNA/DNA and RNA/DNA T/P, respectively (Figure 12B and C). The large (~ 19 -fold) difference between these values is statistically significant ($p < 0.005$). This large difference in IC_{50} value cannot be explained by pre-existing large differences in the rates of AZT-MP excision from RNA/DNA or DNA/DNA T/P in the absence of drug (the apparent rates of AZT-MP excision were calculated to be $0.067 \pm 0.005 \text{ min}^{-1}$ and $0.045 \pm 0.002 \text{ min}^{-1}$ for DNA/DNA and RNA/DNA T/P, respectively) or by differences in apparent affinity of RT for the RNA/DNA and DNA/DNA T/P (Figure 12D and 15A). Studies from the Anderson lab [147, 233] and ours [120] have demonstrated communication between the NNRTI-binding pocket and the DNA polymerase active site in HIV-1 RT, which accounts for the inhibition of RT-catalyzed

nucleotide incorporation and excision reactions on a DNA/DNA T/P via a remote effect on the chemical step of these reactions. However, the data in Figure 12 suggest that additional parameters may also contribute toward the ability of efavirenz to inhibit NRTI-MP excision on RNA/DNA T/P.

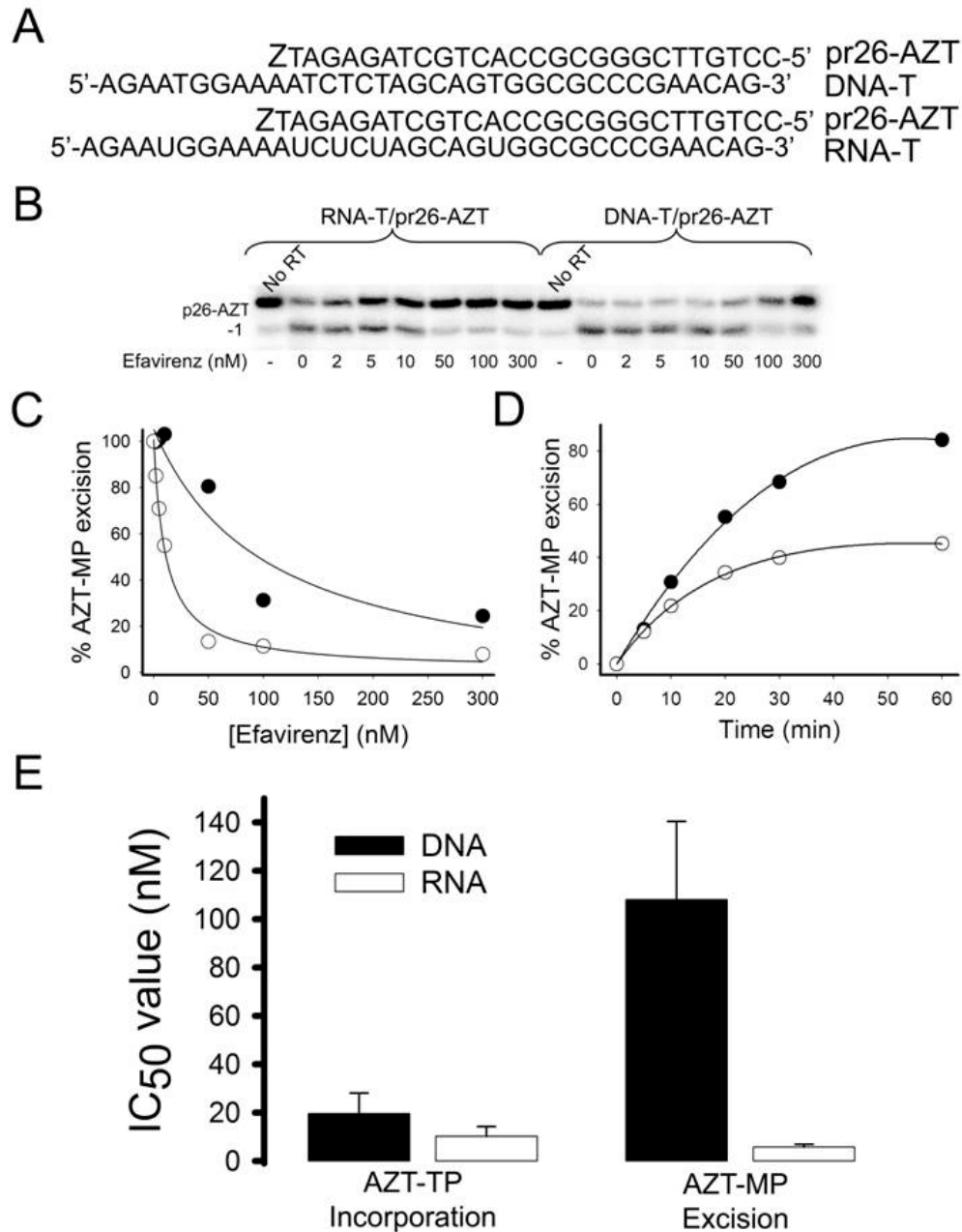


Figure 12. Inhibition of RT-mediated AZT-TP incorporation and AZT-MP excision on RNA/DNA and DNA/DNA T/P by efavirenz.

A, Sequences of RNA and DNA templates and DNA primer used in all experiments. In the ATP-mediated excision assays, the pr26 primer was chain-terminated with AZT-MP (designated as Z). B, Representative gel analysis of AZT-MP excision reaction carried out on RNA/DNA or DNA/DNA T/P in the absence and presence of varying concentrations of efavirenz (0-300 nM). C, Graph of inhibition of AZT-MP excision by efavirenz on RNA/DNA

T/P (○) and DNA/DNA T/P (●) from data in B. IC₅₀ values determined from this isotherm were 11.9 and 100.7 nM for the RNA/DNA and DNA/DNA T/P, respectively. D, HIV-1 RT AZT-MP excision isotherms from RNA/DNA T/P (○) and DNA/DNA T/P (●) in the absence of inhibitor. The apparent rates of AZT-MP excision were calculated to be $0.067 \pm 0.005 \text{ min}^{-1}$ and $0.045 \pm 0.002 \text{ min}^{-1}$ for DNA/DNA and RNA/DNA T/P, respectively. The burst amplitudes (total amount of product excised at an infinite time point) were 84 and 45% for the DNA/DNA and RNA/DNA T/P, respectively. E, IC₅₀ values for the inhibition of AZT-TP incorporation and AZT-MP excision by efavirenz under single-turnover conditions. The concentrations of efavirenz used in the incorporation assays were 5, 10, 20, 30, 50, 100, 150, 250, and 500 nM. The concentrations of efavirenz used in the excision assays were 2, 5, 10, 30, 50, and 100 nM and 25, 50, 100, 150, 200, and 500 nM for the RNA/DNA and DNA/DNA T/P, respectively. The calculated IC₅₀ values for incorporation of AZT-TP were 19.6 ± 8.5 and 10.2 ± 4.0 nM for the DNA/DNA and RNA/DNA T/P, respectively. The calculated IC₅₀ values for ATP-mediated excision of AZT-MP were 108.1 ± 32.3 and 5.8 ± 1.1 nM for the same two substrates, respectively. The difference between these two values was found to be statistically significant ($p < 0.005$).

3.5.2 Effect of Efavirenz on RNase H Activity

Recent reports have suggested that the NRTI excision phenotype might also be influenced by the RNase H activity of RT [175]. In this regard, several studies have demonstrated that NNRTIs modulate the enzyme's RNase H activity. For example, others have shown that this class of drugs can accelerate the enzyme's 3'end -directed (or DNA polymerase-directed) RNase H activity [214, 232]. Accordingly, the RNase H cleavage events that occurred during the AZT-MP excision reaction were assessed. It was then delineated whether these affected the efficiency of the excision reaction. Figure 13 shows that efavirenz accelerates HIV-1 RT RNase H cleavage, data that is consistent with the results of the Shaw-Reid *et al.* and Hang *et al.* studies. Specifically, efavirenz increased the rate of appearance of a secondary RNase H cleavage event that reduced the RNA/DNA duplex length to 10 nucleotides (Figure 13A). It is noteworthy that

an inverse relationship between the efficiency of AZT-MP excision and the appearance of this secondary RNase H cleavage event was also found in time course assays carried out in the absence and presence of efavirenz (Figure 13B and C). Shaw-Reid *et al.* further suggested that the NNRTI (±)-4-(1-chloro-1,1-difluoromethyl)-4-(2-phenylethynyl)-6-chloro-2H-3,1-benzoxazin-2-one, an analog of efavirenz, in addition to accelerating the rate of RT RNase H activity also altered the specific RNase H cleavage pattern. However, this analysis was based on data from a single time point, and our data clearly show that the overall RNase H cleavage pattern of RT, including the primary and secondary cuts, was not affected by efavirenz (Figure 13A).

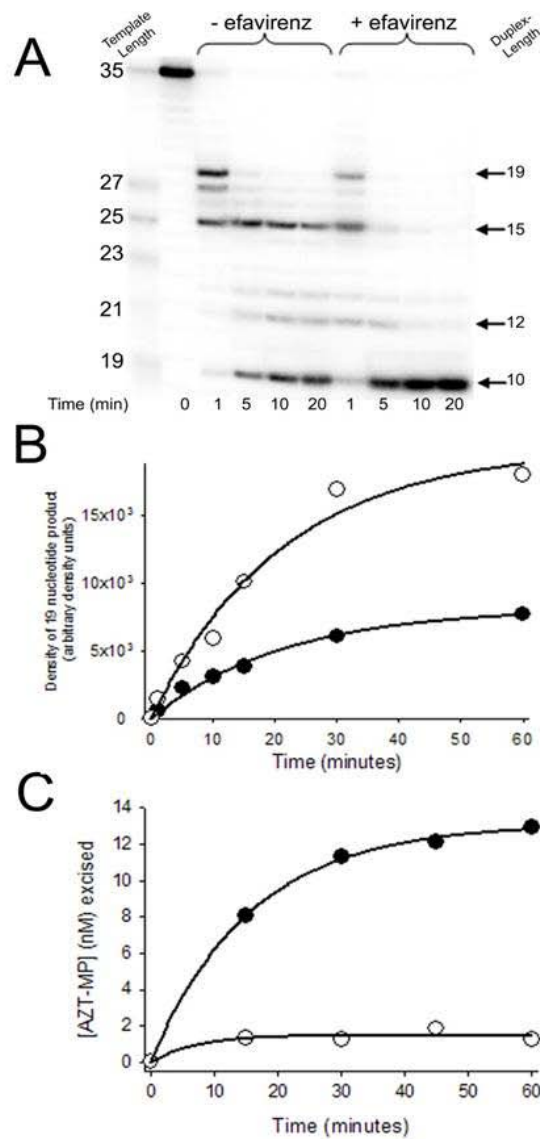


Figure 13. Efavirenz accelerates HIV-1 RT RNase H activity.

A, Autoradiogram of RNase H products generated during ATP-mediated excision assays in the absence and presence of efavirenz. Experiments were carried out as described in Section 3.4.4; the 5'-end of the RNA template is radioactively labeled in these experiments. The primary RNase H cleavage events occur 17 or 18 nucleotides downstream from the polymerase active site. These cleavages generate RNA/DNA duplex lengths of 19 and 18 nucleotides, respectively. B, Isotherm for the rate of appearance of the 19 nucleotide secondary RNase H cleavage product generated in the absence (●) or presence (○) of 150 nM efavirenz. The intensity of the 19 nucleotide

was determined by densitometric analyses using Bio-Rad GS525 Molecular Imager FX software and is reported as arbitrary units. C, Isotherm for the rate of ATP-mediated AZT-MP excision carried-out by HIV-1 RT in the absence (•) or presence (○) of 150 nM efavirenz.

3.5.3 Excision from T/Ps with Decreasing Template Lengths

To define the relationship between the efficiency of NRTI-MP excision and RNase H activity, I next evaluated the ability of HIV-1 RT to excise AZT-MP from a chain-terminated DNA primer that was annealed to different RNA templates that were recessed from ~~10 to 12~~ therefore incrementally decreasing the RNA/DNA duplex length (Figure 14). These data show that the efficiency of AZT-MP excision (and AZT-TP incorporation) was severely compromised when the RNA/DNA duplex length was decreased to 12 nucleotides or less (Figure 14). If the RNA/DNA duplex was reduced to 10 nucleotides - a duplex length consistent with the secondary RNase H cleavage event described in Figure 13 - RT was essentially unable to carry-out ATP-mediated AZT-MP excision.

3.5.4 Effect of Efavirenz on RT-T/P Association

Gel mobility shift assays demonstrated that RT exhibited a decrease in affinity for the RNA/DNA T/P each time the duplex length was decreased (Figure 15). This decrease in RT-T/P affinity provides a plausible explanation for the observed decrease in the efficiency of AZT-MP excision (Figure 14). Taken together, these results provide convincing evidence that the sensitivity of the AZT-MP excision reaction on RNA/DNA T/P to efavirenz may be explained by the drug-induced accelerated RNase H activity of the enzyme in addition to effects on the

chemistry step of the AZT-MP excision reaction. This data also show that AZT-TP incorporation is affected by decreasing the RNA/DNA duplex length (Figure 14). However, the rate of AZT-TP incorporation is significantly faster than the rate of AZT-MP excision, (8.78 s^{-1} versus $0.54 \times 10^{-3} \text{ s}^{-1}$; [171]) and therefore we would not expect the observed increase in the secondary cleavage event that accumulates in a minute time-scale (see Figure 13) to adversely affect the IC_{50} for incorporation of AZT-TP.

Nikolenko *et al.* proposed that an equilibrium exists between 1) NRTI incorporation, NRTI excision, and resumption of DNA synthesis and 2) degradation of the RNA template by RNase H activity that leads to dissociation of the template-primer and abrogation of HIV-1 replication [175]. In this regard, the authors elegantly showed that mutations in the RNase H domain of RT that reduce RT RNase H activity confer AZT resistance. This study lends biochemical support to our model and clearly demonstrates that the efficiency of ATP-mediated excision reactions on RNA/DNA templates can be influenced by the enzyme's RNase H activity. However, the data in Figure 14 show that it is not a decrease in the absolute rate of RNase H activity that will contribute to increased NRTI-MP excision, but a decrease in the rate or appearance of secondary cleavage events that generate RNA/DNA T/P with duplexes less than 13 nucleotides.

Duplex Length

Efficiency of AZT-TP Incorporation and AZT-MP Excision

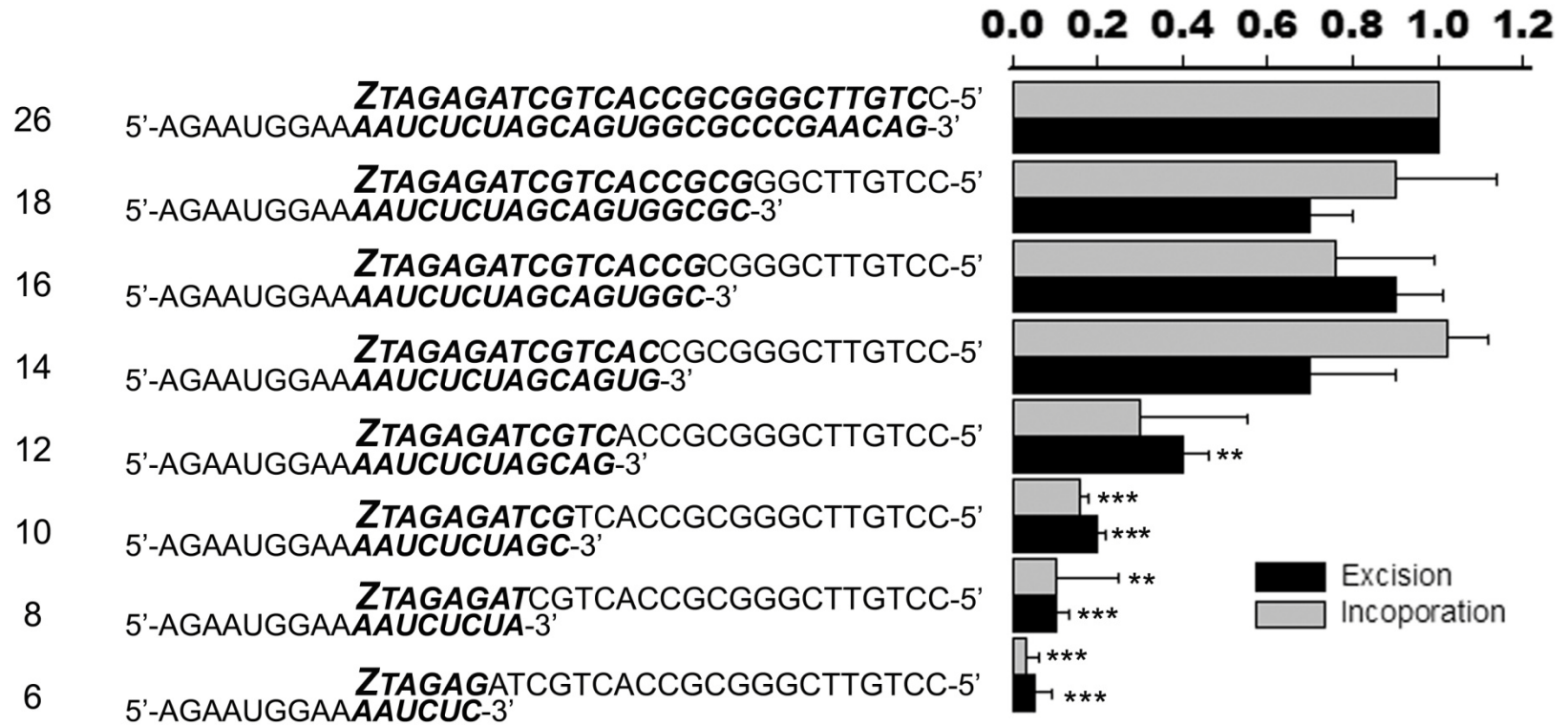


Figure 14. Ability of HIV-1 RT to incorporate or excise AZT on RNA/DNA T/P with decreasing duplex lengths

Sequences of RNA templates that were annealed to pr26 (for incorporation of AZT-TP) or pr26-AZT (for excision of AZT-MP) are shown. The RNA/DNA duplex length is highlighted in bold. Assays were carried out as described in Section 3.4.3. Incorporation and excision activity on the RNA-T template was assumed as the reference (100%). Statistical difference is denoted as ** ($p < 0.01$) and *** ($p < 0.001$).

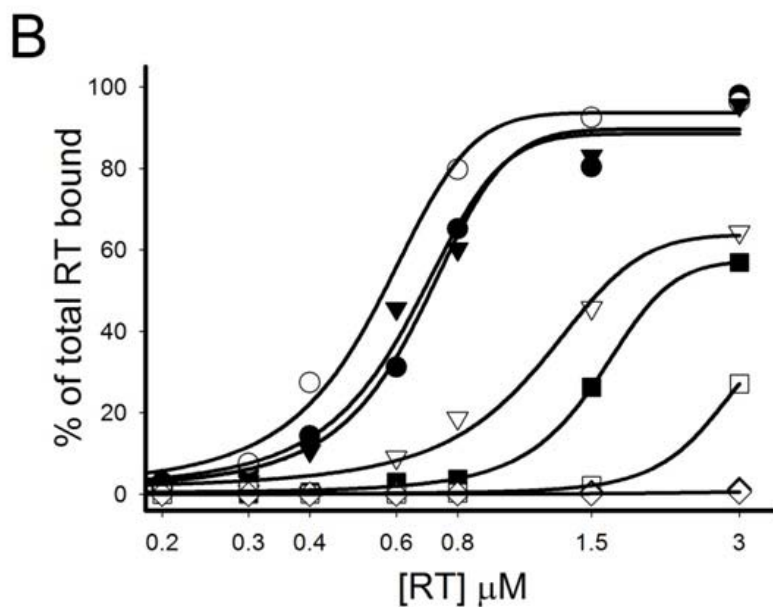
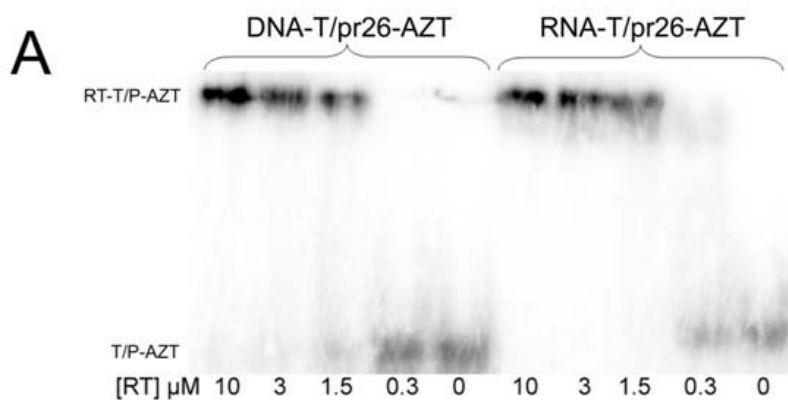


Figure 15. Mobility gel shift assays to assess RT-T/P interactions

A, representative gel for the binding of RT to RNA-T/pr26-AZT and DNA-T/pr26-AZT. Assays were carried out as described in Section 3.4.5. The bound and free T/P substrates are labeled as RT-T/P-AZT and T/P-AZT, respectively. The concentrations of RT used in the assay are also indicated. B, plots of RT binding to the RNA/DNA T/P substrates with decreasing duplex lengths, as indicated in Figure 14. RNA/DNA T/P with duplex lengths of 26 nucleotides (●), 18 nucleotides (○), 16 nucleotides (▲), 14 nucleotides (△), 12 nucleotides (■), 10 nucleotides (□), 8 nucleotides (◆), and 6 nucleotides (◇) are shown.

4.0 CHAPTER TWO: EFAVIRENZ ALTERS THE INTERACTION BETWEEN HIV-1 REVERSE TRANSCRIPTASE AND TEMPLATE/PRIMER

4.1 PREFACE

This work was presented at the *XVI International HIV Drug Resistance Workshop*, June 12-16, 2007; Barbados, West Indies. (abstract published in Radzio J, Sheen C and Sluis-Cremer N. Efavirenz Alters the Interaction Between HIV-1 Reverse Transcriptase and Template/Primer. *Antiviral Therapy* 2007; 12 Suppl.2; S133)

The work described in this chapter is in partial fulfillment of Specific Aim 1.

4.2 ABSTRACT

We previously demonstrated that efavirenz exhibits a greater capacity to inhibit HIV-1 RT-mediated AZT-MP excision from an RNA/DNA T/P than a DNA/DNA T/P (Section 3.0) [225]. This was due, in part, to efavirenz increasing the appearance of secondary RNase H cleavage products and altering the precise positioning of the T/P. To gain insight into the mechanism by which efavirenz affects RT RNase H activity and T/P binding, I have used fluorescence resonance energy transfer (FRET) to measure distances between specific residues in the RNase H domain of RT and the 5'-end of the T/P. Recombinant enzymes that could be modified to incorporate AlexaFluor555 (AF555) at two unique sites in the RNase H domain (449 and 560) of RT were constructed. The 5'-ends of the DNA or RNA templates were labeled with AlexaFluor647 (AF647). FRET was determined under equilibrium conditions and analyzed according to the Förster theory. Recombinant enzymes were purified and labeled (~70% efficiency) without appreciable loss of RT polymerase or RNase H activity. Energy transfer between the fluorescent donor (AF-555) at residues 449 and 560 in RT and fluorescent acceptor (AF647) at the 5'-end of the DNA template was readily measured. The efficiency of energy transfer (E) was calculated to be 0.36 from residue 449 and 0.44 from residue 560. When efavirenz was added to the energy transfer experiments, E decreased to 0.17 from residue 449 and increased to 0.31 from residue 560. These data provide direct evidence that efavirenz binding to RTs alters the precise positioning of the T/P in the DNA binding tract of RT, and I

hypothesize that these changes significantly contribute to the mechanism by which efavirenz inhibits both nucleotide incorporation and AZT excision and contributes to the observed effect on RNase H activity.

4.3 GOAL OF THE STUDY

The previous study demonstrated an additional mechanism of synergy between NRTIs and NNRTIs. It was demonstrated that efavirenz exhibits a greater capacity to inhibit HIV-1 RT-mediated AZT-MP excision from an RNA/DNA T/P than a DNA/DNA T/P (Section 3.0) [225]. This was due, in part, to efavirenz increasing the appearance of the enzyme's secondary RNase H cleavage products. Additionally, it has previously been demonstrated that NNRTIs inhibit dNTP incorporation via an indirect effect on the chemistry step of the reaction [120].

Despite the wealth of structural information that is available for HIV-1 RT, no structures exist in which both NNRTI and the T/P are bound or in which the RNA/DNA hybrid extends through both active sites of the enzyme. Therefore, the effect of the NNRTI on the position of the T/P in the binding cleft of RT has not been investigated. In this regard, I hypothesized that the NNRTI affects the efficiency of dNTP incorporation as well as RNase H cleavage by altering the precise positioning of the T/P. Accordingly in this study, I have used FRET to probe RT-T/P interactions in the absence and presence of bound NNRTI (i.e. efavirenz). Determining the position of RT on both DNA/DNA and RNA/DNA T/P systems will provide further insight into how the bound NNRTI may be modulating RNase H activity and contributing to synergy in the absence of a crystal structure.

4.4 MATERIALS AND METHODS

4.4.1 Materials.

Efavirenz was obtained from the National Institutes of Health AIDS Research and Reference Reagent Program. Both RNA and DNA oligonucleotides were synthesized by Integrated DNA Technologies (Coralville, IA). The AZT-TP was purchased from Sierra Bioresearch (Tuscon, AZ). AlexaFluor 555 C₅ maleimide conjugate (AF555) was purchased from Molecular Probes (Invitrogen, Carlsbad, CA). All other reagents were of the highest quality available and were used without further purification.

4.4.2 Template/Primer Substrates.

All assays were carried out using an AlexaFluor-labeled 26-nucleotide DNA primer (pr26-AF647, 5'-/AF647/-CCTGTTCGGGCGCCACTGCTAGAGAT-3') annealed to either a 35-nucleotide RNA template (RNA-T, 5'-AGAAUGGAAAAUCUCUAGCAGUGGCGCCCGAACAG-3') or to a DNA template that was identical in sequence to the RNA template (DNA-T, 5'-AGAATGGAAAATCTCTAGCAGTGGCGCCCGAACAG-3'). The pr26-AF647 primer was chain-terminated with AZT-MP to generate pr26-AF647-AZT, as described previously (Section 3.4.2). The 5'-end of the RNA template was radioactively labeled with [γ -³²P]ATP (GE Healthcare, Piscataway, NJ) for the RNase H activity evaluation.

4.4.3 Generation and Characterization of Labeled Recombinant Mutant Enzymes

Point mutations were added in the prokaryotic expression vector p6HRT-PROT containing HIV-1 LAI RT by GenScript (Piscataway, NJ). Mutations C38V and C280S were inserted in all clones to removed naturally occurring cysteine residues. Mutations E449C and L560C were introduced into separate clones to allow labeling of the RNase H domain in specific locations. Recombinant RTs were overexpressed as an N-terminal hexahistidine fusion protein and purified to homogeneity as described previously (Section 3.4.1). Enzyme concentration was determined spectrophotometrically at 280 nm using an extinction coefficient (ϵ_{280}) of $260,450 \text{ M}^{-1} \text{ cm}^{-1}$. Recombinant RT enzymes containing a cysteine residue at one position were incubated with AF555, allowing the formation of a carbon-sulfur bond between the maleimide and the thiol group of the cysteine in RT. RT was incubated over night at 4°C in a reaction containing $50 \mu\text{M}$ RT, 2% dye and reaction buffer (Section 3.4.1). The labeled RT (RT-AF555) was separated from unreacted compound using a NAP-5 column equilibrated with reaction buffer. A polymerase activity assay was used to determine polymerase activity and the previously described RNase H assay was used to check that rate and pattern were similar to previously seen results (Section 3.4.4).

4.4.4 FRET Assays

RT-AF555 (800 nM) was allowed to equilibrate with $1 \mu\text{M}$ efavirenz in 50 mM Tris-HCl, pH 7.5 and 50 mM KCl for 5 minutes at 37°C . T/P-AF647 (200 nM) was then added and allowed to equilibrate with the mixture for an additional 15 minutes. All data was collected from a SpectraMax M2 from Molecular Devices (Sunnyvale, CA) at 37°C in relative fluorescence units

(RFU). The scan speed for the instrument is $45 \cdot K$ nm/min (K = wavelength interval), readings were taken at 1 nm intervals using the photomultiplier tube precise setting (Readings: 30), excitation wavelength = 502 nm and cutoff wavelength = 550 nm.

4.4.5 Analysis of Data

The efficiency of energy transfer (E) is defined as:

Equation 1

$$E = 1 - \frac{F_{DA} - F_D (1 - f_A)}{F_D f_A}$$

where F_{DA} and F_D are the donor fluorescence intensities measured at 570 nm with and without an acceptor, respectively, and f_A is the fractional labeling of the acceptor [234]. Assuming fractional labeling to be equivalent, the following equation can be used.

Equation 2

$$E = 1 - \frac{F_{DA}}{F_D}$$

The distance (r) between donor and acceptor molecules can be determined from the following equation:

Equation 3

$$E = R_0^6 / (R_0^6 + r^6)$$

where R_0 is the critical Förster distance of the donor and acceptor pair at which the FRET efficiency is 50%. R_0 for the AF555/AF647 pair is 51 Å.

4.5 RESULTS AND DISCUSSION

The effects of NNRTI binding on the association of RT and T/P are unknown due to a lack of crystallography data. There are no crystal structures available for the binary complex of RT with a bound NNRTI or RNA/DNA T/P extending through both the polymerase and RNase H active sites. Therefore, it is difficult to anticipate the structural effects which could modulate RNase H cleavage in the presence of an NNRTI. In light of data suggesting that NNRTIs alter template cleavage during excision (Section 3.0) I wanted to determine the effects of efavirenz binding on the position of the terminated T/P. To do this in the absence of a crystal structure, I utilized FRET.

4.5.1 Characterization of Labeled RT

The distance between two fluorophores can be measured by the efficiency of energy transfer between them. By conjugating a donor molecular to RT and an acceptor molecule to the 5'-end of the T/P the change in distance between the two can be measured. To determine the change in interaction between the RT and T/P in the presence of an NNRTI, I labeled the RT molecule with the maleimide-conjugated AF555 donor at amino acid positions 490 and 560. Both positions are on the superficial layer of the folded enzyme, allowing for energy transfer to the AF647-conjugated 5'-end of the DNA primer.

Point mutations were made in the RTs to remove the naturally occurring cysteine residues at C38 and C280. Site-directed mutagenesis was also used to replace the residues at 490 and 560 to allow addition of the AF555 at specific locations on the enzyme. The RTs containing the mutations and chemical modifications were evaluated for polymerase and RNase H activities

to establish that the modifications did not affect the enzyme functionality (Fig. 16). Previously described polymerase activity assays were used to evaluate the polymerase activity of the modified enzymes in the absence and presence of efavirenz (Section 3.4.1, Fig. 16A). The polymerase and RNase H activity of the labeled enzymes were not affected by the presence of the dyes as determined by comparison to WT enzyme. Additionally, the NNRTI inhibited the polymerase activity of the WT and conjugated enzymes equivalently, decreasing polymerization to 5-10% (Fig. 16A). The appearance of secondary RNase H cleavage products was also enhanced in the presence of efavirenz for all three RTs (Fig. 16B).

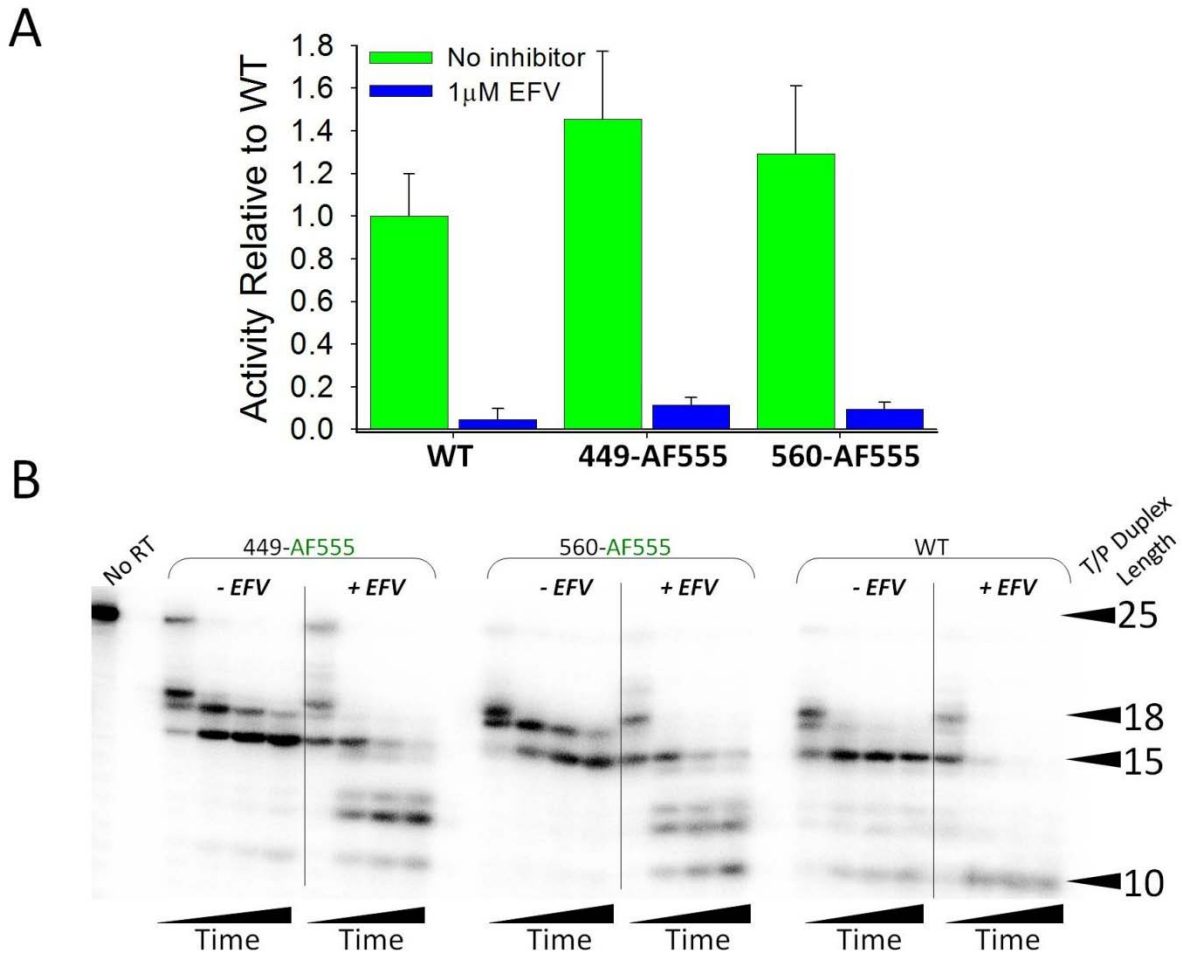


Figure 16. Characterization of modified recombinant RT function.

A, DNA polymerase activity of the WT and modified RTs was performed as described using a fixed time point activity assay in the absence and presence of 1 μ M efavirenz. B, The RNase H activity of WT and modified RTs was evaluated in absence and presence of 1 μ M efavirenz as described. Time points were taken at 1, 5, 10 and 20 minutes.

4.5.2 Effect of NNRTI Binding as Evaluated by FRET Analysis

FRET is governed by the distance between the donor (AF555) and acceptor (AF647) as well as the overlap of the donor emission spectra and the acceptor absorbance spectra. The spectral overlap of the chosen pair (Fig. 17) shows the maximum possible energy transfer between AF555 and AF647. The wavelength at which the donor is most excited does not overlap with the excitation spectra of the acceptor and therefore the excitation of the acceptor is generated by the emission of the donor. Accordingly, the chosen donor/accept pair has a high level of maximal energy transfer according to their excitation and emission spectra and minimal overlap of excitation spectra.

To determine the changes in association of RT with T/P in the presence of an NNRTI, AF-labeled RT was incubated with 1 μ M efavirenz, then bound to a terminated AF-labeled T/P, containing either a DNA or RNA template. The donor molecule was excited at 502 nm and the energy transferred was measured at 570 nm according to the quenching of the donor (Fig. 18). The quenching of the donor molecule is evident by the decrease in emission at 570 nm in the presence of the donor-labeled RT and the acceptor-labeled T/P (Fig. 18, yellow shading). Conversely, the increase in emission from the acceptor molecule in the presence of the donor-labeled RT at 670 nm reveals energy transfer (Fig. 18, orange shading). Using the equations shown in Section 4.4.5, the distance between the two dyes was calculated for each set of conditions (Table 3). In each case, with the exception of the 560 residue in the context of the DNA template, the distance between the two molecules increased when the NNRTI was present, indicating that the RNase H domain and the labeled 5'-end of the primer separated, on both RNA and DNA templates, when the NNRTI-BP was formed by the presence of efavirenz.

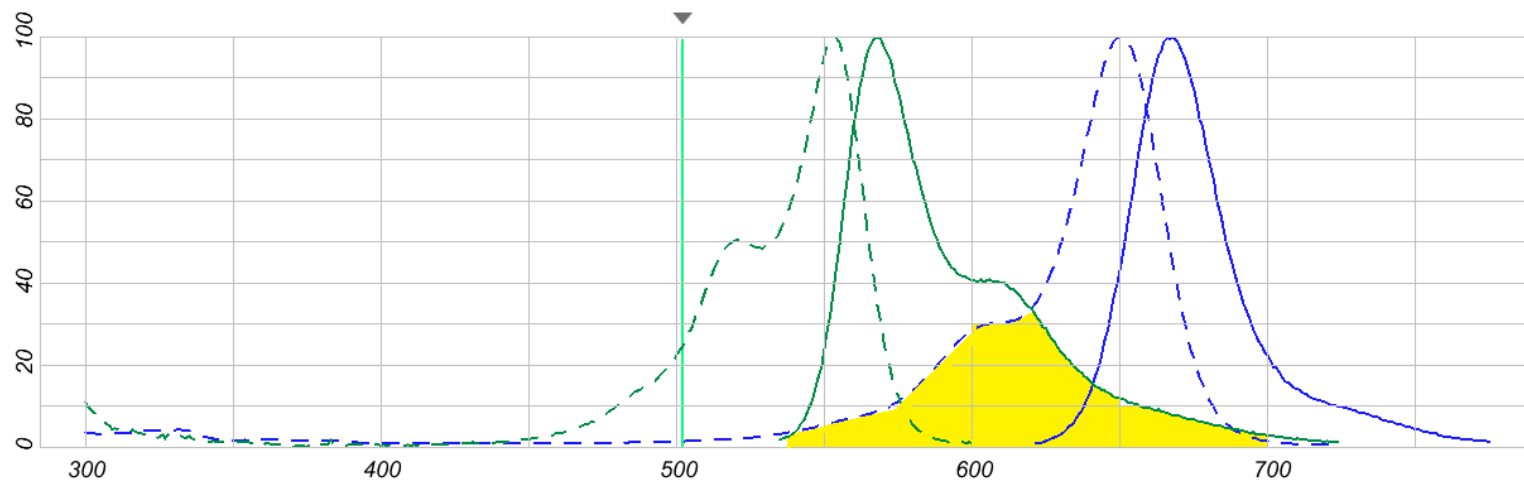


Figure 17. Fluorescence spectra for donor dye AlexaFluro555 and acceptor dye AlexaFluor647.

Donor (AF555, dark green lines) and acceptor (AF647, blue lines) dyes were chosen based on their spectral overlap. The excitation (dashed lines) and emission (solid lines) spectral curves are shown. The highlighted area under the curve is the spectral overlap representative of energy available for transfer when the donor is excited at 502 nm (gray arrow, bright green line). This figure was generated and adapted using the Fluorescence SpectraViewer (<http://www.invitrogen.com/site/us/en/home/support/Research-Tools/Fluorescence-SpectraViewer.html>)

The goal of this study was to use FRET analysis to elucidate how the effect of efavirenz on RNase H activity is contributing to synergy between NRTIs and NNRTIs. My previous data showed that NNRTIs enhance the appearance of the 10-nucleotide hybrid product (Fig. 13), a template that is not a suitable substrate for the excision reaction (Fig. 14). In this study, the change in distance between the RNase H domain of RT and the 5'-end of the DNA primer were measured using FRET. The data show that the binding of efavirenz causes a shift of RT away from the 5'-end of the DNA primer, consistent with the enzyme leaving the polymerase-competent conformation (Fig. 19). Recent FRET studies done by Liu, *et. al*, show that the binding of an NNRTI causes increased dynamic motion of RT on the T/P and destabilizes the polymerase competent mode of binding [122]. Additionally, recent studies on the RNA/DNA T/P equivalent to the PPT RNA primer demonstrated that NNRTIs increase the frequency at which the enzyme “flips” and reorients such that the RNase H domain is poised for removal of the PPT primer [54]. These FRET data do not demonstrate “flipping,” which reinforces the hypothesis that the effect of NNRTIs on the PPT T/P is specific to that structure. Together, these studies demonstrate that NNRTIs are synergistic with NRTIs by two mechanisms: (1) They can accelerate the accumulation of shorted hybrid T/Ps, which are not sufficient substrates for excision, and (2) these increased cleavage events may be a result of NNRTIs destabilizing the polymerase-competent binding mode, which also decreases DNA polymerization and excision.

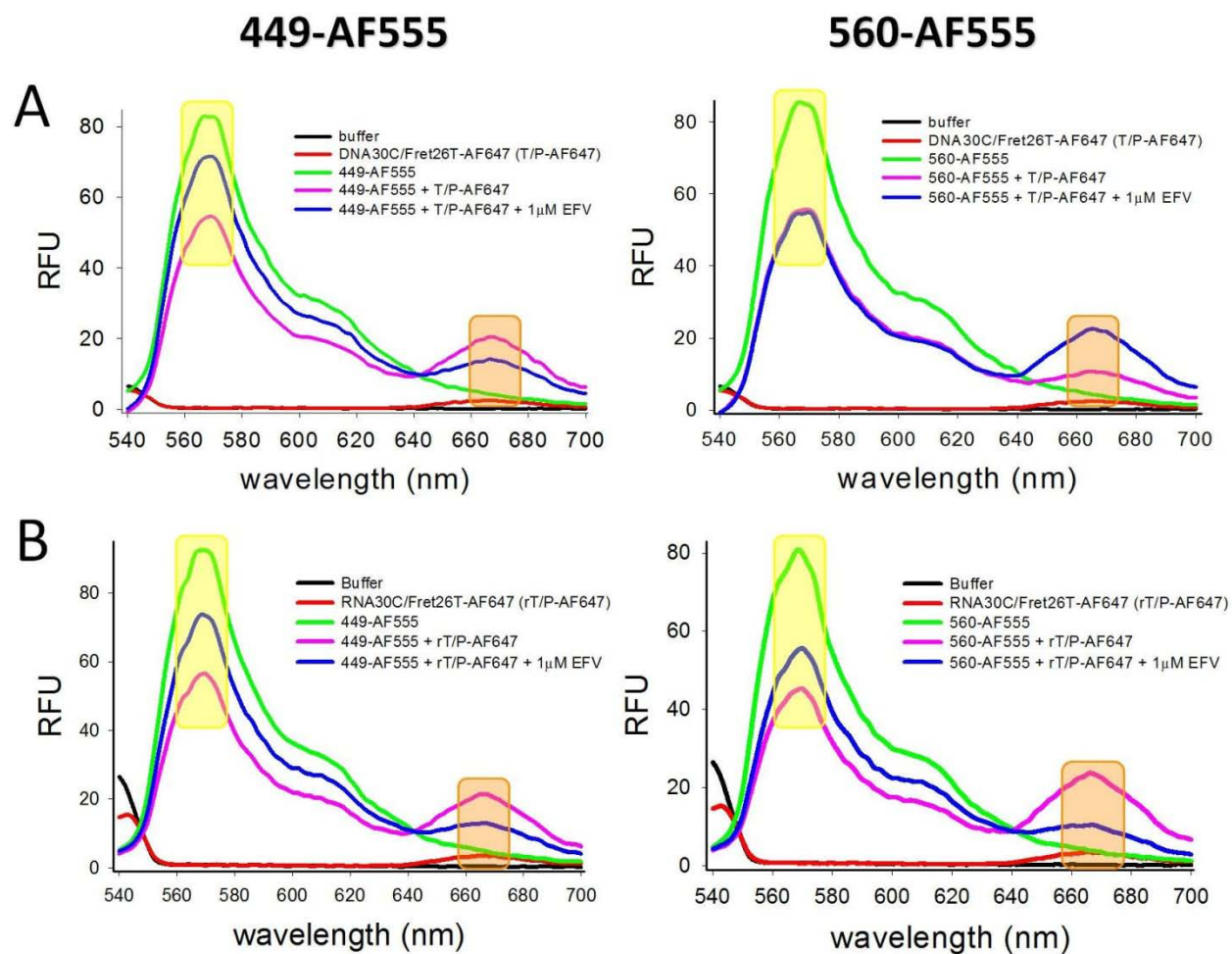


Figure 18. FRET analysis of RT-AF555 bound to a AF-647 labeled T/P in the absence and presence of 1 μ M efavirenz.

RT (800 nM) was allowed to equilibrate with 1 μ M efavirenz in reaction buffer for 5 minutes at 37°C. T/P (200 nM of either DNA/DNA, A, or RNA/DNA, B) was added and incubated at 37°C for an additional 15 minutes. All readings were taken at 37°C. The highlighted regions represent either the donor quenching (yellow) or enhanced acceptor emission (orange).

Table 3. Efficiency of energy transfer (E) and distances (r) calculated.

Template	Labeled Residue	NNRTI present	E	r (Å)	Change in distance
DNA	449	--	0.35	46.10	6.49 Å
		EFV	0.18	39.61	
	560	--	0.35	46.10	0
		EFV	0.35	46.10	
RNA	449	--	0.36	46.20	7.05 Å
		EFV	0.17	39.16	
	560	--	0.44	48.91	4.19 Å
		EFV	0.31	44.72	

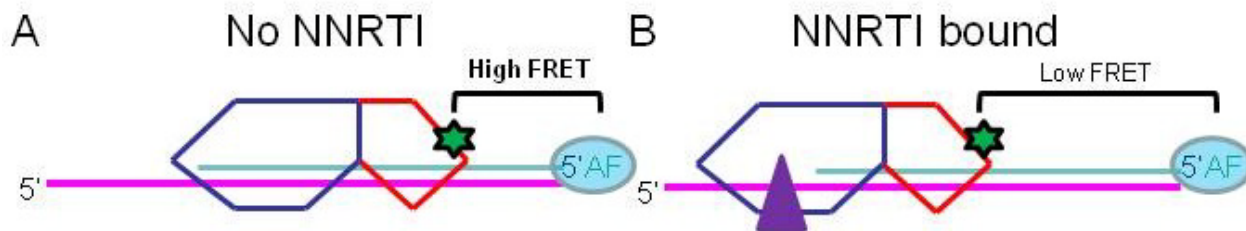


Figure 19. Model depicting effect of efavirenz on T/P association.

A, Under polymerizing conditions, RT binds such that the polymerase active site (pol domain, dark blue) is positioned over the 3' -end of the DNA primer (light blue). The AF555 label (green star) in the RNase H domain (red) is close to the AF647 on the 5' end of the primer (blue circle). This facilitates high energy transfer from one dye to the other. B, When the NNRTI, efavirenz (purple triangle) is bound, the energy transfer is decreased, suggesting that RT shifts away from the 5' end of the primer.

**5.0 CHAPTER THREE: N348I REVERSE TRANSCRIPTASE PROVIDES A
GENETIC PATHWAY FOR HIV-1 TO SELECT TAMS AND MUTATIONS
ANTAGONISTIC TO TAMS**

5.1 PREFACE

This work was presented in part at the *16th Annual Conference on Retroviruses and Opportunistic Infections* February 8-11, 2009, Montreal, Canada (abstract 68; Radzio J, Yap SH, Harrigan R, Tachedjian G and Sluis-Cremer N. N348I in HIV-1 Reverse Transcriptase Counteracts the Antagonism Between Thymidine Analog Mutations and Y181C) and at the *2nd Annual World Summit of Antivirals* July 18-25, 2009 Beijing, China (abstract; Radzio J and Sluis-Cremer N. Mechanisms by which N348I in the connection domain of HIV-1 reverse transcriptase (RT) confers RT inhibitor resistance).

Additionally, this chapter is adapted from Radzio J, Yap S-H, Tachedjian G, Sluis-Cremer N. N348I in Reverse Transcriptase Provides a Genetic Pathway for HIV-1 to Select TAMS and Mutations Antagonistic to TAMS. *AIDS* 2010 Mar 13;24(5):659-67 reprinted with permission from *Wolters Kluwer Health*.

This work is in partial fulfillment of Specific Aim 2.

5.2 ABSTRACT

Several nonnucleoside (e.g. Y181C) and nucleoside (e.g. L74V, M184V) resistance mutations in HIV-1 RT are antagonistic toward TAMs that confer AZT resistance. The N348I mutation in the connection domain of RT also confers AZT resistance, however the mechanisms involved are different than those of TAMs. In this study, we examined whether N348I compensates for the antagonism of the TAM K70R by Y181C, L74V and M184V. The efficiency of AZT-MP excision and RNase H activity of recombinant purified HIV-1 RT containing combinations of K70R and N348I with Y181C, L74V or M184V were assessed using standard biochemical and antiviral assays. As expected, the introduction of the Y181C, L74V or M184V mutations into K70R HIV-1 RT significantly diminished the ATP-mediated AZT-MP excision activity of the enzyme. However, the N348I mutation compensated for this antagonism on RNA/DNA T/P by significantly decreasing the frequency of secondary RNase H cleavages that reduces the overall efficiency of the excision reaction. The acquisition of N348I in HIV-1 RT - which can occur early in therapy, often before TAMs - may provide a simple genetic pathway that allows the virus to select both TAMs and mutations that are antagonistic toward TAMs.

5.3 GOAL OF THE STUDY

Although the mechanism by which the Y181C mutation antagonizes AZT resistance has been described [187-188], it is not known if this mutation also antagonizes the N348I AZT resistance phenotype. Accordingly, in this study my goals were to confirm antagonism of AZT resistance at the polymerase active site using recombinant RTs containing the K70R and Y181C mutations.

Next, I wanted to analyze the effects of N348I on the AZT-MP excision phenotype in combination with the antagonistic mutations. Finally, I wanted to determine the effect of the N348I mutation on RNase H activity in an enzyme harboring the K70R and Y181C mutations.

5.4 MATERIALS AND METHODS

5.4.1 Materials

The K70R, L74V, Y181C, M184V and N348I mutations were introduced into the WT p6HRT-PROT prokaryotic expression vector using the QuikChange Site Directed Mutagenesis Kit from Stratagene (Santa Clara, CA). Full-length sequencing of mutant RTs was performed to confirm the presence of the desired mutations and to exclude adventitious mutations introduced during mutagenesis. The WT, K70R, Y181C, N348I, K70R/Y181C, K70R/Y181C/N348I, K70R/L74V, K70R/L74V/N348I, K70R/M184V, K70R/M184V/N348I HIV-1 RTs were purified as previously described (Section 3.4.1). The protein concentration of the purified enzymes was determined spectrophotometrically at 280 nm using an extinction coefficient (ϵ_{280}) of $260450 \text{ M}^{-1} \text{ cm}^{-1}$, and by Bradford protein assays (Sigma-Aldrich, St. Louis, MO). The polymerase activities of the purified WT and mutant enzymes were essentially identical, performed as described (Section 3.4.1). The AZT-TP was purchased from Sierra Bioresearch (Tuscon, AZ). ATP, dNTPs, and ddNTPs were purchased from GE Healthcare (Piscataway, NJ), and [γ - ^{32}P]ATP was acquired from PerkinElmer Life Sciences (Boston, MA). RNA and DNA oligonucleotides were synthesized by Integrated DNA Technologies (Coralville, IA).

5.4.2 Single-Round AZT-MP Excision Assays

The DNA primer pr26 was 5'-radiolabeled with [γ - ^{32}P]ATP and chain-terminated with AZT-MP to generate pr26-AZT as reported previously (Chapter 3.4.2). P_{AZT} was then annealed to either a 35-nucleotide DNA (T_{DNA}: 5'-AGAATGGAAAATCTCTAGCAGTGGCGCCCGAACAG-3') or RNA (T_{RNA}: 5'-AGAAUGGAAAUCUCUAGCAGUGGCGCCCGAACAG-3') template. ATP-mediated AZT-MP excision assays were carried out by first incubating 20 nM T_{RNA}/pr26-AZT or T_{DNA}/pr26-AZT with 3 mM ATP, 10 mM MgCl₂, 1 μM dTTP and 10 μM ddCTP in a buffer containing 50 mM Tris-HCl (pH 7.5) and 50 mM KCl. Reactions were initiated by the addition of 200 nM WT or mutant RT. Aliquots were removed at defined times, quenched with sample loading buffer (98% deionized formamide, 1 mg/ml each of bromophenol blue and xylene cyanol), denatured at 95 °C for 8 min, and then product was resolved from substrate by denaturing polyacrylamide gel electrophoresis and analyzed as described (Section 3.4.3).

5.4.3 Assay for RT RNase H Activity

WT and mutant RT RNase H activity was evaluated using the same AZT-MP chain-terminated RNA/DNA T/P substrate described above, except the 5'-end of the RNA was ^{32}P -end-labeled. Assays were carried out using 20 nM T_{RNA}/pr26-AZT, 3 mM ATP and 10 mM MgCl₂ in a buffer containing 50 mM Tris-HCl (pH 7.5) and 50 mM KCl. Reactions were initiated by the addition of 200 nM WT or mutant HIV-1 RT. Aliquots were removed, quenched at varying times, and analyzed as described (Section 3.4.3).

5.4.4 RT Polymerization Products Formed Under Continuous DNA Polymerization

Conditions

Heteropolymeric RNA-dependent or DNA-dependent DNA polymerase T/Ps were prepared as reported previously [171, 235]. DNA polymerization reactions were carried out by incubating 20 nM heteropolymeric T/P complex with 1 μ M concentration of each dNTP, 2 μ M of AZT-TP, 3 mM ATP and 10 mM MgCl₂ in buffer containing 50 mM Tris-HCl (pH 7.5) and 50 mM KCl. Reactions were initiated by the addition of 200 nM WT or mutant RT. After defined incubation periods, aliquots were removed from the reaction tube and quenched with equal volumes of gel loading dye. Products were separated by denaturing gel electrophoresis and quantified.

5.5 RESULTS AND DISCUSSION

The Y181C mutation in RT increases HIV-1 sensitivity to AZT even when multiple TAMs are co-selected on the same genome [186]. Previous biochemical studies suggested that this phenotype was due to the Y181C mutation decreasing the AZT-MP excision activity of both WT and D67N/K70R/T215F/K219Q HIV-1 RT by directly impacting ATP binding and/or the rate of AZT-MP excision [187-188]. Because the mechanism by which N348I in HIV-1 RT confers AZT resistance is different from that conferred by TAMs, I hypothesized that Y181C might not antagonize the excision activity of N348I HIV-1 RT and, accordingly, that N348I may compensate for the Y181C-mediated antagonism of TAMs. To investigate this hypothesis, I examined the ability of recombinant HIV-1 RT containing combinations of Y181C, K70R and N348I to excise AZT-MP using established biochemical assay systems. In this study, I focused

on a single TAM (i.e. K70R) to determine how N348I influenced the interplay between TAMs and Y181C at the onset of resistance development. In this regard, the K70R mutation is one of the first TAMs to appear under AZT drug pressure [236]. Furthermore, K70R in HIV-1 RT is associated with a strong ATP-mediated excision phenotype *in vitro* [237].

5.5.1 N348I Rescues the Excision Phenotype on RNA Templates

I first examined the ability of WT, K70R, Y181C, K70R/Y181C, and K70R/Y181C/N348I HIV-1 RT to excise AZT-MP and rescue DNA synthesis from chain-terminated DNA/DNA and RNA/DNA T/Ps (Fig. 20). As described previously, Y181C HIV-1 RT unblocked AZT-MP chain-terminated primers inefficiently on both DNA/DNA and RNA/DNA T/Ps (Fig. 20B and C). As expected, Y181C also antagonized the ability of K70R RT to excise AZT-MP and recover DNA synthesis, although this defect was more pronounced on an RNA/DNA T/P than on a DNA/DNA T/P (Fig. 20B and C). Introduction of the N348I mutation into RT containing K70R/Y181C RT increased the enzymes excision activity on the RNA/DNA T/P but not on the DNA/DNA T/P (Fig. 20B and C).

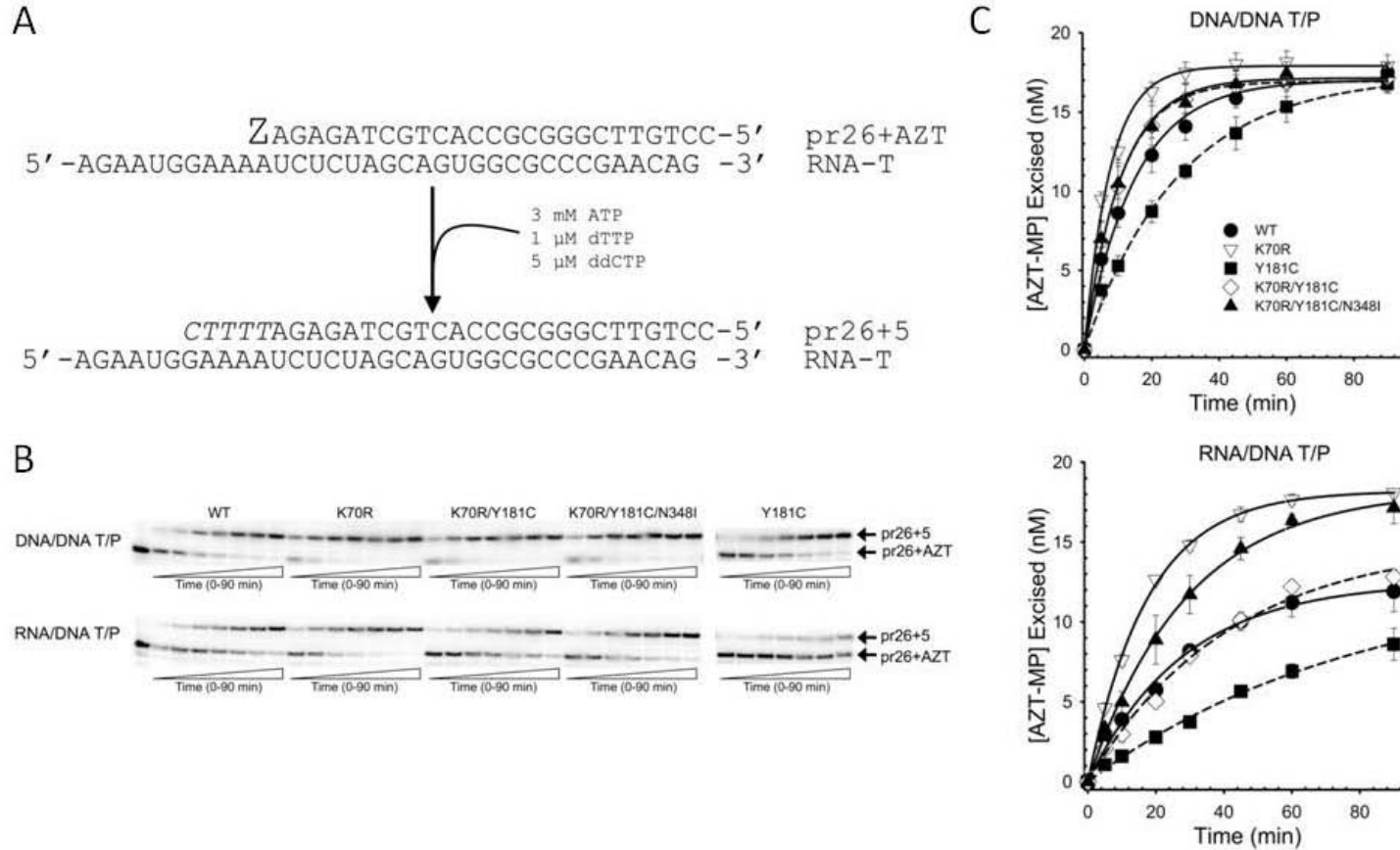


Figure 20. ATP-mediated AZT-MP excision activity of HIV-1 RT on RNA/DNA and DNA/DNA T/Ps

A, Schematic representation of the ATP-mediated excision assay used in this study. AZT-MP is designated as “Z” B, Representative autoradiogram of AZT-MP excision reactions carried out by WT and mutant RT on RNA/DNA and DNA/DNA T/Ps. The reaction times were 3, 5, 10, 15, 30, 60 and 90 min. C, Isotherms of ATP-mediated AZT-MP excision reactions carried out by WT and mutant HIV-1 RT on a DNA/DNA T/P (left-hand curve) and on an RNA/DNA T/P (right-hand curve). Data are the mean \pm standard deviation from at least three independent experiments

5.5.2 N348I Decreases RNase H Cleavage Alone and When Combine with Antagonistic Mutations.

Our group, as well as those of Drs. Matthias Götte [204] and Vinay Pathak [238], have demonstrated that the N348I mutation in HIV-1 RT increases AZT resistance by decreasing the frequency of secondary RNase H cleavages that significantly reduce the RNA/DNA duplex length of the T/P and diminish the efficiency of AZT-MP excision (Fig. 14). Previously, I delineated the relationship between AZT-MP excision efficiency and RNase H activity on the RNA/DNA T/P substrate used in these experiments. These studies showed that the primary polymerase-dependent RNase H cleavage by RT does not impact the AZT-MP excision efficiency of the enzyme, but subsequent cleavages that reduce the RNA/DNA duplex length to less than 12 nucleotides abolish AZT-MP excision activity (Fig. 14). In light of these data, I next evaluated the RNase H activity of WT and mutant RT that occurred during the ATP-mediated excision reactions described in Figure 18. A schematic of the cleavage positions are depicted in Figure 21A. As reported previously, N348I significantly reduced the frequency of cleavage events that decreased the RNA/DNA duplex to 10 nucleotides (Fig. 21B). In comparison with the WT enzyme, the K70R and Y181C mutations had minimal impact on the RNase H activity of RT (Fig. 21). Introduction of the N348I mutation into K70R/Y181C RT, however, significantly reduced the frequency of this terminal cleavage event (Fig. 21), which is consistent with the notion that N348I in HIV-1 RT impacts the efficiency of the AZT-MP excision reaction by RNase H-dependent mechanism.

This study suggests that the acquisition of N348I in HIV-1 RT, which can occur early during therapy often before TAMs [201], may provide a simple genetic pathway that allows the

virus to select both TAMs and mutations that are antagonistic to TAMs (e.g. L74V, Y181C and M184V). This finding is consistent with recent studies that show a strong association between N348I with TAMs, M184V/I and Y181C and that N348I is frequently observed in AZT- and/or ddI-containing therapies [203]. In fact, in the Stanford University HIV Database, N348I is frequently observed in viruses from patients failing combination antiretroviral therapies that contained an NNRTI and either AZT/3TC (frequency of N348I = 22.2%) or AZT/ddI (frequency of N348I = 9.5%). Finally, this study further highlights the complex but potentially important role of mutations in the C-terminal domains of HIV-1 RT drug resistance.

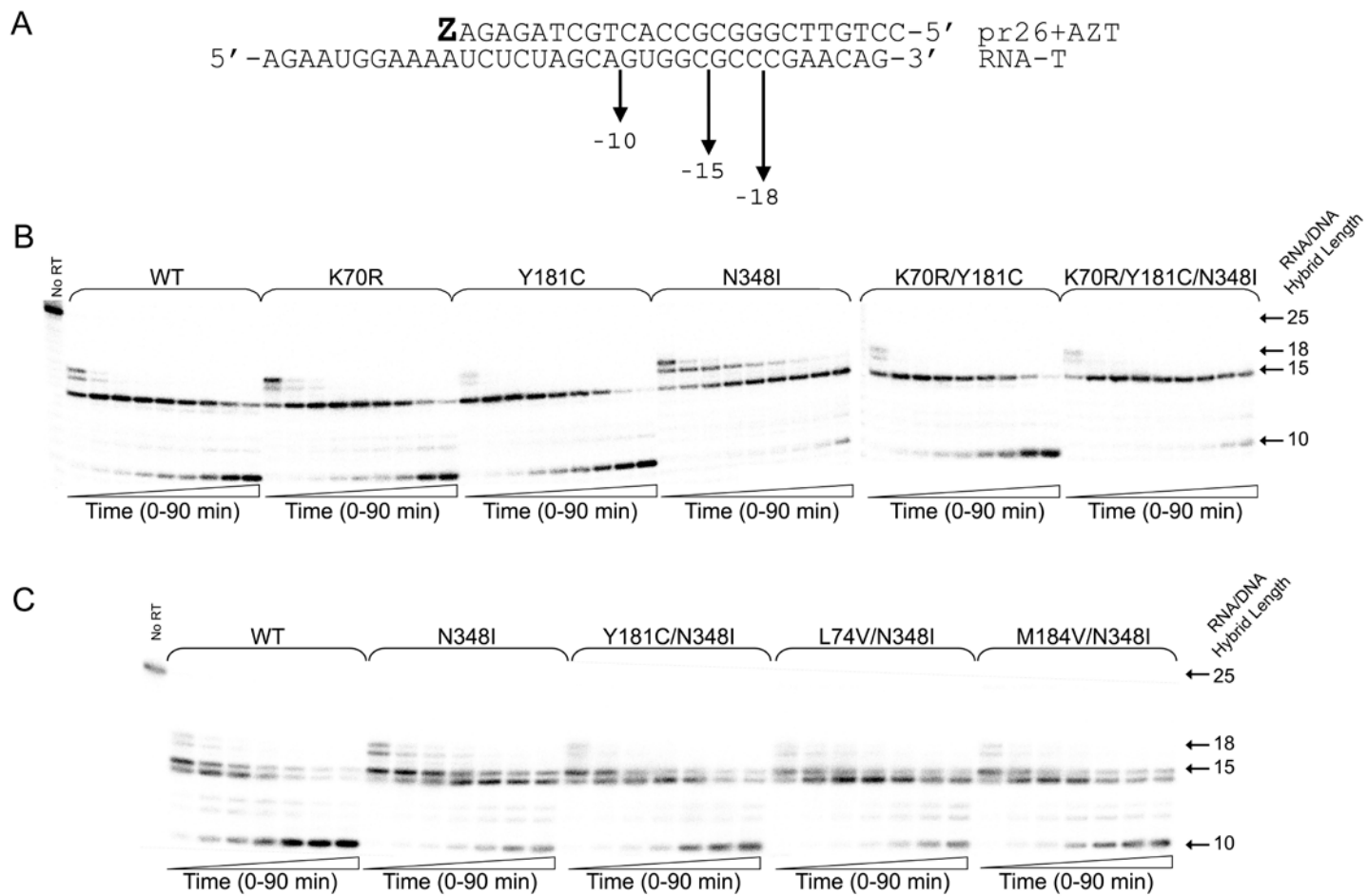


Figure 21. RNase H cleavage activity of HIV-1 RT that occurs during the AZT-MP excision reaction.

A, Schematic illustrating the location of the RNase H cleavage sites in the RNA template. B and C, Representative autoradiogram of the RNase H cleavage activity of the WT and mutant HIV-1 RTs. The reaction times were 1, 3, 5, 10, 20, 30, 45, 60 and 90 min.

In the experiments described above, I evaluated the AZT-MP excision and RNase H cleavage activities of the WT and mutant enzymes on a defined (in terms of sequence and length) RNA/DNA T/P. Because both excision and RNase H activities of RT are likely affected by nucleic acid sequence and length, I next evaluated the ability of WT and mutant enzymes to synthesize DNA in the presence of AZT-TP and ATP using a long heteropolymeric RNA template, corresponding to the HIV-1 sequence used for γ -ssDNA synthesis, and primed with a DNA oligonucleotide. The 173- nucleotide incorporation events needed to produce full-length DNA product in this assay system allow for multiple AZT-TP incorporation and AZT-MP excision events to occur during the formation of full-length final product [171, 235]. In the presence of 3 mM ATP, the N348I and K70R enzymes were significantly more efficient than WT RT in synthesizing full-length DNA product (Fig. 22). By contrast, both the Y181C and K70R/Y181C enzymes were less efficient in generating full-length DNA product. Consistent with the data in Figure 20, the N348I mutation partially compensated for the antagonism between K70R and Y181C: more final DNA synthesis product was observed for the K70R/Y181C/N348I RT compared to the WT, Y181C and K70R/Y181C RTs (Fig. 22).

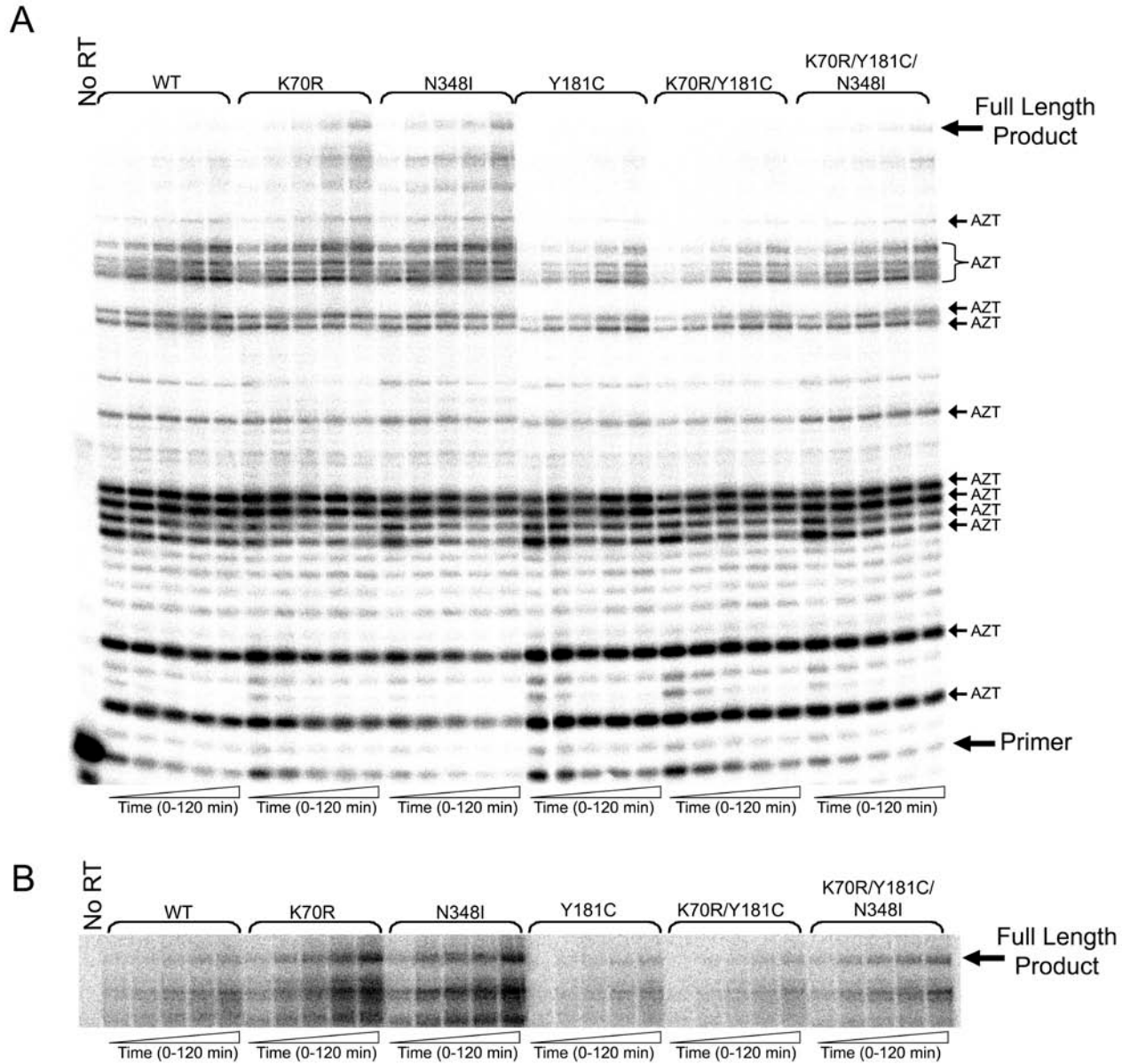


Figure 22. Autoradiogram of steady-state DNA synthesis by WT and mutant HIV-1 RT in the presence of AZT-TP and 3 mM ATP

A, Complete autoradiogram indicating primer, final product, and AZT-MP chain-termination sites. The time points for the reactions were 15, 30, 60, 90 and 120 min. B, Different contrast of the final product bands from the autoradiogram presented in (A).

Taken together, these data show that the Y181C mutation does not antagonize the ability of N348I to excise AZT-MP via an RNase H-dependent mechanism in HIV-1 RT containing K70R. Accordingly, N348I in HIV-1 RT compensates for the antagonism between TAMs and Y181C.

5.5.3 N348I in HIV-1 RT Also Compensates for the Antagonism of K70R by L74V and M184V

Previous studies have demonstrated that the NRTI discrimination mutations L74V and M184V antagonize the AZT-MP excision phenotype of RT containing TAMs. To determine whether L74V- or M184V-mediated antagonism of TAMs could also be rescued by the N348I mutation, I compared the AZT-MP excision and RNase H activities of K70R/L74V HIV-1 RT with K70R/L74V/N348I HIV-1 RT and K70R/M184V HIV-1 RT with K70R/M184V/N348I HIV-1 RT (Fig. 23, Fig. 24). Consistent with previously published data [189-190, 239], the introduction of either the L74V or the M184V mutations into HIV-1 RT containing K70R dramatically decreased the ATP-mediated AZT-MP excision activity of HIV-1 RT (Fig. 23). However, the N348I mutation partially compensated for the antagonism of K70R by M184V (Fig. 23A) and completely alleviated the antagonism of K70R by L74V (Fig. 23B). As expected, N348I decreased the formation of the terminal RNase H cleavage product that reduced the RNA/DNA duplex to 10 nucleotides in length for both the K70R/M184V (Fig. 24A) and K70R/L74V (Fig. 24B) RTs.

Taken together, these findings demonstrate that neither L74V nor M184V antagonizes the ability of N348I in HIV-1 RT to excise AZT-MP via an RNase H-dependent mechanism. Therefore, N348I in HIV-1 RT can also compensate for the antagonism of TAMs by L74V and M184V.

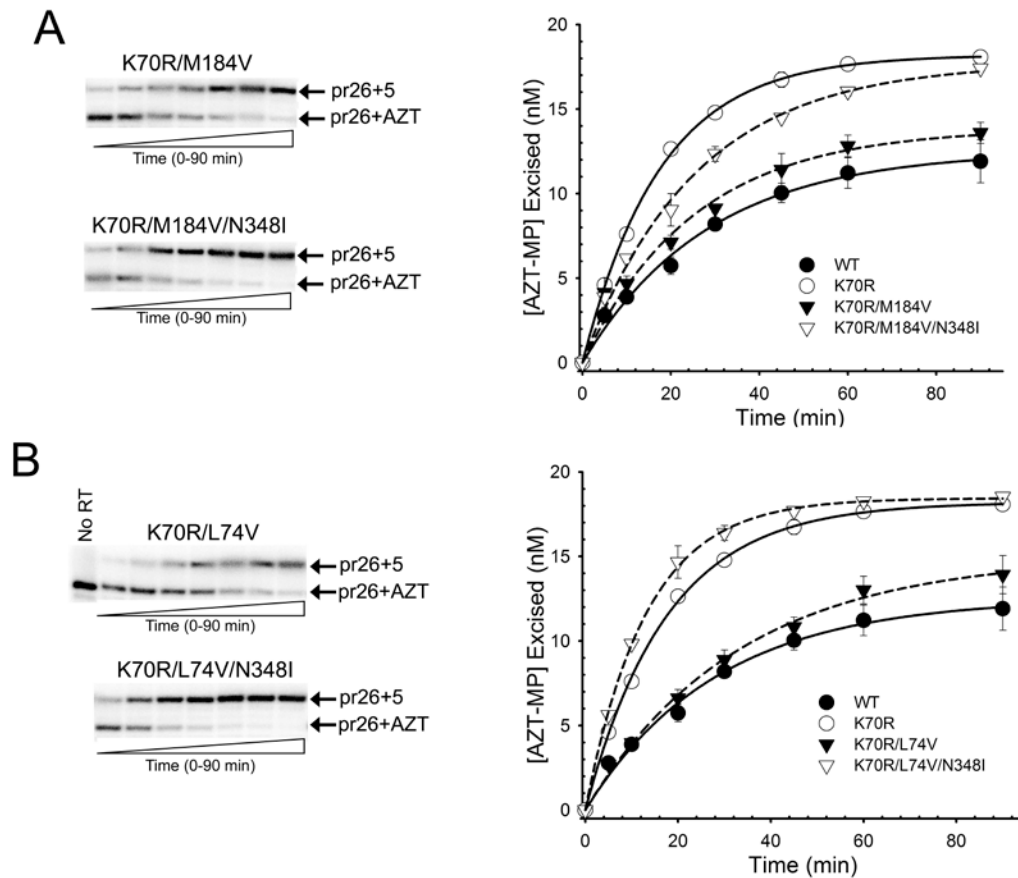


Figure 23. AZT-MP excision activities of WT and mutant HIV-1 RT on an RNA/DNA T/P.

A, The autoradiogram shows the AZT-MP excision reactions carried out by K70R/M184V and K70R/M184V/N348I HIV-1 RT. The reaction times were 3, 5, 10, 20, 30, 60 and 90 min. The isotherm shows ATP-mediated AZT-MP excision reactions carried out by WT, K70R, K70R/M184V and K70R/M184V/N348I HIV-1 RT. B, The autoradiogram shows the AZT-MP excision reactions carried out by K70R/L74V and K70R/L74V/N348I HIV-1 RT. The reaction times were 3, 5, 10, 20, 30, 60 and 90 min. The isotherm shows ATP-mediated AZT-MP excision reactions carried out by WT, K70R, K70R/L74V and K70R/L74V/N348I HIV-1 RT. Data are the mean \pm standard deviation from at least three independent experiments.

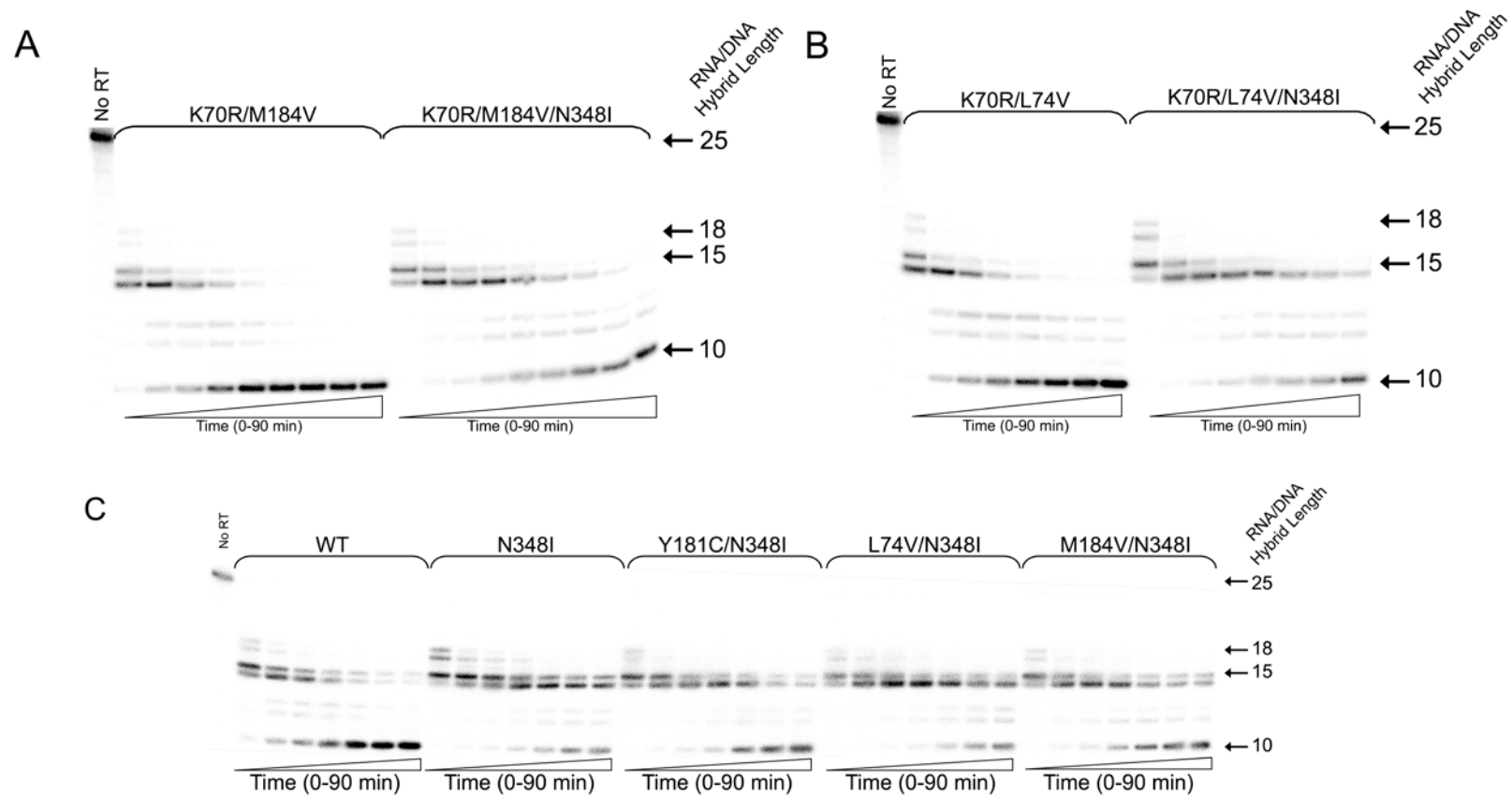


Figure 24. RNase H cleavage during ATP-mediated AZT-MP excision by WT and mutant HIV-1 RT.

A, Representative autoradiogram of the RNase H cleavage activities of K70R/LM184V and K70R/M184V/N348I HIV-1 RT. The reaction times are 1, 3, 5, 10, 20, 30, 40, 60 and 90 min. B, Representative autoradiogram of the RNase H cleavage activities of K70R/L74V and K70R/L74V/N348I HIV-1 RT. The reaction times are 1, 3, 5, 10, 20, 30, 60 and 90 min. C, Representative autoradiogram of the RNase H cleavage activities of WT, N348I, Y181C/N348I, L74V/N348I and M184V/N348I HIV-1 RT. The reaction times are 1, 3, 5, 10, 20, 30, 60 and 90 min.

6.0 CHAPTER FOUR: SUBUNIT-SPECIFIC MUTATIONAL ANALYSIS OF RESIDUE N348 IN HIV-1 REVERSE TRANSCRIPTASE

6.1 PREFACE

This work was presented in part at the XVIII *International HIV Drug Resistance Workshop*. June 9-12, 2009. Fort Myers, FL (abstract published in Radzio J, Tachedjian G, Sluis-Cremer N. Mutational Analysis of Residue Asn348 in HIV-1 Reverse Transcriptase. *Antiviral Therapy* 2009; 14 Suppl 2;A32) and at the *International HIV and Hepatitis Virus Drug Resistance Workshop and Curative Strategies*. June 8-12, 2010. Dubrovnik, Croatia (abstract published in Radzio J, Sluis-Cremer N. Subunit Specific Mutational Analysis of Residue N348 in HIV-1 Reverse Transcriptase. *Antiviral Therapy* 2010; 15 Suppl 2; A79)

This work is in partial fulfillment of Specific Aim 2.

6.2 ABSTRACT

N348I in HIV-1 RT confers both AZT and nevirapine resistance. Several studies have demonstrated that the AZT resistance phenotype is due to the decreased appearance of the secondary RNase H cleavage products of the N348I mutant RT [201, 204, 240]. The mechanism(s) by which N348I in RT confer nevirapine resistance are poorly understood, although Nikolenko *et al* suggest that it also may be related to the enzyme's RNase H activity [241]. Furthermore, it is not clear whether it is N348I in the p66, p51 or both subunits of RT that is responsible for the resistance phenotypes. Here, mutational analyses of residue Asn348 were performed to address these questions. The N348A, N348I, N348L N348E, N348R or N348Q mutations were introduced into WT HIV-1 RT. RTs were purified in which the mutations were present in both subunits. RTs with the N348I, N348A N348E or N348Q mutations in p66 only, and one RT with N348L present in p51 only were also purified. The polymerase and RNase H activities of the enzymes, as well as their sensitivities to AZT and nevirapine, were determined using appropriate biochemical assays. For the RTs that harbored mutations in both subunits, it was determined that N348I and N348L decreased the enzyme's RNase H activity and increased its capacity to excise AZT-MP, using ATP as a pyrophosphate donor. In contrast, the N348A and N348Q mutations exhibited RNase H and AZT-MP excision activities comparable to WT enzyme. All of the mutant enzymes containing the mutations in both subunits or p51 alone exhibited nevirapine resistance. The RTs that contained mutations in p66 only, exhibited RNase

H activities similar to WT. In contrast, the RT with N348L in the p51 subunit exhibited decreased RNase H activity. This study suggests that AZT and nevirapine resistance may be due to N348I in the p51 but not the p66 subunit of HIV-1 RT.

6.3 GOAL OF THE STUDY

Our group has previously demonstrated that the N348I mutation in the connection domain of HIV-1 RT confers both AZT and nevirapine resistance [201]. Previous biochemical studies by us [201, 240] and others [204, 238] have suggested that N348I confers AZT resistance, in part, via an RNase H-dependent mechanism. Recent biochemical studies have suggested mechanisms of nevirapine resistance conferred by N348I [241-242]. However, these studies fail to demonstrate empirical evidence to validate their model and are unable to elucidate which subunit is contributing to the resistance phenotype. Residue N348 in both subunits of HIV-1 RT resides distal to the DNA polymerase active site, the RNase H active site, the T/P binding tract and the NNRTI-binding pocket (Fig. 10). Therefore, the structural mechanism by which N348I confers dual AZT/nevirapine resistance is not known. There is no structural data available for RT in a binary complex with an RNA/DNA hybrid T/P which extends through the RNase H active site. Therefore, the mechanisms by which N348I decreases RT RNase H activity and drug susceptibility cannot be inferred. Furthermore, it is not clear whether it is N348I in the p66, p51 or both subunits of RT that is responsible for the resistance phenotypes. However, modeling studies performed in our lab suggest that the position of the Asn348 residue in the p51 subunit may affect interaction with the RNA/DNA T/P. The goal of this study was to determine the relevance of the N348 residue in the p51 and p66 subunits and determine how it relates to an

effect on RNase H activity as well as NNRTI resistance. The effect of substitutions at Asn348 in the p51 subunit was evaluated using modeling studies, followed by biochemical analysis. Mutational analyses of residue Asn348 were carried out to specifically address structure-activity-resistance relationships.

6.4 MATERIALS AND METHODS

6.4.1 Materials

Nevirapine was obtained from the AIDS Research and Reference Reagent Program, National Institute for Allergy and Infectious Diseases, National Institutes of Health (NIH). The AZT-TP was purchased from TriLink Biotechnologies. All other nucleotides were purchased from GE Healthcare.

6.4.2 Cloning, Expression and Purification of Recombinant HIV-1 RT

6.4.2.1 Asn348 Mutations in Both Subunits

The N348A, N348E, N348I, N348L, N348Q and N348R mutations were introduced into WT HIV-1_{LAI} RT in p6HRT-PROT by GenScript (Piscataway, NJ). Recombinant WT and mutant HIV-1 RT was expressed as previously described (Chapter 3.4.1). All enzymes were found to exhibit similar levels of DNA polymerization activity based on activity assays (except for the N348R and N348E which were left out of subsequent studies).

6.4.2.2 Subunit-Specific Mutagenesis

RTs in which the N348I, N348A, N348E or N348Q mutations were present in p66 only, and one RT in which N348L was present in p51 only were also purified. Chimeric RTs containing mutations in either p51 or p66 were expressed from the pETDuet-1 vector system purchased from EMD Biosciences (San Diego, CA). The WT or mutant p66 subunit was cloned into the MCS 1 by PCR from the p6HRT-PROT vector. Primers used to amplify the full length gene contained restriction sites for 5'-end BamH 1 and 3'-end Hind III. The WT or mutant p51 subunit was cloned by PCR from p6HRT into the pT7-FLAG-1 expression system purchased from Sigma-Aldrich (St. Louis, MO) to acquire the 5'FLAG tag. The primers used to amplify the p51 subunit contained the 5'-Hind III and 3'-Sac I restriction sites. The 5'-FLAG-p51 was then subcloned by PCR from the pT7-FLAG-1 vector into the MCS2 of the pETDuet vector containing the p66 subunit. Primers used to amplify the p51 subunit with the 5'FLAG contained the 5'-Nde I and 3'-Avr II restriction sites. The sequence of the subunits was confirmed using vector-specific primers. The chimeric RTs were expressed in BL21(DE) *E coli* by induction with 1 mM IPTG at 37°C overnight and purified to homogeneity as previously described (Chapter 3.4.1). Polymerization activity was compared using the activity assay previously described (Chapter 3.4.1).

6.4.3 Recombinant Enzyme Characterization

The sensitivity of the WT and mutant enzymes to nevirapine inhibition was determined using an ELISA plate assay. The template (RNA-T, Chapter 3.4.2) and the pr26 primer (Chapter 3.4.2) containing a 5' end biotin tag used in the assay were purchased from Integrated DNA Technologies. RT (15 nM) was preincubated with various concentrations of nevirapine (0.2 μM-

10 μ M) in reaction buffer for 5 minutes at 37°C. One micromolar dNTPs (a mixture of dATP, dCTP, dGTP and BR-conjugated dUTP) and 200 nM T/P were added and polymerization continued for 20 minutes at 37°C. The reactions were quenched using 0.25 M EDTA and the volume of the reaction was transferred to a 96-well streptavidin coated plate. The plate was incubated at room temperature to allow the biotinylated primer to bind to the wells. The wells were washed, 3 times each, with 5.0 M NaOH followed by wash buffer (1x PBS, 0.5% BSA and 0.2% Tween) to denature and remove the template strand. An anti-Br HRP-conjugated antibody was used to detect the incorporated Br-dUTP and was quantified using chemiluminescence on SpectraMax M2 from Molecular Devices.

6.4.4 Evaluation of RT Polymerization Products Formed Under Continuous DNA

Polymerization Conditions

Heteropolymeric RNA/DNA T/P was prepared as described previously (Section 5.4.4). DNA polymerization reactions were carried out by incubating 200 nM WT or mutant RT with 20 nM heteropolymeric T/P complex in 50 mM Tris-HCl (pH 8.0) and 50 mM KCl for 5 min before the addition of 5 μ M of each dNTP, 2.5 μ M AZT-TP, 3.0 mM ATP, and 10 mM MgCl₂. After defined incubation periods, aliquots were removed from the reaction tube and quenched with equal volumes of gel loading dye. Products were separated by denaturing gel electrophoresis and quantified with a Bio-Rad GS525 Molecular Imager.

6.5 RESULTS AND DISCUSSION

Modeling analyses performed in our lab suggest that mutations at the Asn348 residue in the p51 subunit may cause alterations in RT which could indirectly effect the association of RT and T/P. Recently, a crystal structure of the human RNase H1 was solved in complex with an RNA/DNA substrate which extends directly into the enzyme's active site [33]. Because of the similarity between the human RNase H1 and the RNase H domains of HIV-1 RT, the authors were able to model an RNA/DNA duplex into HIV-1 RT that extends from the RNase H active site into the DNA polymerase active site. In this model, the β 14- β 15 loop (containing the N348 residue) of the p51 subunit of RT directly interacts with the RNA template backbone. Specifically, the Y342, P345 and F346 from this loop directly contact the RNA template backbone. These coordinates were then used to model in N348A, N348E, N348I, N348L, N348Q and N348R substitutions. When the N348I mutation is introduced into the p51 subunit in this structure by molecular modeling (Fig. 25A), the position of the β 14- β 15 loop is shifted such that P345 and F346 no longer contact the RNA template. This loop distortion appears to be due to the bulky size of the isoleucine side-chain because the introduction of an alanine at codon 348 does not appear to influence interactions with the RNA template (Fig. 25B). However, introduction of a leucine at this position distorts the loop structure so that only the F346 residue no longer interacts with the template. (Fig. 25C).

To validate this model, mutational analyses of residue Asn348 were performed. The polymerase and RNase H activities of the enzymes, as well as their sensitivities to AZT and nevirapine, were determined using appropriate biochemical assays.

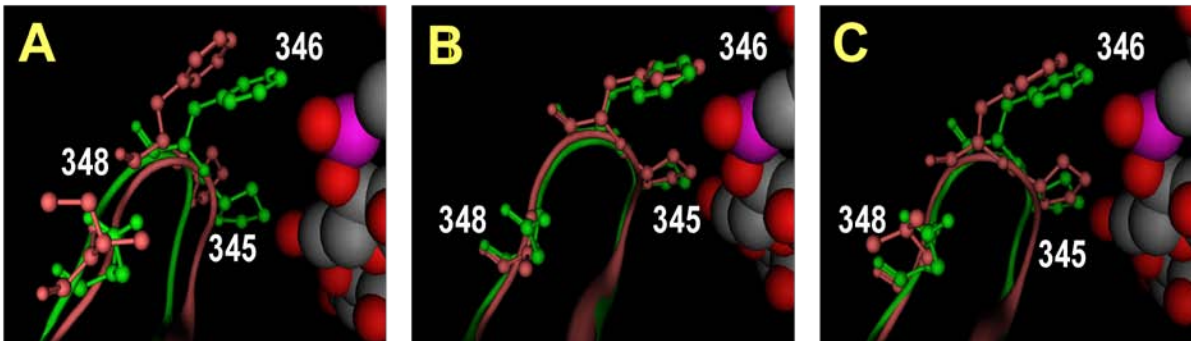


Figure 25. Molecular models of the β 14- β 15 loop in the p51 subunit of HIV-1 RT in complex with an RNA/DNA duplex that extends into the RNase H active site.

The WT (green) structure is overlaid with either N348I (A), N348A (B) or N348L (C), shown in pink. The coordinates for this structure were kindly provided by Dr M. Nowotny (NIDDK, NIH).

6.5.1 Comparison of Polymerization Activity.

The polymerization capacity of each of the enzymes was assessed using the previously described activity assay (Section 3.4.1). The N348A, N348I, N348L and N348Q enzymes harboring mutations in both subunits exhibited comparable DNA polymerase activities to WT HIV-1 RT (Fig. 26A). By contrast, the N348E and N348R enzymes exhibited significantly diminished DNA polymerase activities and, accordingly, were excluded from subsequent analyses. None of the subunit specific mutations decreased RT polymerase activity (Fig. 26B). Interestingly, the N348E mutation produced a functional enzyme when it was present in only the p66 subunit, suggesting that it's affect on the loop position in the p51 subunit causes negative interactions with the T/P. The modeling data show that this substitution caused the loop position to move away from the RNA template.

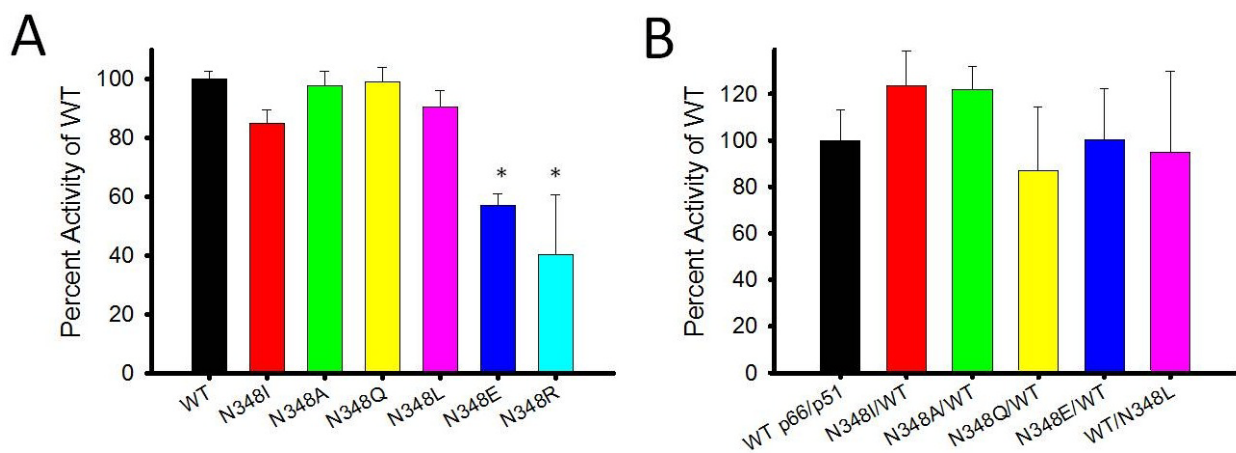


Figure 26. Polymerase activity of Asn348 mutants.

A, Polymerase activity of Asn348 mutants when the mutation is in both the p66 and p51 subunits (p -value <0.01).

B, Polymerase activity of Asn348 mutants when the mutation is in the p66 or the p51 subunit.

6.5.2 Evaluation of RNase H activity

It is known that the N348I mutation present in both subunits decreases the appearance of the terminal band which appears during RNase H cleavage using our T/P system (Fig. 24C). To determine if the loop containing this residue modulates this effect, the RNase H activity of the recombinant RTs was evaluated as described. When the mutations were in both subunits, a decrease in the appearance of the 10 nucleotide cleavage products relative to the WT was evident for the N348I and N348L mutations (Figure 27A). This observation could be the result of the fact that both of these substitutions at the N348 residue cause the β 14- β 15 loop in the p51 subunit to move away from the RNA template backbone. To confirm that it was the mutation in the p51 subunit causing this effect, the assay was repeated with the RTs containing subunit-specific mutations. The RTs that contained mutations in p66 only (including N348I), exhibited

RNase H activities similar to WT. By contrast, the RT with N348L in the p51 subunit exhibited decreased RNase H activity (Fig. 27B).

Based on this data, the decrease we see in RNase H activity when N348I is present is the result of the isoleucine replacement in the the β 14- β 15 loop in the p51 subunit. Although I was unable to directly test this using an enzyme containing the N348I mutation in the p51 subunit, the N348L mutation, which has a similar effect on the position of the loop based on our model, decreased the RNase H activity in the p51 subunit. Interestingly the N348I change causes both the P345 and F346 residues to lose contact with the RNA template. However, the N348L substitution allows the P345 residue to maintain contact suggesting that the loss of contact between the F346 residue and the RNA template is responsible for the decrease in activity. As discussed earlier, the N348I mutation can allow extended time for excision because the RNA/DNA hybrid duplex is maintained for a longer period of time.

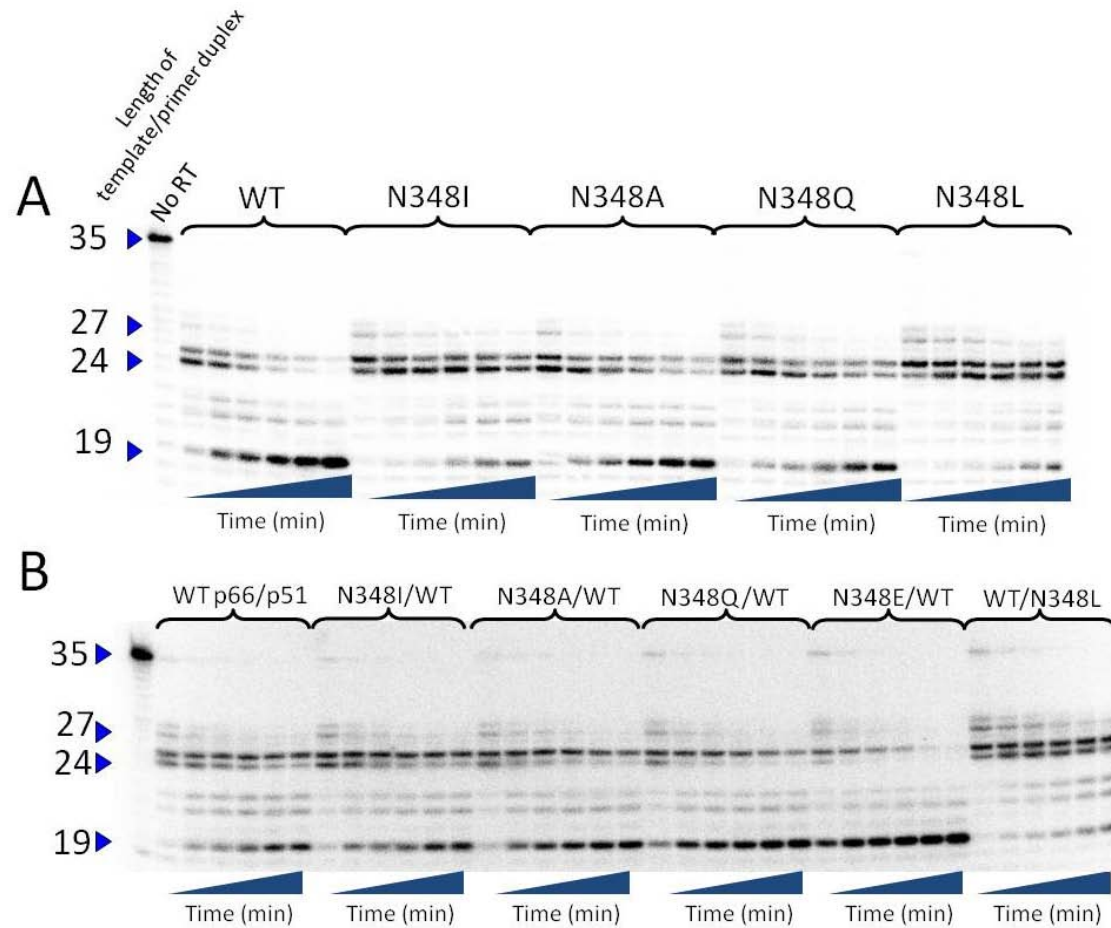


Figure 27. RNase H cleavage activity of WT and N348 mutant HIV-1 RT.

A, Autoradiogram of the cleavage activity of WT and N348 mutant HIV-1 RT where the mutation shown is in both RT subunits B, Autoradiogram of the cleavage activity of HIV-1 RT where the subunits were cloned in separate MCS in the pETDuet expression system, allowing the N348 mutations to be expressed in each subunit separately.

6.5.3 Analysis of RT Polymerization Under Continuous DNA Polymerization Conditions in the Presence of AZT-TP

I analyzed steady-state synthesis by both WT and mutant enzymes in the presence of AZT-TP and ATP. Heteropolymeric RNA template, corresponding to the HIV-1 sequence used for ssDNA synthesis, primed with a DNA oligonucleotide was used to confirm that the increased excision was a result of the decreased RNase H activity. The 173- nucleotide incorporation events needed to produce full-length DNA product in this assay system allow for multiple AZT-TP incorporation and AZT-MP excision events during the formation of full-length final product. The full length product was separated on a polyacrylamide gel and the data was analyzed by phosphoimaging analysis. Figure 28 shows the amount of completed DNA product over time in relative density units (RDUs). For the enzymes harboring the mutations in both subunits, the N348I and N348L RTs synthesized significantly greater amounts of full-length DNA as compared to the WT or the other mutant enzymes (Fig. 28A). The efficiency of AZT-MP excision can be ordered: N348I RT > N348L RT > N348Q RT > WT > N348A RT. By contrast, the enzyme harboring the N348L mutation in the p51 subunit was the only one to display high levels of completed product when compared with the other chimeric enzymes (Fig. 28B).

As expected, the relative AZT-MP excision activity for each enzyme correlated with its RNase H activity, suggesting that the AZT resistance conferred by the N348 residue is an indirect result of the decreased RNase H activity. Previous studies have demonstrated that N348I increases the processivity of the enzyme [204]. This could also appear to increase the AZT resistance in this assay, although it is not known whether this observation is a result of the

mutation in the p66 or p51 subunit. The N348I substitution in the p66 subunit did not increase AZT resistance but it was determined if this enzyme had increased processivity over WT. Additionally, studies suggest that this mutation also possesses an RNase H-independent mechanism of AZT resistance in similar assays [204]. Again, the AZT resistance assay was not performed on a DNA/DNA T/P so this observation cannot be made or correlated with a subunit.

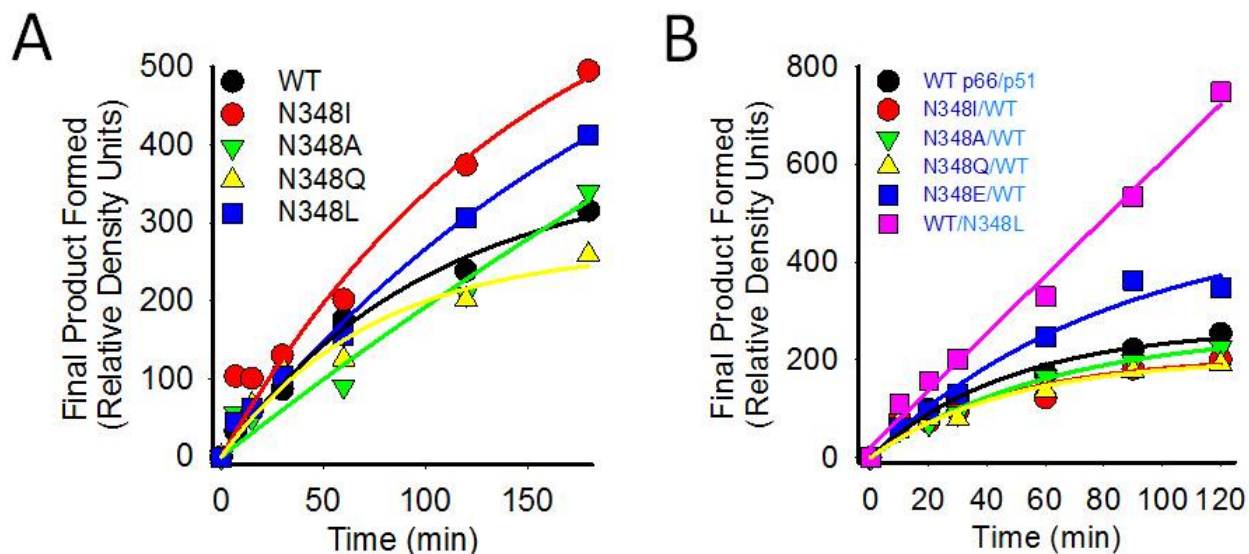


Figure 28. DNA synthesis by WT and mutant HIV-1 RT in the presence of AZT-TP and 3 mM ATP.

Two hundred nanomolar RT was incubated with 20 nM RNA/DNA T/P, 0.75 μ M AZT-TP and 1 μ M dNTP in reaction buffer. Aliquots were removed at the indicated times, quenched with formamide and products were separated from substrates by gel electrophoresis. Product formation was analyzed by densitometry. A, Data for enzymes containing mutations in both subunits. B, Data for enzymes containing the subunit-specific mutations.

6.5.4 Nevirapine Resistance of Recombinant Mutant HIV-1 RTs

It has been suggested that the nevirapine resistance observed for the N348I mutation is a result of the decrease in RNase H activity [241]. To evaluate if a correlation is seen between nevirapine resistance and effects on RNase H activity, the NNRTI resistance of the mutant and chimeric mutant RTs was evaluated. Under continuous polymerization conditions, all RTs harboring the

mutations in both subunits displayed significant resistance to nevirapine. Both N348I and N348L showed the highest level of resistance at 8- and 11-fold respectively (Fig. 29). N348A and N348Q showed low levels of resistance, 3- and 2-fold, respectively. Interestingly, none of the chimeric RTs containing the mutations in the p66 subunits (including the N348I mutation) showed significant nevirapine resistance. However, the RT harboring the N348L mutation in the p51 subunit demonstrated ~ 6-fold resistance. This observation suggests that the N348 residue confers significant nevirapine resistance in the p51 subunit, but not the p66 subunit.

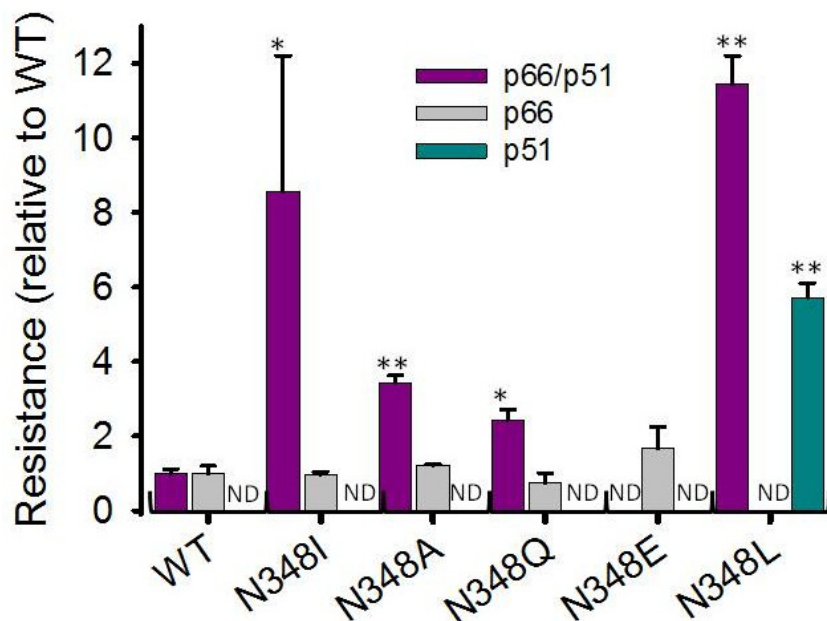


Figure 29. Nevirapine resistance of WT and N348 HIV-1 RTs.

In this ELISA-based assay, 15nM RT was incubated with 200 nM RNA/DNA T/P and 1 μ M dNTPs in reaction buffer with increasing concentrations of inhibitor. Reactions quenched after 20 minutes with 0.25M EDTA and a Br-conjugated dNTP was detected using a conjugated antibody. Statistical significance was based on the WT data from each group (* = p -value<0.001, ** = p -value<0.009)

This study demonstrates a mechanism of resistance both for AZT as well as nevirapine. The inversely correlated decrease in RNase H activity and increase in AZT-MP excision has been described [201], but the structural mechanism by which this occurs has been elusive. In the absence of appropriate crystal structures of the binary complex of RT with an RNA/DNA T/P passing through both the polymerase and RNase H active sites, it has been impossible to determine the structural mechanism influencing the decreased RNase H activity, AZT resistance or NNRTI resistance. However, recent modeling studies in our lab have used related modeling based on the human RNase H1 molecule to hypothesize how the isoleucine substitution at residue Asn348 could affect the association of RT and T/P [33]. From this analysis, it was determined that the Asn348 residue, although not contacting the T/P itself, did reside in a loop that may interact with the RNA template. When this asparagine is replaced with a leucine or isoleucine, the loop no longer fully contacts the template. The goal of this work was to validate this model through biochemical analysis. As the model predicted, the N348L mutation in the p51 subunit caused a decreased in RNase H activity, whereas the N348I mutation the p66 subunit had no effect on cleavage.

A recent report by the Pathak group suggested a model for the correlation between RNase H activity and NNRTI resistance [241]. In that study, it was demonstrated that in many cases, mutations that cause decreased RNase H activity also increase resistance to NNRTIs. In the present study, I also observed an inverse correlation between the decreased in RNase H cleavage increased resistance to nevirapine. However, it is important to note that resistance to the NNRTIs is seen in the context of a DNA template as well. Therefore, in the case of N348I, it is not correct to hypothesize that this decrease in sensitivity is purely a result of the effect of these mutations on the RNase H activity of the enzyme.

7.0 CONCLUSIONS AND FUTURE DIRECTIONS

7.1 SUMMARY OF PROJECT

The idea for this project was born from the initial observation that NNRTIs display different levels of inhibition depending on the assay system used (Table 2). Most strikingly, more drug is required to inhibit *in vitro* polymerization by recombinant HIV-1 RT than reverse transcription *in vivo*, suggesting that, *in vivo*, polymerization is not the only mechanism of inhibition. This raised the question: in addition to polymerization, are other activities of RT affected by NNRTIs? Although it has been known for years that both NNRTIs and mutations that confer resistance to these inhibitors could impact the cleavage rate and pattern, the governing factors of this interaction had not been understood. For example, various studies have shown that RNase H cleavage can be inhibited [125], enhanced [213] or remain unaffected [211-212] in the presence of NNRTIs. In order to better understand this modulation, a study was performed using a panel of NNRTIs and T/P substrates [214]. This work revealed that inconsistent substrates generated conflicting data. Therefore, the effect of NNRTIs on the RNase H activity of RT is dictated by the nature of the T/P.

The balance between polymerase and RNase H activity has been overlooked for some time, likely because little is known about the kinetic interplay of the two active sites. Because processive polymerization is continuous and RNase H activity is periodic, it's assumed that the

rates of the two activities are different and that they are not functioning simultaneously. However, recent biochemical studies have shown that locking the 3'-end of the primer at the polymerase active site in the ternary complex or with the inhibitor foscarnet produces efficient RNase H cleavage demonstrating the RT can engage both active sites [40, 243]. Although it is unclear whether or not the two activities are temporally coordinated, this does demonstrate that the two are not mutually exclusive.

The observation that both active sites can simultaneously interact with the T/P suggests that the activity or an effect on one could influence the activity of the other despite a distance of at least 60 Å between them. The dependence between the two has been demonstrated empirically as well. Because the binding constant (K_D) of the primer grip in the polymerase domain is significantly lower than the RNase H domain, mutations in the polymerase T/P grip region can affect RNase H activity [244]. Previous studies have shown that alterations in the polymerase domain can translate into observable effects in the RNase H domain [37, 215-216]

In light of these observations, I hypothesized that any compound (or mutation) that has an effect on one active site could potentially affect the functioning of the other. Therefore, the therapeutic efficacy of an inhibitor combined with an NNRTI that affects RNase H activity would be determined by how that inhibitor reacts to the shift in the polymerase/RNase H equilibrium caused by the NNRTI. The goals of this study were (1) to determine the mechanisms of synergy between NRTIs and NNRTIs, including the influence of the nature of the template, and (2) to elucidate the mechanisms by which RT can gain resistance to combination therapy.

7.1.1 Mechanisms of Synergy Between NRTIs and NNRTIs

There are examples in the literature of synergy between NRTIs and NNRTIs, both in clinical studies [245] as well as biochemical analyses [246-248]. The major mechanism proposed in the literature is that NNRTIs inhibit ATP-mediated removal of NRTIs from chain-terminated primers by negatively affecting both affinity of ATP for RT and the rate of the chemical step in the excision reaction, thus sustaining NRTI chain termination [147, 229]. However, these studies were carried out using a DNA/DNA T/P only. In light of the recent evidence demonstrating the connection between decreased RNase H activity and increased NRTI excision [175], it was postulated that increased RNase H activity could decrease NRTI excision. As discussed, I have previously observed that under certain conditions, NNRTIs can enhance RNase H cleavage, possibly contributing to an additional mechanism of synergy (Fig. 3).

The first goal was to determine if there was in a difference between excision on an RNA template as compared to a DNA template in the presence of an NNRTI. To evaluate this, the IC_{50} value for the inhibition of excision by efavirenz was determined (Fig 12E). The IC_{50} for the inhibition of excision on the RNA template was much lower than for the DNA template. Because the rate of excision on RNA and DNA templates is similar ($0.067 \pm 0.005 \text{ min}^{-1}$ and $0.045 \pm 0.002 \text{ min}^{-1}$ for DNA/DNA and RNA/DNA T/P, respectively), the data suggest that there is an additional factor playing a role in the inhibition of excision on the RNA template. I next evaluated the cleavage pattern in the presence of efavirenz under excision conditions and noticed an increase of the 10 nucleotide duplex product as compared to in the absence of inhibitor (Fig 13). Because a larger proportion of the T/P was in the 10 nucleotide duplex state during the excision reaction, I evaluated the excision on that T/P system. Figure 14 demonstrates that when the T/P duplex is reduced below 12 nucleotides, the excision reaction is inefficient. Efavirenz

accelerates the appearance of the reduced T/P hybrid, and therefore decreases the absolute amount of excision that can take place on the substrate. As a result, efavirenz can decrease excision, not only by the increase in K_D of ATP as demonstrated by pre-steady state kinetics [188], but also by reducing the T/P hybrid length.

In an effort to elucidate the mechanism by which the NNRTI affect RNase H cleavage, I wanted to determine if the presence of the NNRTI affected the association of RT with the T/P. Unfortunately, due to the lack of a relevant crystal structures containing RT bound to T/P and an NNRTI, the effect of the compound on T/P association has only been speculative. Additionally, it was not known if the nature of the T/P (DNA or RNA) has an effect on this association. Accordingly, a FRET system was created to assess the position of the T/P in reference to the RNase H domain of RT in the presence of an NNRTI. RT was pre-bound with a saturating concentration of efavirenz and AZT-MP-terminated T/P was added in the absence of magnesium to prevent catalysis. The efficiency of energy transfer from the donor molecule, which was covalently attached to the RT molecule, to the acceptor on the 5'-end of the DNA primer was measured.

The distance between the two labeled residues on RT and the 5'-end of the DNA primer increased when efavirenz was bound on both the DNA/DNA and RNA/DNA T/P systems (Table 3). This suggests that RT binds in a similar fashion, with the RNase H domain moving away in space from the 5'-end of the DNA primer, in the presence of efavirenz regardless of the nature of the template. However, the position of the RNase H domain seemed to change more dramatically in the context of the RNA template. Residue 449 moved 7.05Å and residue 560 moved 4.19Å, creating more distance between the two dyes. In contrast, on the DNA template, residue 449 moved 6.49Å. The lack of change in the distance between residue 560 and the 5'-

end of the DNA primer annealed to the DNA template may be the result of a lack of structural consistency at this residue as it is located at the end of the C-terminus of the enzyme.

Since this study, recent work has demonstrated that RT has the ability to “shuttle” on a T/P [122]. While the next complimentary dNTP causes RT to favor a polymerase-competent mode and stabilize at the 3-end of the DNA primer, the presence of an NNRTI destabilizes the structure at the 3’ end increasing “shuttling” [122]. Having less RT bound at the 3’ end for polymerization in the presence of NNRTIs constitutes an additional mode of inhibition not previously described. The data shown in Section 4.0 supports this model. Additionally, “flipping” was noted in the presence of an NNRTI on RNA/DNA T/Ps identical to the PPT region [54]. This phenomenon did not occur in the T/P system used here, confirming that this “flipping” is specific to the PPT region. Combined with my data, this suggests that the binding of the NNRTI allowed RT to move away from the 5’-end of the primer in a polymerase-incompetent mode. This motion of RT on the T/P may also explain the increased presence of the shorter RNA/DNA hybrids during RNase H cleavage seen in the presence of the NNRTI. When RT is favoring the polymerase-dependent mode, cleavage occurs approximately 18 base pairs from the 3’-end of the DNA primer (Fig. 19A). When the polymerase active site of RT is shifted out of this configuration on the T/P, as demonstrated in the presence of an NNRTI, the RNase H active site is positioned closer to the 5’-end of the RNA template strand, resulting in smaller cleavage products (Fig. 19B).

Due to the flexibility of the RT enzyme, it is also possible that the RNase H domain alone is shifting away from the 5’-end of the primer. The described experiments do not remove the possibility that, although the RNase H domain is lifting away from the DNA primer, the

polymerase domain is still positioned at the 3'-end, poised for polymerization. Additional FRET experiments could be done to confirm the location of the N-terminus of the enzyme.

With the ongoing development of RNase H inhibitors and new NNRTIs, it is important to evaluate and understand the mechanism by which combinations of drugs inhibit RT. RNase H activity is an attractive therapeutic target as this activity is absolutely required for virus replication. However, we now know that decreased RNase H activity can facilitate NRTI excision therefore, it will be important to evaluate these combinations of classes *in vitro* and *in vivo* prior to use as therapy.

7.1.2 Mechanisms by Which HIV-1 RT is able to Circumvent Combination Therapy

The most powerful tool physicians have to combat the development of resistance to RTIs is effective combination therapy. Selection of inhibitors that work synergistically and give rise to antagonistic pathways of resistance delays or prevents rebounding plasma viremia. Unfortunately, resistance can arise even in the presence of drug combinations proven to be synergistic or that give rise to antagonistic mutational pathways [249-251]. To prevent the establishment of multidrug resistance mutations and to develop inhibitors that prevent viral replication in the context of current available therapies, it is important to understand how RT can overcome different drug combinations. The work described here further elucidates the mechanisms by which HIV-1 RT can develop resistance to combination therapies including commonly prescribed NRTIs and NNRTIs.

The recently described N348I mutation is able to confer resistance to NRTIs and NNRTIs by a new mechanism; modulation of RNase H activity [201]. Because this mutation is highly correlated with TAMs as well as mutations antagonistic to the excision phenotype, such as

L74V, M184V and Y181C [201, 252], I wanted to determine if this mutation allows the maintenance of antagonistic combinations. As previously observed, the excision phenotype (conferred by K70R) is antagonized in the presence of Y181C (Fig. 20B and C), M184V (Fig. 23A) and L74V (Fig. 23B). When N348I was added, the excision was increased on the RNA template in all cases. N348I was able to recover the excision phenotype on the RNA template, suggesting that the RNase H activity may be playing a role in facilitating dual resistance.

Because N348I confers NRTI resistance by an RNase H-dependent mechanism, I wanted to determine if this mutation was affecting the basal level of RNase H activity of the mutants. The RNase H activity of the RTs harboring the antagonistic mutations in the absence and presence of the N348I mutation was evaluated. From this analysis it was determined that the N348I mutation decreased the RNase H activity of the enzymes both alone (Fig. 21B), in combination with K70R, L74V, M184V and Y181C; (Fig. 21C) and in the presence of K70R paired with L74V (Fig. 24B), M184V (Fig. 24C) and Y181C (Fig. 21B). These observations support previous data suggesting that N348I increases AZT-MP excision by an RNase H-dependent mechanism [201]. This data also suggests that N348I can compensate for antagonism of the excision phenotype by the same mechanism. Additionally, the increased RNase H activity of Y181C alone (Fig. 21B) suggests an added mechanism of antagonism between the K70R and Y181C mutations.

Finally, I determined the effect of the N348I mutation in combination with the mutations correlated with multiple rounds of incorporation and excision, using a biologically relevant, heteropolymeric RNA/DNA T/P system. This experiment demonstrates how each set of mutations functions during γ -ssDNA synthesis in the presence of AZT-TP during reverse transcription. N348I had the greatest amount of completed product (Fig 22). Previous studies

have demonstrated that N348I can compensate for a decrease in processive DNA synthesis caused by TAMs [204] that, paired with RNase H-mediated increased AZT-MP excision, allows the formation of more product. N348I affects RNase H activity causing an indirect effect which circumvents the antagonism. In this case, the biochemical antagonism is still present, but the N348I mutation can overcome this by extending the time for excision.

Despite the data showing the effects of the N348I mutation in biochemical assays, the lack of structural data hindered our understanding of the structural characteristics which could lead to the resistant phenotype. In an effort to understand how N348I was modulating RNase H activity, we used a model of RT complexed with an RNA/DNA template primer based on the crystal structure of the human RNase H1. In this structure, the N348 residue resides on a β loop that contacts the RNA template (Fig. 25). When N348I is substituted at this position, the loop moves away from the template, suggesting a mechanism of RNase H modulation.

To validate the hypothesis that the isoleucine substitution was decreasing RNase H activity through the effect in the p51 subunit, I characterized RTs containing various mutations at the Asn348 residue in both subunits and each subunit individually. When the leucine and isoleucine residues at 348 were present in both subunits, a decrease was noted in RNase H activity (Fig. 27A). This translated into increased AZT-MP excision on the heteropolymeric RNA/DNA T/P (Fig. 28A). Interestingly, these RTs also conferred the highest level of NNRTI resistance (Fig. 29, purple bars). However, the level of resistance seen when the N348L mutation was in the p51 subunit does not explain the 11-fold resistance when the mutation is in both subunits. This demonstrates that the highest level of nevirapine resistance is achieved when the mutation is in both subunits. When the N348I mutation was in the p66 subunit only, the RNase H activity (Fig. 27B) and AZT-MP excision (Fig. 28B) were similar to that of WT. The

mutation also did not confer NNRTI resistance when present only in the p66 subunit of RT. However, N348L in the p51 subunit displayed decreased RNase H activity (Fig. 27B), increased AZT-MP excision (Fig. 28B) and ~6-fold nevirapine resistance over WT (Fig. 29, blue bar).

The modeling study suggests that when the N348I mutation is present in the p51 subunit, the β 14- β 15 loop is farther away from the RNA template such that residues P345 and F346 do not make contact with the template (Fig. 25A, pink). However, when leucine is present at this position, only the F346 is not in contact with the template (Fig. 25C, pink). Therefore, it seems that the loss of contact between the F346 residue in the p51 subunit and the RNA template affects RNase H activity.

In addition to NRTI resistance, these data suggest the NNRTI resistance is also associated with the decreased RNase H activity. When taken in the context of my previous data, we can describe the following model (Fig. 30). In the presence of NNRTIs, HIV-1 RT can shift from a polymerase-competent mode of binding, to an incompetent mode. This accounts for decreased polymerization, accelerated appearance of shorter RNase H products and decreased excision of terminating nucleosides. However, when N348I is present, it is able to compensate for the shift in the presence of NNRTIs and favor the polymerase-competent binding mode, allowing increased polymerization (NNRTI resistance), WT levels of RNase H cleavage and enhanced NRTI excision. This may also explain why N348I has increased processivity and can bind shorter substrates for a longer period of time [204]. Because the primer grip region in the polymerase domain is more valuable in RT-T/P association than the grip region in the RNase H domain [35], RT may be able to remain bound to the shorter T/P longer when the polymerase

competent mode is favored. Additional experiments need to be performed to determine if the polymerase activity is, in fact, moved from the 3'-end of the DNA primer both in the absence and presence of an NNRTI as well as in the presence of the N348I mutation.

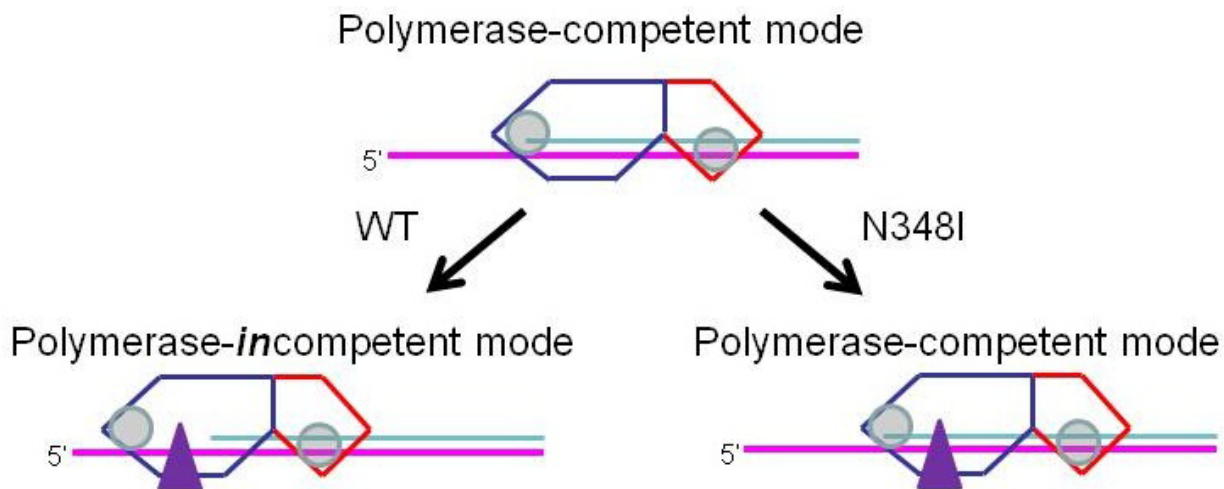


Figure 30. N348I confers NNRTI resistance by favoring a polymerase-competent binding mode.

RT is shown with the polymerase (dark blue) and RNase H (red) active site (gray circles). In the absence of inhibitor, RT favors binding to a T/P substrate with a recessed 3' DNA end in a polymerase competent mode. When an NNRTI binds to RT, it causes RT to favor sliding into a polymerase-incompetent mode, where the active site is not positioned for polymerization and the RNase H active site is closer to the 5' end of the RNA template. In the presence of the N348I mutation, RT favors the polymerase-competent mode of binding, which decreases the appearance of smaller RNase H cleavage products and allows greater levels polymerization (and excision of NRTIs).

7.2 PUBLIC HEALTH SIGNIFICANCE

Since the approval of delavirdine in 1996, NNRTIs have been used in combination with NRTIs to maintain low plasma viremia and to delay the onset of drug-resistant mutants [143, 253].

Globally, NNRTI-containing regimens are now the most widely prescribed combinations for initial therapy [177]. Currently, many clinicians choose to prescribe the NNRTI-based regimens *in lieu* of those containing a protease inhibitor due to the metabolic side effects associated with protease inhibitors (i.e. lipodystrophy) and the low cytotoxicity of NNRTIs [254-255]. For example, nevirapine is safe for use during pregnancy and, therefore, has been recommended for the prevention of mother-to-child transmission [256-257]. The World Health Organization also includes NNRTIs in their antiretroviral regimen for developing nations due to their low cost (relative to other options) and their potency [258].

In light of the popularity of NNRTI-containing regimens, it is important to understand the mechanisms by which they inhibit HIV-1 as well as the mechanisms by which RT can overcome these therapies. Determining the mechanisms of resistance can allow the development of inhibitors with greater potency against resistance virus and possibly delay the onset of resistance. Elucidating how the interplay between these mutations affects RT function is necessary for the treatment of ARV-experienced patients as well as the development of new, effective therapies. This study and previously published work demonstrating the importance of RNase H activity in resistance to NRTIs as well as NNRTIs highlights new drug targets as well as the importance of the interplay between the enzyme functions. For example, because decreased RNase H activity can enhance resistance to NRTIs, therapies which inhibit virus replication by inhibiting RNase H activity will facilitate NRTI resistance. However, the acceleration of RNase H activity may inhibit viral replication by prematurely removing the RNA template prior to strand transfer or by having effects on primer RNA removal. Understanding the mechanisms by which RTIs function in the context of reverse transcription is vital to our ability to curb virus replication, especially when these compounds are used in combination therapy.

Additionally, transmission of RTI-resistant virus has been increasing. To allow physicians to make the best choice for the treatment of their patients, a full understanding of clinically significant mutations is needed. The currently available drug-resistance data base is an important tool to preventing rebounding virus but it needs to be expanded to include other regions of RT such as the connection and RNase H domains. The work presented demonstrates that resistance can be present in the C-terminal domain of RT and should be considered during treatment.

7.3 FUTURE DIRECTIONS

Although this study adds to the field of drug resistance, a deeper understanding of these observations in the context of current therapy is necessary to evaluate the additional mechanisms by which NNRTIs inhibit HIV-1 RT and consequences of mutations that can alleviate this inhibition.

7.3.1 Mechanism(s) by which NNRTIs inhibit RT and reverse transcription

This work demonstrates that NNRTIs are inhibiting RT by a mechanism that was previously disregarded. The interaction of RT with the RNA/DNA T/P substrate during reverse transcription provides different functions and binding modes for RT. Although a shift in the binding mode of RT occurs on both T/P systems, this effect was highlighted on the RNA template. Certain steps during reverse transcription that require multiple functions of RT have not been explored in the context of an NNRTI and may be particularly sensitive to inhibition by

this class of compounds. For example, it is now understood that NNRTIs cause RT to bind differently to T/P and that RNase H activity is perturbed. Steps during reverse transcription during which RT relies on the coordinated functions of RNase H activity and polymerase activity, may be uniquely affected by NNRTIs and/or RNase H modulating mutations.

The process of strand transfer requires both RNase H and polymerase activity. As described in section 1.1.3.2, the models proposed for mechanism of strand transfer rely heavily on RNase H activity. Enhancement of this function (by mutation or NNRTI) could cause premature dissociation of RT prior annealing of the template acceptor or alter the formation of secondary structures which enhance the strand transfer events [37]. Studies have already demonstrated that NNRTI-resistant mutations are more resistant during the process of strand transfer [210] suggesting that strand transfer may be inhibited during reverse transcription.

Recent data also demonstrates that NNRTIs can affect RNA primer removal [54], an important process to determine the ends of the LTR for proper integration into the host cell genome. The study presented here as well as single-molecule FRET studies show that the presence of NNRTIs can cause RT to change its position on the T/P. Acceleration or alteration of the cleavage position during primer removal could alter the LTRs and inhibit integration. Therefore, *in vitro* assays to evaluate the effect of NNRTIs specifically on strand transfer and primer removal need to be developed.

7.3.2 More questions about N348I and the connection between decreased RNase H activity and NNRTI-resistance.

Although the basic mechanism of NNRTI resistance conferred by N348I has been described, this model can be further confirmed by additional FRET experiments. A similar FRET analysis

using RT with the N348I mutation (and other such mutations which decrease RNase H activity and increase NNRTI resistance) would confirm our model. Additionally, the model suggests that the actual rate of RNase H cleavage is not altered by the N348I mutation. This assumption can be confirmed by pre-steady state analysis of the initial polymerase-dependent cleavage as well as the rate of subsequent polymerase-independent cleavages.

Due to the lack of a relevant crystal structure, the structural effects of the N348I mutation in the p51 subunit that cause RT to favor the polymerase-competent binding mode is still unknown. Crystal structures with N348I RT may provide clues to this. However, in the absence of the T/P connection with both active sites, a structure may be inconclusive.

7.3.3 Resistance Mutations in Non-subtype B

Although subtype B is most prominent in the industrialized world, subtype C is most prevalent overall [7]. Despite this, subtype B clones have been used in most studies for the development of effective antiretroviral inhibitors as well as to understand drug resistance mechanisms. This raises the question of whether individuals infected with non-subtype B viruses will fully benefit from current treatments. A growing body of evidence suggests that different subtypes may respond differently to therapeutic interventions [259]. Furthermore, the presence of polymorphisms in non-B subtypes which are considered secondary resistance mutations in subtype B [260-262], supports the idea that the acquisition of drug resistance mutations might be enhanced in non-B subtypes of HIV-1. For example, it has been demonstrated that the genetic variation at NNRTI-resistance positions such as V106M and A98S was substantially greater in subtype C-infected patients than in subtype B-infected patients [263]. Accordingly, V106M seems to be a signature mutation in subtype-C patients treated with efavirenz [264]. Moreover,

one study conducted in Uganda, revealed that selection of genotypic mutations associated with resistance occurred more frequently in women infected with subtype D than in women infected with subtype-A viruses [265]. Additionally, intrinsic difference in the subtypes may lead to differential resistance among them. One study found that subtype D had diminished drug sensitivity as a result of more rapid growth kinetics as compared to subtypes A, B, C and E [266], highlighting that there are fundamental differences between subtypes. These observations suggest that subtype B may not be an appropriate model for the study of all HIV-1 resistance development.

The development of specific mutations in various subtypes is also worth investigating. Recent studies have already demonstrated the development of N348I in subtype C virus in South Africa [267]. However, more data is needed to properly correlate the increase in the frequency of this mutation with specific therapies as well as co-selected mutations. This would suggest if the N348I mutation also appears with TAMs, NNRTI resistance mutations and M184V as has been determined with this mutation in subtype B. Additionally, biochemical evaluation of the mutation in the context of the subtype C RT would be important to further understand the development and mechanisms of resistance in non-subtype B viruses. Because the genotypes of the different subtypes lead to different replication kinetics, the mutational pathways taken in subtype C as compared to subtype B may be different. Therefore, the compensation we see for antagonism by N348I in the presence of TAMs and mutations such as L74V, M184V and Y181C may not be relevant in the context of subtype C.

BIBLIOGRAPHY

1. Hahn, B.H., et al., *AIDS as a zoonosis: scientific and public health implications*. Science, 2000. **287**(5453): p. 607-14.
2. Plantier, J.C., et al., *A new human immunodeficiency virus derived from gorillas*. Nat Med, 2009. **15**(8): p. 871-2.
3. Keele, B.F., et al., *Chimpanzee reservoirs of pandemic and nonpandemic HIV-1*. Science, 2006. **313**(5786): p. 523-6.
4. Abram, M.E., et al., *The Nature, Position and Frequency of Mutations Made in a Single-Cycle of HIV-1 Replication*. J Virol, 2010.
5. Domingo, E. and J.J. Holland, *RNA virus mutations and fitness for survival*. Annu Rev Microbiol, 1997. **51**: p. 151-78.
6. Worobey, M., et al., *Direct evidence of extensive diversity of HIV-1 in Kinshasa by 1960*. Nature, 2008. **455**(7213): p. 661-4.
7. Woodman, Z. and C. Williamson, *HIV molecular epidemiology: transmission and adaptation to human populations*. Curr Opin HIV AIDS, 2009. **4**(4): p. 247-52.
8. Geretti, A.M., *HIV-1 subtypes: epidemiology and significance for HIV management*. Curr Opin Infect Dis, 2006. **19**(1): p. 1-7.
9. Kwong, P.D., et al., *Oligomeric modeling and electrostatic analysis of the gp120 envelope glycoprotein of human immunodeficiency virus*. J Virol, 2000. **74**(4): p. 1961-72.
10. Bieniasz, P.D., *The cell biology of HIV-1 virion genesis*. Cell Host Microbe, 2009. **5**(6): p. 550-8.
11. Nakai, M. and T. Goto, *Ultrastructure and morphogenesis of human immunodeficiency virus*. J Electron Microsc (Tokyo), 1996. **45**(4): p. 247-57.
12. Fassati, A. and S.P. Goff, *Characterization of intracellular reverse transcription complexes of human immunodeficiency virus type 1*. J Virol, 2001. **75**(8): p. 3626-35.
13. Forshey, B.M., et al., *Formation of a human immunodeficiency virus type 1 core of optimal stability is crucial for viral replication*. J Virol, 2002. **76**(11): p. 5667-77.
14. Auewarakul, P., et al., *Uncoating of HIV-1 requires cellular activation*. Virology, 2005. **337**(1): p. 93-101.
15. Towers, G.J., et al., *Cyclophilin A modulates the sensitivity of HIV-1 to host restriction factors*. Nat Med, 2003. **9**(9): p. 1138-43.
16. Towers, G.J., *The control of viral infection by tripartite motif proteins and cyclophilin A*. Retrovirology, 2007. **4**: p. 40.
17. Zhang, H., et al., *Morphologic changes in human immunodeficiency virus type 1 virions secondary to intravirion reverse transcription: evidence indicating that reverse transcription may not take place within the intact viral core*. J Hum Virol, 2000. **3**(3): p. 165-72.
18. Saadatmand, J., et al., *Interactions of reverse transcriptase sequences in Pol with Gag and LysRS in the HIV-1 tRNA^{Lys3} packaging/annealing complex*. Virology, 2008. **380**(1): p. 109-17.
19. Campbell, E.M. and T.J. Hope, *Live cell imaging of the HIV-1 life cycle*. Trends Microbiol, 2008. **16**(12): p. 580-7.

20. McDonald, D., et al., *Visualization of the intracellular behavior of HIV in living cells*. J Cell Biol, 2002. **159**(3): p. 441-52.
21. Warrilow, D., G. Tachedjian, and D. Harrich, *Maturation of the HIV reverse transcription complex: putting the jigsaw together*. Rev Med Virol, 2009. **19**(6): p. 324-37.
22. Miller, M.D., C.M. Farnet, and F.D. Bushman, *Human immunodeficiency virus type 1 preintegration complexes: studies of organization and composition*. J Virol, 1997. **71**(7): p. 5382-90.
23. Nisole, S. and A. Saib, *Early steps of retrovirus replicative cycle*. Retrovirology, 2004. **1**: p. 9.
24. Warrilow, D., D. Stenzel, and D. Harrich, *Isolated HIV-1 core is active for reverse transcription*. Retrovirology, 2007. **4**: p. 77.
25. Rey, M.A., et al., *Characterization of the RNA dependent DNA polymerase of a new human T-lymphotropic retrovirus (lymphadenopathy associated virus)*. Biochem Biophys Res Commun, 1984. **121**(1): p. 126-33.
26. Chandra, A., et al., *Serological relationship between reverse transcriptases from human T-cell lymphotropic viruses defined by monoclonal antibodies. Evidence for two forms of reverse transcriptases in the AIDS-associated virus, HTLV-III/LAV*. FEBS Lett, 1986. **200**(2): p. 327-32.
27. Kohlstaedt, L.A., et al., *Crystal structure at 3.5 Å resolution of HIV-1 reverse transcriptase complexed with an inhibitor*. Science, 1992. **256**(5065): p. 1783-90.
28. Tachedjian, G., H.E. Aronson, and S.P. Goff, *Analysis of mutations and suppressors affecting interactions between the subunits of the HIV type 1 reverse transcriptase*. Proc Natl Acad Sci U S A, 2000. **97**(12): p. 6334-9.
29. Jacobo-Molina, A., et al., *Crystal structure of human immunodeficiency virus type 1 reverse transcriptase complexed with double-stranded DNA at 3.0 Å resolution shows bent DNA*. Proc Natl Acad Sci U S A, 1993. **90**(13): p. 6320-4.
30. Huang, H., et al., *Structure of a covalently trapped catalytic complex of HIV-1 reverse transcriptase: implications for drug resistance*. Science, 1998. **282**(5394): p. 1669-75.
31. Kati, W.M., et al., *Mechanism and fidelity of HIV reverse transcriptase*. J Biol Chem, 1992. **267**(36): p. 25988-97.
32. Rittinger, K., G. Divita, and R.S. Goody, *Human immunodeficiency virus reverse transcriptase substrate-induced conformational changes and the mechanism of inhibition by nonnucleoside inhibitors*. Proc Natl Acad Sci U S A, 1995. **92**(17): p. 8046-9.
33. Nowotny, M., et al., *Structure of human RNase H1 complexed with an RNA/DNA hybrid: insight into HIV reverse transcription*. Mol Cell, 2007. **28**(2): p. 264-76.
34. Szyperski, T., et al., *NMR structure of the chimeric hybrid duplex r(gcaguggc).r(gcca)d(CTGC) comprising the tRNA-DNA junction formed during initiation of HIV-1 reverse transcription*. J Biomol NMR, 1999. **13**(4): p. 343-55.
35. Julias, J.G., et al., *Mutations in the RNase H domain of HIV-1 reverse transcriptase affect the initiation of DNA synthesis and the specificity of RNase H cleavage in vivo*. Proc Natl Acad Sci U S A, 2002. **99**(14): p. 9515-20.
36. Boyer, P.L., et al., *Mutational analysis of the fingers and palm subdomains of human immunodeficiency virus type-1 (HIV-1) reverse transcriptase*. J Mol Biol, 1994. **243**(3): p. 472-83.

37. Gao, H.Q., et al., *Effects of mutations in the polymerase domain on the polymerase, RNase H and strand transfer activities of human immunodeficiency virus type 1 reverse transcriptase*. J Mol Biol, 1998. **277**(3): p. 559-72.
38. Wohrl, B.M. and K. Moelling, *Interaction of HIV-1 ribonuclease H with polypurine tract containing RNA-DNA hybrids*. Biochemistry, 1990. **29**(44): p. 10141-7.
39. DeStefano, J.J., et al., *Polymerization and RNase H activities of the reverse transcriptases from avian myeloblastosis, human immunodeficiency, and Moloney murine leukemia viruses are functionally uncoupled*. J Biol Chem, 1991. **266**(12): p. 7423-31.
40. Beilhartz, G.L., et al., *HIV-1 reverse transcriptase can simultaneously engage its DNA/RNA substrate at both DNA polymerase and RNase H active sites: implications for RNase H inhibition*. J Mol Biol, 2009. **388**(3): p. 462-74.
41. Tisne, C., *Structural bases of the annealing of primer tRNA(3Lys) to the HIV-1 viral RNA*. Curr HIV Res, 2005. **3**(2): p. 147-56.
42. Saadatmand, J., et al., *The contribution of the primer activation signal to differences between Gag- and NCp7-facilitated tRNA(Lys3) annealing in HIV-1*. Virology, 2009. **391**(2): p. 334-41.
43. Yu, H., et al., *The nature of human immunodeficiency virus type 1 strand transfers*. J Biol Chem, 1998. **273**(43): p. 28384-91.
44. Heath, M.J. and J.J. Destefano, *A complementary single-stranded docking site is required for enhancement of strand exchange by human immunodeficiency virus nucleocapsid protein on substrates that model viral recombination*. Biochemistry, 2005. **44**(10): p. 3915-25.
45. Balakrishnan, M., et al., *Template dimerization promotes an acceptor invasion-induced transfer mechanism during human immunodeficiency virus type 1 minus-strand synthesis*. J Virol, 2003. **77**(8): p. 4710-21.
46. Beerens, N. and J. Kjems, *Circularization of the HIV-1 genome facilitates strand transfer during reverse transcription*. RNA, 2010. **16**(6): p. 1226-35.
47. Coffin, J.M., *Structure, replication, and recombination of retrovirus genomes: some unifying hypotheses*. J Gen Virol, 1979. **42**(1): p. 1-26.
48. Negroni, M., et al., *Homologous recombination promoted by reverse transcriptase during copying of two distinct RNA templates*. Proc Natl Acad Sci U S A, 1995. **92**(15): p. 6971-5.
49. Nikolenko, G.N., et al., *Antiretroviral drug resistance mutations in human immunodeficiency virus type 1 reverse transcriptase increase template-switching frequency*. J Virol, 2004. **78**(16): p. 8761-70.
50. Wisniewski, M., et al., *Unique progressive cleavage mechanism of HIV reverse transcriptase RNase H*. Proc Natl Acad Sci U S A, 2000. **97**(22): p. 11978-83.
51. Schultz, S.J. and J.J. Champoux, *RNase H activity: structure, specificity, and function in reverse transcription*. Virus Res, 2008. **134**(1-2): p. 86-103.
52. Furfine, E.S. and J.E. Reardon, *Reverse transcriptase.RNase H from the human immunodeficiency virus. Relationship of the DNA polymerase and RNA hydrolysis activities*. J Biol Chem, 1991. **266**(1): p. 406-12.
53. Rausch, J.W. and S.F. Le Grice, *'Binding, bending and bonding': polypurine tract-primed initiation of plus-strand DNA synthesis in human immunodeficiency virus*. Int J Biochem Cell Biol, 2004. **36**(9): p. 1752-66.

54. Gotte, M., et al., *Reverse transcriptase in motion: conformational dynamics of enzyme-substrate interactions*. *Biochim Biophys Acta*, 2010. **1804**(5): p. 1202-12.
55. Hwang, C.K., E.S. Svarovskaia, and V.K. Pathak, *Dynamic copy choice: steady state between murine leukemia virus polymerase and polymerase-dependent RNase H activity determines frequency of in vivo template switching*. *Proc Natl Acad Sci U S A*, 2001. **98**(21): p. 12209-14.
56. DeStefano, J.J., et al., *Requirements for strand transfer between internal regions of heteropolymer templates by human immunodeficiency virus reverse transcriptase*. *J Virol*, 1992. **66**(11): p. 6370-8.
57. de Noronha, C.M., et al., *Dynamic disruptions in nuclear envelope architecture and integrity induced by HIV-1 Vpr*. *Science*, 2001. **294**(5544): p. 1105-8.
58. Bouyac-Bertoia, M., et al., *HIV-1 infection requires a functional integrase NLS*. *Mol Cell*, 2001. **7**(5): p. 1025-35.
59. Nadler, S.G., et al., *Differential expression and sequence-specific interaction of karyopherin alpha with nuclear localization sequences*. *J Biol Chem*, 1997. **272**(7): p. 4310-5.
60. Reil, H., et al., *Efficient HIV-1 replication can occur in the absence of the viral matrix protein*. *EMBO J*, 1998. **17**(9): p. 2699-708.
61. Rexach, M. and G. Blobel, *Protein import into nuclei: association and dissociation reactions involving transport substrate, transport factors, and nucleoporins*. *Cell*, 1995. **83**(5): p. 683-92.
62. Gallay, P., et al., *Role of the karyopherin pathway in human immunodeficiency virus type 1 nuclear import*. *J Virol*, 1996. **70**(2): p. 1027-32.
63. Brass, A.L., et al., *Identification of host proteins required for HIV infection through a functional genomic screen*. *Science*, 2008. **319**(5865): p. 921-6.
64. Ebina, H., et al., *Role of Nup98 in nuclear entry of human immunodeficiency virus type 1 cDNA*. *Microbes Infect*, 2004. **6**(8): p. 715-24.
65. Konig, R., et al., *Global analysis of host-pathogen interactions that regulate early-stage HIV-1 replication*. *Cell*, 2008. **135**(1): p. 49-60.
66. Schroder, A.R., et al., *HIV-1 integration in the human genome favors active genes and local hotspots*. *Cell*, 2002. **110**(4): p. 521-9.
67. Brady, T., et al., *HIV integration site distributions in resting and activated CD4+ T cells infected in culture*. *AIDS*, 2009. **23**(12): p. 1461-71.
68. Meehan, A.M. and E.M. Poeschla, *Chromatin tethering and retroviral integration: Recent discoveries and parallels with DNA viruses*. *Biochim Biophys Acta*, 2010. **1799**(3-4): p. 182-191.
69. Kalpana, G.V., et al., *Binding and stimulation of HIV-1 integrase by a human homolog of yeast transcription factor SNF5*. *Science*, 1994. **266**(5193): p. 2002-6.
70. Mulder, L.C., L.A. Chakrabarti, and M.A. Muesing, *Interaction of HIV-1 integrase with DNA repair protein hRad18*. *J Biol Chem*, 2002. **277**(30): p. 27489-93.
71. Violot, S., et al., *The human polycomb group EED protein interacts with the integrase of human immunodeficiency virus type 1*. *J Virol*, 2003. **77**(23): p. 12507-22.
72. Delelis, O., et al., *Integrase and integration: biochemical activities of HIV-1 integrase*. *Retrovirology*, 2008. **5**: p. 114.
73. Skalka, A.M. and R.A. Katz, *Retroviral DNA integration and the DNA damage response*. *Cell Death Differ*, 2005. **12 Suppl 1**: p. 971-8.

74. Pereira, L.A., et al., *A compilation of cellular transcription factor interactions with the HIV-1 LTR promoter*. Nucleic Acids Res, 2000. **28**(3): p. 663-8.
75. Richman, D.D., et al., *The challenge of finding a cure for HIV infection*. Science, 2009. **323**(5919): p. 1304-7.
76. Pollard, V.W. and M.H. Malim, *The HIV-1 Rev protein*. Annu Rev Microbiol, 1998. **52**: p. 491-532.
77. Freed, E.O., *HIV-1 replication*. Somat Cell Mol Genet, 2001. **26**(1-6): p. 13-33.
78. Kobayashi, Y., et al., *Identification of a cellular factor that modulates HIV-1 programmed ribosomal frameshifting*. J Biol Chem, 2010. **285**(26): p. 19776-84.
79. Jacks, T., et al., *Characterization of ribosomal frameshifting in HIV-1 gag-pol expression*. Nature, 1988. **331**(6153): p. 280-3.
80. Resh, M.D., *Intracellular trafficking of HIV-1 Gag: how Gag interacts with cell membranes and makes viral particles*. AIDS Rev, 2005. **7**(2): p. 84-91.
81. Chu, H., J.J. Wang, and P. Spearman, *Human immunodeficiency virus type-1 gag and host vesicular trafficking pathways*. Curr Top Microbiol Immunol, 2009. **339**: p. 67-84.
82. Pettit, S.C., et al., *Initial cleavage of the human immunodeficiency virus type 1 GagPol precursor by its activated protease occurs by an intramolecular mechanism*. J Virol, 2004. **78**(16): p. 8477-85.
83. Louis, J.M., et al., *Kinetics and mechanism of autoprocessing of human immunodeficiency virus type 1 protease from an analog of the Gag-Pol polyprotein*. Proc Natl Acad Sci U S A, 1994. **91**(17): p. 7970-4.
84. Morellet, N., et al., *Helical structure determined by NMR of the HIV-1 (345-392)Gag sequence, surrounding p2: implications for particle assembly and RNA packaging*. Protein Sci, 2005. **14**(2): p. 375-86.
85. Zhou, J., et al., *Small-molecule inhibition of human immunodeficiency virus type 1 replication by specific targeting of the final step of virion maturation*. J Virol, 2004. **78**(2): p. 922-9.
86. Broder, S., *The development of antiretroviral therapy and its impact on the HIV-1/AIDS pandemic*. Antiviral Res, 2010. **85**(1): p. 1-18.
87. Mitsuya, H., et al., *3'-Azido-3'-deoxythymidine (BW A509U): an antiviral agent that inhibits the infectivity and cytopathic effect of human T-lymphotropic virus type III/lymphadenopathy-associated virus in vitro*. Proc Natl Acad Sci U S A, 1985. **82**(20): p. 7096-100.
88. Choe, H., et al., *The beta-chemokine receptors CCR3 and CCR5 facilitate infection by primary HIV-1 isolates*. Cell, 1996. **85**(7): p. 1135-48.
89. Deng, H., et al., *Identification of a major co-receptor for primary isolates of HIV-1*. Nature, 1996. **381**(6584): p. 661-6.
90. Zhang, L., et al., *In vivo distribution of the human immunodeficiency virus/simian immunodeficiency virus coreceptors: CXCR4, CCR3, and CCR5*. J Virol, 1998. **72**(6): p. 5035-45.
91. Liu, R., et al., *Homozygous defect in HIV-1 coreceptor accounts for resistance of some multiply-exposed individuals to HIV-1 infection*. Cell, 1996. **86**(3): p. 367-77.
92. Liu, S., S. Wu, and S. Jiang, *HIV entry inhibitors targeting gp41: from polypeptides to small-molecule compounds*. Curr Pharm Des, 2007. **13**(2): p. 143-62.

93. Lalezari, J.P., et al., *T-1249 retains potent antiretroviral activity in patients who had experienced virological failure while on an enfuvirtide-containing treatment regimen*. J Infect Dis, 2005. **191**(7): p. 1155-63.
94. Yu, F., et al., *Recent advances in the research of HIV-1 RNase H inhibitors*. Mini Rev Med Chem, 2008. **8**(12): p. 1243-51.
95. Arts, E.J. and M.A. Wainberg, *Mechanisms of nucleoside analog antiviral activity and resistance during human immunodeficiency virus reverse transcription*. Antimicrob Agents Chemother, 1996. **40**(3): p. 527-40.
96. Furman, P.A., et al., *Phosphorylation of 3'-azido-3'-deoxythymidine and selective interaction of the 5'-triphosphate with human immunodeficiency virus reverse transcriptase*. Proc Natl Acad Sci U S A, 1986. **83**(21): p. 8333-7.
97. Richman, D.D., et al., *The toxicity of azidothymidine (AZT) in the treatment of patients with AIDS and AIDS-related complex. A double-blind, placebo-controlled trial*. N Engl J Med, 1987. **317**(4): p. 192-7.
98. White, A.J., *Mitochondrial toxicity and HIV therapy*. Sex Transm Infect, 2001. **77**(3): p. 158-73.
99. Arnaudo, E., et al., *Depletion of muscle mitochondrial DNA in AIDS patients with zidovudine-induced myopathy*. Lancet, 1991. **337**(8740): p. 508-10.
100. Lewis, W. and M.C. Dalakas, *Mitochondrial toxicity of antiviral drugs*. Nat Med, 1995. **1**(5): p. 417-22.
101. Horwitz, J.P., J. Chua, and M. Noel, *1.Nucleosides. V. The Monomesylates of 1-(2'-Deoxy-β-D-lyxofuranosyl)thymine 1,2*. Journal of Organic Chemistry, 1964. **29**(7): p. 2076-2078.
102. Boyer, P.L., et al., *Why do HIV-1 and HIV-2 use different pathways to develop AZT resistance?* PLoS Pathog, 2006. **2**(2): p. e10.
103. Lindblad, G., G. Jonsson, and J. Falk, *Adenine toxicity: a three week intravenous study in dogs*. Acta Pharmacol Toxicol (Copenh), 1973. **32**(3): p. 246-56.
104. Martin, J.C., et al., *Early nucleoside reverse transcriptase inhibitors for the treatment of HIV: a brief history of stavudine (D4T) and its comparison with other dideoxynucleosides*. Antiviral Res, 2010. **85**(1): p. 34-8.
105. Horwitz, J.R., et al., *Nucleosides. IX. The formation of 2',2'-unsaturated pyrimidine nucleosides via a novel beta-elimination reaction*. J Org Chem, 1966. **31**(1): p. 205-11.
106. Mansuri, M.M., et al., *Comparison of in vitro biological properties and mouse toxicities of three thymidine analogs active against human immunodeficiency virus*. Antimicrob Agents Chemother, 1990. **34**(4): p. 637-41.
107. Balzarini, J., et al., *Differential antiherpesvirus and antiretrovirus effects of the (S) and (R) enantiomers of acyclic nucleoside phosphonates: potent and selective in vitro and in vivo antiretrovirus activities of (R)-9-(2-phosphonomethoxypropyl)-2,6-diaminopurine*. Antimicrob Agents Chemother, 1993. **37**(2): p. 332-8.
108. Emau, P., et al., *Post-exposure prophylaxis for SIV revisited: animal model for HIV prevention*. AIDS Res Ther, 2006. **3**: p. 29.
109. Faletto, M.B., et al., *Unique intracellular activation of the potent anti-human immunodeficiency virus agent 1592U89*. Antimicrob Agents Chemother, 1997. **41**(5): p. 1099-107.

110. Daluge, S.M., et al., *1592U89, a novel carbocyclic nucleoside analog with potent, selective anti-human immunodeficiency virus activity*. *Antimicrob Agents Chemother*, 1997. **41**(5): p. 1082-93.
111. Jarvis, B. and D. Faulds, *Lamivudine. A review of its therapeutic potential in chronic hepatitis B*. *Drugs*, 1999. **58**(1): p. 101-41.
112. Cahn, P., *Emtricitabine: a new nucleoside analogue for once-daily antiretroviral therapy*. *Expert Opin Investig Drugs*, 2004. **13**(1): p. 55-68.
113. Frampton, J.E. and C.M. Perry, *Emtricitabine: a review of its use in the management of HIV infection*. *Drugs*, 2005. **65**(10): p. 1427-48.
114. Smerdon, S.J., et al., *Structure of the binding site for nonnucleoside inhibitors of the reverse transcriptase of human immunodeficiency virus type 1*. *Proc Natl Acad Sci U S A*, 1994. **91**(9): p. 3911-5.
115. Hsiou, Y., et al., *Structure of unliganded HIV-1 reverse transcriptase at 2.7 Å resolution: implications of conformational changes for polymerization and inhibition mechanisms*. *Structure*, 1996. **4**(7): p. 853-60.
116. Balzarini, J., *Current status of the non-nucleoside reverse transcriptase inhibitors of human immunodeficiency virus type 1*. *Curr Top Med Chem*, 2004. **4**(9): p. 921-44.
117. Esnouf, R., et al., *Mechanism of inhibition of HIV-1 reverse transcriptase by non-nucleoside inhibitors*. *Nat Struct Biol*, 1995. **2**(4): p. 303-8.
118. Sarafianos, S.G., et al., *Structure and function of HIV-1 reverse transcriptase: molecular mechanisms of polymerization and inhibition*. *J Mol Biol*, 2009. **385**(3): p. 693-713.
119. Das, K., et al., *Crystal structures of clinically relevant Lys103Asn/Tyr181Cys double mutant HIV-1 reverse transcriptase in complexes with ATP and non-nucleoside inhibitor HBY 097*. *J Mol Biol*, 2007. **365**(1): p. 77-89.
120. Xia, Q., et al., *Probing nonnucleoside inhibitor-induced active-site distortion in HIV-1 reverse transcriptase by transient kinetic analyses*. *Protein Sci*, 2007. **16**(8): p. 1728-37.
121. Grobler, J.A., et al., *HIV-1 reverse transcriptase plus-strand initiation exhibits preferential sensitivity to non-nucleoside reverse transcriptase inhibitors in vitro*. *J Biol Chem*, 2007. **282**(11): p. 8005-10.
122. Liu, S., et al., *Slide into action: dynamic shuttling of HIV reverse transcriptase on nucleic acid substrates*. *Science*, 2008. **322**(5904): p. 1092-7.
123. Dueweke, T.J., et al., *U-90152, a potent inhibitor of human immunodeficiency virus type 1 replication*. *Antimicrob Agents Chemother*, 1993. **37**(5): p. 1127-31.
124. Esnouf, R.M., et al., *Unique features in the structure of the complex between HIV-1 reverse transcriptase and the bis(heteroaryl)piperazine (BHAP) U-90152 explain resistance mutations for this nonnucleoside inhibitor*. *Proc Natl Acad Sci U S A*, 1997. **94**(8): p. 3984-9.
125. Merluzzi, V.J., et al., *Inhibition of HIV-1 replication by a nonnucleoside reverse transcriptase inhibitor*. *Science*, 1990. **250**(4986): p. 1411-3.
126. Mellors, J.W. and J.Y. Chow, *Single-dose nevirapine to prevent mother-to-child transmission of HIV type 1: balancing the benefits and risks*. *Clin Infect Dis*, 2009. **48**(4): p. 473-5.
127. Richman, D.D., et al., *Nevirapine resistance mutations of human immunodeficiency virus type 1 selected during therapy*. *J Virol*, 1994. **68**(3): p. 1660-6.

128. Young, S.D., et al., *L-743, 726 (DMP-266): a novel, highly potent nonnucleoside inhibitor of the human immunodeficiency virus type 1 reverse transcriptase*. *Antimicrob Agents Chemother*, 1995. **39**(12): p. 2602-5.
129. Watts, D.H., *Teratogenicity risk of antiretroviral therapy in pregnancy*. *Curr HIV/AIDS Rep*, 2007. **4**(3): p. 135-40.
130. Bacheler, L.T., et al., *Human immunodeficiency virus type 1 mutations selected in patients failing efavirenz combination therapy*. *Antimicrob Agents Chemother*, 2000. **44**(9): p. 2475-84.
131. Tachedjian, G., et al., *Nonnucleoside reverse transcriptase inhibitors are chemical enhancers of dimerization of the HIV type 1 reverse transcriptase*. *Proc Natl Acad Sci U S A*, 2001. **98**(13): p. 7188-93.
132. Venezia, C.F., et al., *Effects of efavirenz binding on the subunit equilibria of HIV-1 reverse transcriptase*. *Biochemistry*, 2006. **45**(9): p. 2779-89.
133. Tachedjian, G. and S.P. Goff, *The effect of NNRTIs on HIV reverse transcriptase dimerization*. *Curr Opin Investig Drugs*, 2003. **4**(8): p. 966-73.
134. de Bethune, M.P., *Non-nucleoside reverse transcriptase inhibitors (NNRTIs), their discovery, development, and use in the treatment of HIV-1 infection: a review of the last 20 years (1989-2009)*. *Antiviral Res*, 2010. **85**(1): p. 75-90.
135. Andries, K., et al., *TMC125, a novel next-generation nonnucleoside reverse transcriptase inhibitor active against nonnucleoside reverse transcriptase inhibitor-resistant human immunodeficiency virus type 1*. *Antimicrob Agents Chemother*, 2004. **48**(12): p. 4680-6.
136. Hicks, C. and R.M. Gulick, *Raltegravir: the first HIV type 1 integrase inhibitor*. *Clin Infect Dis*, 2009. **48**(7): p. 931-9.
137. McColl, D., S. Fransen, and S. Gupta, *Resistance and cross-resistance to first generation integrase inhibitors: insights from a phase II study of elvitegravir (GS-9137)*. *Antiviral Therapy*, 2007. **12**(S11).
138. Hare, S., et al., *Retroviral intasome assembly and inhibition of DNA strand transfer*. *Nature*, 2010. **464**(7286): p. 232-6.
139. Wlodawer, A. and J.W. Erickson, *Structure-based inhibitors of HIV-1 protease*. *Annu Rev Biochem*, 1993. **62**: p. 543-85.
140. Wu, T.D., et al., *Mutation patterns and structural correlates in human immunodeficiency virus type 1 protease following different protease inhibitor treatments*. *J Virol*, 2003. **77**(8): p. 4836-47.
141. Johnson, V.A., et al., *Two-drug combinations of zidovudine, didanosine, and recombinant interferon-alpha A inhibit replication of zidovudine-resistant human immunodeficiency virus type 1 synergistically in vitro*. *J Infect Dis*, 1991. **164**(4): p. 646-55.
142. Merrill, D.P., et al., *Lamivudine or stavudine in two- and three-drug combinations against human immunodeficiency virus type 1 replication in vitro*. *J Infect Dis*, 1996. **173**(2): p. 355-64.
143. Balzarini, J., et al., *Marked inhibitory activity of non-nucleoside reverse transcriptase inhibitors against human immunodeficiency virus type 1 when combined with (-)-2',3'-dideoxy-3'-thiacytidine*. *Mol Pharmacol*, 1996. **49**(5): p. 882-90.
144. Pauwels, R., et al., *New tetrahydroimidazo[4,5,1-jk][1,4]-benzodiazepin-2(1H)-one and -thione derivatives are potent inhibitors of human immunodeficiency virus type 1*

- replication and are synergistic with 2',3'-dideoxynucleoside analogs. Antimicrob Agents Chemother, 1994. 38(12): p. 2863-70.*
145. Richman, D., et al., *BI-RG-587 is active against zidovudine-resistant human immunodeficiency virus type 1 and synergistic with zidovudine. Antimicrob Agents Chemother, 1991. 35(2): p. 305-8.*
 146. Feng, J.Y., et al., *The triple combination of tenofovir, emtricitabine and efavirenz shows synergistic anti-HIV-1 activity in vitro: a mechanism of action study. Retrovirology, 2009. 6: p. 44.*
 147. Basavapathruni, A., C.M. Bailey, and K.S. Anderson, *Defining a molecular mechanism of synergy between nucleoside and nonnucleoside AIDS drugs. J Biol Chem, 2004. 279(8): p. 6221-4.*
 148. Hoggard, P.G., et al., *Effects of drugs on 2',3'-dideoxy-2',3'-didehydrothymidine phosphorylation in vitro. Antimicrob Agents Chemother, 1997. 41(6): p. 1231-6.*
 149. Havlir, D.V., et al., *In vivo antagonism with zidovudine plus stavudine combination therapy. J Infect Dis, 2000. 182(1): p. 321-5.*
 150. Coghlan, M.E., et al., *Symptomatic lactic acidosis in hospitalized antiretroviral-treated patients with human immunodeficiency virus infection: a report of 12 cases. Clin Infect Dis, 2001. 33(11): p. 1914-21.*
 151. Boubaker, K., et al., *Hyperlactatemia and antiretroviral therapy: the Swiss HIV Cohort Study. Clin Infect Dis, 2001. 33(11): p. 1931-7.*
 152. Hammer, S.M., et al., *Antiretroviral treatment of adult HIV infection: 2008 recommendations of the International AIDS Society-USA panel. JAMA, 2008. 300(5): p. 555-70.*
 153. Services, U.D.o.H.a.H. *Adult and Adolescent Antiretroviral Treatment Guidelines. 2009 [cited 2010 June 28].*
 154. Halvas, E.K., et al., *Low frequency nonnucleoside reverse-transcriptase inhibitor-resistant variants contribute to failure of efavirenz-containing regimens in treatment-experienced patients. J Infect Dis, 2010. 201(5): p. 672-80.*
 155. Taiwo, B., *Understanding transmitted HIV resistance through the experience in the USA. Int J Infect Dis, 2009. 13(5): p. 552-9.*
 156. Parikh, U.M., et al., *In vitro activity of structurally diverse nucleoside analogs against human immunodeficiency virus type 1 with the K65R mutation in reverse transcriptase. Antimicrob Agents Chemother, 2005. 49(3): p. 1139-44.*
 157. Shah, F.S., et al., *Differential influence of nucleoside analog-resistance mutations K65R and L74V on the overall mutation rate and error specificity of human immunodeficiency virus type 1 reverse transcriptase. J Biol Chem, 2000. 275(35): p. 27037-44.*
 158. Deval, J., et al., *A loss of viral replicative capacity correlates with altered DNA polymerization kinetics by the human immunodeficiency virus reverse transcriptase bearing the K65R and L74V dideoxynucleoside resistance substitutions. J Biol Chem, 2004. 279(24): p. 25489-96.*
 159. Sarafianos, S.G., et al., *Lamivudine (3TC) resistance in HIV-1 reverse transcriptase involves steric hindrance with beta-branched amino acids. Proc Natl Acad Sci U S A, 1999. 96(18): p. 10027-32.*
 160. Deval, J., et al., *Mechanistic basis for reduced viral and enzymatic fitness of HIV-1 reverse transcriptase containing both K65R and M184V mutations. J Biol Chem, 2004. 279(1): p. 509-16.*

161. Menendez-Arias, L., *Molecular basis of human immunodeficiency virus drug resistance: an update*. Antiviral Res, 2010. **85**(1): p. 210-31.
162. Meyer, P.R., et al., *Unblocking of chain-terminated primer by HIV-1 reverse transcriptase through a nucleotide-dependent mechanism*. Proc Natl Acad Sci U S A, 1998. **95**(23): p. 13471-6.
163. Arion, D. and M.A. Parniak, *HIV resistance to zidovudine: the role of pyrophosphorolysis*. Drug Resist Updat, 1999. **2**(2): p. 91-95.
164. Caliendo, A.M., et al., *Effects of zidovudine-selected human immunodeficiency virus type 1 reverse transcriptase amino acid substitutions on processive DNA synthesis and viral replication*. J Virol, 1996. **70**(4): p. 2146-53.
165. Canard, B., S.R. Sarfati, and C.C. Richardson, *Enhanced binding of azidothymidine-resistant human immunodeficiency virus 1 reverse transcriptase to the 3'-azido-3'-deoxythymidine 5'-monophosphate-terminated primer*. J Biol Chem, 1998. **273**(23): p. 14596-604.
166. Whitcomb, J.M., et al., *Broad nucleoside reverse-transcriptase inhibitor cross-resistance in human immunodeficiency virus type 1 clinical isolates*. J Infect Dis, 2003. **188**(7): p. 992-1000.
167. Tong, W., et al., *Nucleotide-induced stable complex formation by HIV-1 reverse transcriptase*. Biochemistry, 1997. **36**(19): p. 5749-57.
168. Boyer, P.L., et al., *Selective excision of AZTMP by drug-resistant human immunodeficiency virus reverse transcriptase*. J Virol, 2001. **75**(10): p. 4832-42.
169. Arion, D., et al., *Phenotypic mechanism of HIV-1 resistance to 3'-azido-3'-deoxythymidine (AZT): increased polymerization processivity and enhanced sensitivity to pyrophosphate of the mutant viral reverse transcriptase*. Biochemistry, 1998. **37**(45): p. 15908-17.
170. Marchand, B. and M. Gotte, *Site-specific footprinting reveals differences in the translocation status of HIV-1 reverse transcriptase. Implications for polymerase translocation and drug resistance*. J Biol Chem, 2003. **278**(37): p. 35362-72.
171. Sluis-Cremer, N., et al., *The 3'-azido group is not the primary determinant of 3'-azido-3'-deoxythymidine (AZT) responsible for the excision phenotype of AZT-resistant HIV-1*. J Biol Chem, 2005. **280**(32): p. 29047-52.
172. Sluis-Cremer, N., et al., *Molecular mechanism by which the K70E mutation in human immunodeficiency virus type 1 reverse transcriptase confers resistance to nucleoside reverse transcriptase inhibitors*. Antimicrob Agents Chemother, 2007. **51**(1): p. 48-53.
173. Rigourd, M., et al., *Primer unblocking and rescue of DNA synthesis by azidothymidine (AZT)-resistant HIV-1 reverse transcriptase: comparison between initiation and elongation of reverse transcription and between (-) and (+) strand DNA synthesis*. J Biol Chem, 2002. **277**(21): p. 18611-8.
174. Ray, A.S., et al., *Probing the molecular mechanisms of AZT drug resistance mediated by HIV-1 reverse transcriptase using a transient kinetic analysis*. Biochemistry, 2003. **42**(29): p. 8831-41.
175. Nikolenko, G.N., et al., *Mechanism for nucleoside analog-mediated abrogation of HIV-1 replication: balance between RNase H activity and nucleotide excision*. Proc Natl Acad Sci U S A, 2005. **102**(6): p. 2093-8.

176. Delviks-Frankenberry, K.A., et al., *Mutations in human immunodeficiency virus type 1 RNase H primer grip enhance 3'-azido-3'-deoxythymidine resistance*. J Virol, 2007. **81**(13): p. 6837-45.
177. Adams, J., et al., *Nonnucleoside reverse transcriptase inhibitor resistance and the role of the second-generation agents*. Ann Pharmacother, 2010. **44**(1): p. 157-65.
178. De Clercq, E., *The role of non-nucleoside reverse transcriptase inhibitors (NNRTIs) in the therapy of HIV-1 infection*. Antiviral Res, 1998. **38**(3): p. 153-79.
179. Sarafianos, S.G., et al., *Taking aim at a moving target: designing drugs to inhibit drug-resistant HIV-1 reverse transcriptases*. Curr Opin Struct Biol, 2004. **14**(6): p. 716-30.
180. Hsiou, Y., et al., *The Lys103Asn mutation of HIV-1 RT: a novel mechanism of drug resistance*. J Mol Biol, 2001. **309**(2): p. 437-45.
181. Ren, J., et al., *Structural mechanisms of drug resistance for mutations at codons 181 and 188 in HIV-1 reverse transcriptase and the improved resilience of second generation non-nucleoside inhibitors*. J Mol Biol, 2001. **312**(4): p. 795-805.
182. Das, K., et al., *Roles of conformational and positional adaptability in structure-based design of TMC125-R165335 (etravirine) and related non-nucleoside reverse transcriptase inhibitors that are highly potent and effective against wild-type and drug-resistant HIV-1 variants*. J Med Chem, 2004. **47**(10): p. 2550-60.
183. Manosuthi, W., et al., *Patients infected with HIV type 1 subtype CRF01_AE and failing first-line nevirapine- and efavirenz-based regimens demonstrate considerable cross-resistance to etravirine*. AIDS Res Hum Retroviruses, 2010. **26**(6): p. 609-11.
184. Larder, B.A., S.D. Kemp, and P.R. Harrigan, *Potential mechanism for sustained antiretroviral efficacy of AZT-3TC combination therapy*. Science, 1995. **269**(5224): p. 696-9.
185. Shafer, R.W., et al., *Combination therapy with zidovudine and didanosine selects for drug-resistant human immunodeficiency virus type 1 strains with unique patterns of pol gene mutations*. J Infect Dis, 1994. **169**(4): p. 722-9.
186. Larder, B.A., *3'-Azido-3'-deoxythymidine resistance suppressed by a mutation conferring human immunodeficiency virus type 1 resistance to nonnucleoside reverse transcriptase inhibitors*. Antimicrob Agents Chemother, 1992. **36**(12): p. 2664-9.
187. Selmi, B., et al., *The Y181C substitution in 3'-azido-3'-deoxythymidine-resistant human immunodeficiency virus, type 1, reverse transcriptase suppresses the ATP-mediated repair of the 3'-azido-3'-deoxythymidine 5'-monophosphate-terminated primer*. J Biol Chem, 2003. **278**(42): p. 40464-72.
188. Basavapathruni, A., et al., *Modulation of human immunodeficiency virus type 1 synergistic inhibition by reverse transcriptase mutations*. Biochemistry, 2006. **45**(23): p. 7334-40.
189. Frankel, F.A., et al., *Impaired rescue of chain-terminated DNA synthesis associated with the L74V mutation in human immunodeficiency virus type 1 reverse transcriptase*. Antimicrob Agents Chemother, 2005. **49**(7): p. 2657-64.
190. Gotte, M., et al., *The M184V mutation in the reverse transcriptase of human immunodeficiency virus type 1 impairs rescue of chain-terminated DNA synthesis*. J Virol, 2000. **74**(8): p. 3579-85.
191. Parikh, U.M., et al., *The K65R mutation in human immunodeficiency virus type 1 reverse transcriptase exhibits bidirectional phenotypic antagonism with thymidine analog mutations*. J Virol, 2006. **80**(10): p. 4971-7.

192. White, K.L., et al., *The K65R reverse transcriptase mutation in HIV-1 reverses the excision phenotype of zidovudine resistance mutations*. *Antivir Ther*, 2006. **11**(2): p. 155-63.
193. Das, K., et al., *Structural basis for the role of the K65R mutation in HIV-1 reverse transcriptase polymerization, excision antagonism, and tenofovir resistance*. *J Biol Chem*, 2009. **284**(50): p. 35092-100.
194. Johnson, V.A., et al., *Update of the Drug Resistance Mutations in HIV-1: December 2009*. *Topics in HIV Medicine*, 2009. **17**(5): p. 138-145.
195. Kagan, R., et al. *Expanded range of HIV-1 reverse transcriptase mutations detected through long range sequencing*. in *11th Conference on Retroviruses and Opportunistic Infections*. 2004. San Francisco, CA, USA.
196. Galli, R., et al. *Beyond codon 240: Mutations in the HIV-1 reverse transcriptase selected after exposure to antiretrovirals*. in *15th International AIDS Conference*. 2004. Bangkok, Thailand.
197. Gallego, O., et al., *Prevalence of G333D/E in naive and pretreated HIV-infected patients*. *AIDS Res Hum Retroviruses*, 2002. **18**(12): p. 857-60.
198. Kemp, S.D., et al., *A novel polymorphism at codon 333 of human immunodeficiency virus type 1 reverse transcriptase can facilitate dual resistance to zidovudine and L-2',3'-dideoxy-3'-thiacytidine*. *J Virol*, 1998. **72**(6): p. 5093-8.
199. Zelina, S., et al., *Mechanisms by which the G333D mutation in human immunodeficiency virus type 1 Reverse transcriptase facilitates dual resistance to zidovudine and lamivudine*. *Antimicrob Agents Chemother*, 2008. **52**(1): p. 157-63.
200. Nikolenko, G.N., et al., *Mutations in the connection domain of HIV-1 reverse transcriptase increase 3'-azido-3'-deoxythymidine resistance*. *Proc Natl Acad Sci U S A*, 2007. **104**(1): p. 317-22.
201. Yap, S.H., et al., *N348I in the connection domain of HIV-1 reverse transcriptase confers zidovudine and nevirapine resistance*. *PLoS Med*, 2007. **4**(12): p. e335.
202. von Wyl, V., et al., *Epidemiological and biological evidence for a compensatory effect of connection domain mutation N348I on M184V in HIV-1 reverse transcriptase*. *J Infect Dis*, 2010. **201**(7): p. 1054-62.
203. Hachiya, A., et al., *Amino acid mutation N348I in the connection subdomain of human immunodeficiency virus type 1 reverse transcriptase confers multiclass resistance to nucleoside and nonnucleoside reverse transcriptase inhibitors*. *J Virol*, 2008. **82**(7): p. 3261-70.
204. Ehteshami, M., et al., *Connection domain mutations N348I and A360V in HIV-1 reverse transcriptase enhance resistance to 3'-azido-3'-deoxythymidine through both RNase H-dependent and -independent mechanisms*. *J Biol Chem*, 2008. **283**(32): p. 22222-32.
205. Brehm, J.H., et al., *Selection of mutations in the connection and RNase H domains of human immunodeficiency virus type 1 reverse transcriptase that increase resistance to 3'-azido-3'-dideoxythymidine*. *J Virol*, 2007. **81**(15): p. 7852-9.
206. Gotte, M., *Should we include connection domain mutations of HIV-1 reverse transcriptase in HIV resistance testing*. *PLoS Med*, 2007. **4**(12): p. e346.
207. Quan, Y., et al., *Enhanced impairment of chain elongation by inhibitors of HIV reverse transcriptase in cell-free reactions yielding longer DNA products*. *Nucleic Acids Res*, 1998. **26**(24): p. 5692-8.

208. Gu, Z., et al., *Effects of non-nucleoside inhibitors of human immunodeficiency virus type 1 in cell-free recombinant reverse transcriptase assays*. J Biol Chem, 1995. **270**(52): p. 31046-51.
209. Quan, Y., et al., *Reverse transcriptase inhibitors can selectively block the synthesis of differently sized viral DNA transcripts in cells acutely infected with human immunodeficiency virus type 1*. J Virol, 1999. **73**(8): p. 6700-7.
210. Hang, J., et al., *Compound Specific Differences in the Levels of Resistance of HIV-RT Catalysed Strand Transfer, DNA Polymerase and RNase H Activities to Inhibition by NNRTIs*. Antiviral Therapy, 2006. **11**(S145): p. Abstract No. 129.
211. Goldman, M.E., et al., *Pyridinone derivatives: specific human immunodeficiency virus type 1 reverse transcriptase inhibitors with antiviral activity*. Proc Natl Acad Sci U S A, 1991. **88**(15): p. 6863-7.
212. Debyser, Z., et al., *An antiviral target on reverse transcriptase of human immunodeficiency virus type 1 revealed by tetrahydroimidazo-[4,5,1-jk][1,4]benzodiazepin-2 (1H)-one and -thione derivatives*. Proc Natl Acad Sci U S A, 1991. **88**(4): p. 1451-5.
213. Gopalakrishnan, V. and S. Benkovic, *Effect of a thiobenzimidazolone derivative on DNA strand transfer catalyzed by HIV-1 reverse transcriptase*. J Biol Chem, 1994. **269**(6): p. 4110-5.
214. Hang, J.Q., et al., *Substrate-dependent inhibition or stimulation of HIV RNase H activity by non-nucleoside reverse transcriptase inhibitors (NNRTIs)*. Biochem Biophys Res Commun, 2007. **352**(2): p. 341-350.
215. Talele, T.T., A. Upadhyay, and V.N. Pandey, *Influence of the RNase H domain of retroviral reverse transcriptases on the metal specificity and substrate selection of their polymerase domains*. Virol J, 2009. **6**: p. 159.
216. Boyer, P.L., A.L. Ferris, and S.H. Hughes, *Cassette mutagenesis of the reverse transcriptase of human immunodeficiency virus type 1*. J Virol, 1992. **66**(2): p. 1031-9.
217. Clark, S.A., et al., *Reverse transcriptase mutations 118I, 208Y, and 215Y cause HIV-1 hypersusceptibility to non-nucleoside reverse transcriptase inhibitors*. AIDS, 2006. **20**(7): p. 981-4.
218. Sato, A., et al., *In vitro selection of mutations in human immunodeficiency virus type 1 reverse transcriptase that confer resistance to capravirine, a novel nonnucleoside reverse transcriptase inhibitor*. Antiviral Res, 2006. **70**(2): p. 66-74.
219. Hazen, R.J., et al., *Anti-human immunodeficiency virus type 1 activity of the nonnucleoside reverse transcriptase inhibitor GW678248 in combination with other antiretrovirals against clinical isolate viruses and in vitro selection for resistance*. Antimicrob Agents Chemother, 2005. **49**(11): p. 4465-73.
220. Motakis, D. and M.A. Parniak, *A tight-binding mode of inhibition is essential for anti-human immunodeficiency virus type 1 virucidal activity of nonnucleoside reverse transcriptase inhibitors*. Antimicrob Agents Chemother, 2002. **46**(6): p. 1851-6.
221. Nissley, D.V., et al., *Characterization of novel non-nucleoside reverse transcriptase (RT) inhibitor resistance mutations at residues 132 and 135 in the 51 kDa subunit of HIV-1 RT*. Biochem J, 2007. **404**(1): p. 151-7.
222. Hang, J.Q., et al., *Substrate-dependent inhibition or stimulation of HIV RNase H activity by non-nucleoside reverse transcriptase inhibitors (NNRTIs)*. Biochem Biophys Res Commun, 2007. **352**(2): p. 341-50.

223. Geitmann, M., T. Unge, and U.H. Danielson, *Biosensor-based kinetic characterization of the interaction between HIV-1 reverse transcriptase and non-nucleoside inhibitors*. J Med Chem, 2006. **49**(8): p. 2367-74.
224. Shaw-Reid, C.A., et al., *Dissecting the effects of DNA polymerase and ribonuclease H inhibitor combinations on HIV-1 reverse-transcriptase activities*. Biochemistry, 2005. **44**(5): p. 1595-606.
225. Radzio, J. and N. Sluis-Cremer, *Efavirenz accelerates HIV-1 reverse transcriptase ribonuclease H cleavage, leading to diminished zidovudine excision*. Mol Pharmacol, 2008. **73**(2): p. 601-6.
226. Le Grice, S.F. and F. Gruninger-Leitch, *Rapid purification of homodimer and heterodimer HIV-1 reverse transcriptase by metal chelate affinity chromatography*. Eur J Biochem, 1990. **187**(2): p. 307-14.
227. Le Grice, S.F., C.E. Cameron, and S.J. Benkovic, *Purification and characterization of human immunodeficiency virus type 1 reverse transcriptase*. Methods Enzymol, 1995. **262**: p. 130-44.
228. Borkow, G., et al., *The thiocarboxanilide nonnucleoside inhibitor UC781 restores antiviral activity of 3'-azido-3'-deoxythymidine (AZT) against AZT-resistant human immunodeficiency virus type 1*. Antimicrob Agents Chemother, 1999. **43**(2): p. 259-63.
229. Odriozola, L., et al., *Non-nucleoside inhibitors of HIV-1 reverse transcriptase inhibit phosphorolysis and resensitize the 3'-azido-3'-deoxythymidine (AZT)-resistant polymerase to AZT-5'-triphosphate*. J Biol Chem, 2003. **278**(43): p. 42710-6.
230. Palaniappan, C., P.J. Fay, and R.A. Bambara, *Nevirapine alters the cleavage specificity of ribonuclease H of human immunodeficiency virus 1 reverse transcriptase*. J Biol Chem, 1995. **270**(9): p. 4861-4869.
231. Temiz, N.A. and I. Bahar, *Inhibitor binding alters the directions of domain motions in HIV-1 reverse transcriptase*. Proteins, 2002. **49**(1): p. 61-70.
232. Shaw-Reid, C.A., et al., *Dissecting the effects of DNA polymerase and ribonuclease H inhibitor combinations on HIV-1 reverse-transcriptase activities*. Biochemistry, 2005. **44**(5): p. 1595-1606.
233. Spence, R.A., et al., *Mechanism of inhibition of HIV-1 reverse transcriptase by nonnucleoside inhibitors*. Science, 1995. **267**(5200): p. 988-93.
234. Lakowicz, J.R., *Principles of Fluorescence Spectroscopy*. Second Edition ed. 1999: Kluwer Academic.
235. Brehm, J.H., J.W. Mellors, and N. Sluis-Cremer, *Mechanism by which a glutamine to leucine substitution at residue 509 in the ribonuclease H domain of HIV-1 reverse transcriptase confers zidovudine resistance*. Biochemistry, 2008. **47**(52): p. 14020-7.
236. Boucher, C.A., et al., *Ordered appearance of zidovudine resistance mutations during treatment of 18 human immunodeficiency virus-positive subjects*. J Infect Dis, 1992. **165**(1): p. 105-10.
237. Zelina, S., et al., *Residue K70 in HIV-1 reverse transcriptase: a crossroad between excision and discrimination mechanisms of NRTI resistance*. Antiviral Therapy, 2006. **11**: p. S159.
238. Delviks-Frankenberry, K.A., et al., *HIV-1 reverse transcriptase connection subdomain mutations reduce template RNA degradation and enhance AZT excision*. Proc Natl Acad Sci U S A, 2008. **105**(31): p. 10943-8.

239. Boyer, P.L., et al., *The M184V mutation reduces the selective excision of zidovudine 5'-monophosphate (AZTMP) by the reverse transcriptase of human immunodeficiency virus type 1*. J Virol, 2002. **76**(7): p. 3248-56.
240. Radzio, J., et al., *N348I in reverse transcriptase provides a genetic pathway for HIV-1 to select thymidine analogue mutations and mutations antagonistic to thymidine analogue mutations*. AIDS, 2010. **24**(5): p. 659-67.
241. Nikolenko, G.N., K.A. Delviks-Frankenberry, and V.K. Pathak, *A novel molecular mechanism of dual resistance to nucleoside and nonnucleoside reverse transcriptase inhibitors*. J Virol, 2010. **84**(10): p. 5238-49.
242. Biondi, M.J., et al., *N348I in HIV-1 reverse transcriptase can counteract the nevirapine-mediated bias toward RNase H cleavage during plus-strand initiation*. J Biol Chem, 2010.
243. Gao, H.Q., et al., *The role of steric hindrance in 3TC resistance of human immunodeficiency virus type-1 reverse transcriptase*. J Mol Biol, 2000. **300**(2): p. 403-18.
244. Sarafianos, S.G., et al., *Crystal structure of HIV-1 reverse transcriptase in complex with a polypurine tract RNA:DNA*. EMBO J, 2001. **20**(6): p. 1449-61.
245. Carr, A., et al., *A controlled trial of nevirapine plus zidovudine versus zidovudine alone in p24 antigenaemic HIV-infected patients. The Dutch-Italian-Australian Nevirapine Study Group*. AIDS, 1996. **10**(6): p. 635-41.
246. King, R.W., et al., *Potency of nonnucleoside reverse transcriptase inhibitors (NNRTIs) used in combination with other human immunodeficiency virus NNRTIs, NRTIs, or protease inhibitors*. Antimicrob Agents Chemother, 2002. **46**(6): p. 1640-6.
247. Maga, G., et al., *Potentiation of inhibition of wild-type and mutant human immunodeficiency virus type 1 reverse transcriptases by combinations of nonnucleoside inhibitors and d- and L-(beta)-dideoxynucleoside triphosphate analogs*. Antimicrob Agents Chemother, 2001. **45**(4): p. 1192-200.
248. Carroll, S.S., et al., *Inhibition of HIV-1 reverse transcriptase by a quinazolinone and comparison with inhibition by pyridinones. Differences in the rates of inhibitor binding and in synergistic inhibition with nucleoside analogs*. J Biol Chem, 1994. **269**(51): p. 32351-7.
249. Stoeckli, T.C., et al., *Phenotypic and genotypic analysis of biologically cloned human immunodeficiency virus type 1 isolates from patients treated with zidovudine and lamivudine*. Antimicrob Agents Chemother, 2002. **46**(12): p. 4000-3.
250. Iversen, A.K., et al., *Multidrug-resistant human immunodeficiency virus type 1 strains resulting from combination antiretroviral therapy*. J Virol, 1996. **70**(2): p. 1086-90.
251. Mas, A., et al., *Role of a dipeptide insertion between codons 69 and 70 of HIV-1 reverse transcriptase in the mechanism of AZT resistance*. EMBO J, 2000. **19**(21): p. 5752-61.
252. von Wyl, V., et al., *HIV-1 Reverse Transcriptase Connection Domain Mutations: Dynamics of Emergence and Implications for Success of Combination Antiretroviral Therapy*. Clin Infect Dis, 2010.
253. Balzarini, J., et al., *Concomitant combination therapy for HIV infection preferable over sequential therapy with 3TC and non-nucleoside reverse transcriptase inhibitors*. Proc Natl Acad Sci U S A, 1996. **93**(23): p. 13152-7.

254. Carr, A., et al., *Pathogenesis of HIV-1-protease inhibitor-associated peripheral lipodystrophy, hyperlipidaemia, and insulin resistance*. Lancet, 1998. **351**(9119): p. 1881-3.
255. Pauwels, R., et al., *Potent and selective inhibition of HIV-1 replication in vitro by a novel series of TIBO derivatives*. Nature, 1990. **343**(6257): p. 470-4.
256. Jackson, J.B., et al., *Intrapartum and neonatal single-dose nevirapine compared with zidovudine for prevention of mother-to-child transmission of HIV-1 in Kampala, Uganda: 18-month follow-up of the HIVNET 012 randomised trial*. Lancet, 2003. **362**(9387): p. 859-68.
257. Hitti, J., et al., *Maternal toxicity with continuous nevirapine in pregnancy: results from PACTG 1022*. J Acquir Immune Defic Syndr, 2004. **36**(3): p. 772-6.
258. *Scaling up antiretroviral therapy in resource-limited settings: treatment guidelines for a public health approach*. 2003 [cited 2007 June 19]; 2003:[Available from: Accessed June 19, 2007: http://www.who.int/hiv/pub/prev_care/en/arvrevision2003en.pdf.
259. Dumans, A.T., et al., *Synonymous genetic polymorphisms within Brazilian human immunodeficiency virus Type 1 subtypes may influence mutational routes to drug resistance*. J Infect Dis, 2004. **189**(7): p. 1232-8.
260. Kantor, R., et al., *Impact of HIV-1 subtype and antiretroviral therapy on protease and reverse transcriptase genotype: results of a global collaboration*. PLoS Med, 2005. **2**(4): p. e112.
261. Kantor, R., *Impact of HIV-1 pol diversity on drug resistance and its clinical implications*. Curr Opin Infect Dis, 2006. **19**(6): p. 594-606.
262. Soares, E.A., et al., *Differential drug resistance acquisition in HIV-1 of subtypes B and C*. PLoS One, 2007. **2**(1): p. e730.
263. Grossman, Z., et al., *Genetic variation at NNRTI resistance-associated positions in patients infected with HIV-1 subtype C*. AIDS, 2004. **18**(6): p. 909-15.
264. Brenner, B., et al., *A V106M mutation in HIV-1 clade C viruses exposed to efavirenz confers cross-resistance to non-nucleoside reverse transcriptase inhibitors*. AIDS, 2003. **17**(1): p. F1-5.
265. Eshleman, S.H., et al., *Impact of human immunodeficiency virus type 1 (hiv-1) subtype on women receiving single-dose nevirapine prophylaxis to prevent hiv-1 vertical transmission (hiv network for prevention trials 012 study)*. J Infect Dis, 2001. **184**(7): p. 914-7.
266. Palmer, S., et al., *Drug susceptibility of subtypes A,B,C,D, and E human immunodeficiency virus type 1 primary isolates*. AIDS Res Hum Retroviruses, 1998. **14**(2): p. 157-62.
267. Brehm, J., et al. *Frequent emergence of N348I in the connection domain of reverse transcriptase with virological failure of first-line NNRTI-containing regimens in South Africa*. in *Antiviral Therapy*. 2010.